

**CONTRACTOR REPORT**

*CASE/KELSALL*

SAND86-7001  
Unlimited Release  
UC-70

**Nevada Nuclear Waste Storage Investigations Project**

**Modification of Rock Mass Permeability  
in the Zone Surrounding a  
Shaft in Fractured, Welded Tuff**

John B. Case and Peter C. Kelsall  
IT Corporation  
2340 Alamo SE, Suite 306  
Albuquerque, NM 87106

Prepared by Sandia National Laboratories Albuquerque, New Mexico 87185  
and Livermore, California 94550 for the United States Department of Energy  
under Contract DE-AC04-76DP00789

Printed March 1987

8712100121 870617  
PDR WASTE PDR  
WM-11

"Prepared by Nevada Nuclear Waste Storage Investigations (NNWSI) Project participants as part of the Civilian Radioactive Waste Management Program (CRWM). The NNWSI Project is managed by the Waste Management Project Office (WMPO) of the U. S. Department of Energy, Nevada Operations Office (DOE/NV). NNWSI Project work is sponsored by the Office of Geologic Repositories (OGR) of the DOE Office of Civilian Radioactive Waste Management (OCRWM)."

Issued by Sandia National Laboratories, operated for the United States Department of Energy by Sandia Corporation.

**NOTICE:** This report was prepared as an account of work sponsored by an agency of the United States Government. Neither the United States Government nor any agency thereof, nor any of their employees, nor any of their contractors, subcontractors, or their employees, makes any warranty, express or implied, or assumes any legal liability or responsibility for the accuracy, completeness, or usefulness of any information, apparatus, product, or process disclosed, or represents that its use would not infringe privately owned rights. Reference herein to any specific commercial product, process, or service by trade name, trademark, manufacturer, or otherwise, does not necessarily constitute or imply its endorsement, recommendation, or favoring by the United States Government, any agency thereof or any of their contractors or subcontractors. The views and opinions expressed herein do not necessarily state or reflect those of the United States Government, any agency thereof or any of their contractors or subcontractors.

Printed in the United States of America  
Available from  
National Technical Information Service  
U.S. Department of Commerce  
5235 Port Royal Road  
Springfield, VA 22161

NTIS price codes  
Printed copy: A05  
Microfiche copy: A01

SAND 86-7001  
Unlimited Release  
Printed March 1987

Distribution  
Category UC-70

**MODIFICATION OF ROCK MASS PERMEABILITY  
IN THE ZONE SURROUNDING A  
SHAFT IN FRACTURED, WELDED TUFF**

by  
**John B. Case  
Peter C. Kelsall**

IT Corporation  
2340 Alamo SE, Suite 306  
Albuquerque, NM 87106

for  
**Sandia National Laboratories  
P.O. Box 5800  
Albuquerque, New Mexico 87185**

Under Sandia Contract: 64-6207

Sandia Contract Monitor  
**Joseph A. Fernandez  
Geotechnical Design Division**

**ABSTRACT**

The excavation of a nuclear waste repository at Yucca Mountain, Nevada requires access through shafts and ramps from the ground surface to the repository horizon. To evaluate the need and performance of the sealing subsystem, it is necessary to predict the modifications in the rock immediately surrounding the shaft. The purpose of this study is to develop a model of permeability changes as a function of radial distance from a shaft. The model is based upon analyses which consider modification in rock mass permeability resulting from stress redistribution and blast damage due to excavation around a shaft. Elastic and elastoplastic stress analyses are performed to estimate the stress distributions after excavation for a wide range of rock properties and in situ stress conditions. Changes in stress are related to changes in rock mass permeability using stress-permeability relations for fractures obtained from laboratory and field testing. The effects of blast damage are estimated from case histories. The analyses indicate that rock mass permeability is expected to decline rapidly to the undisturbed value with greater permeability changes occurring at or near the shaft wall. For several conditions evaluated, the equivalent permeability of the modified permeability zone, averaged over an annulus one radius wide around the shaft, ranges from 15 to 80 times the undisturbed rock mass permeability.

## TABLE OF CONTENTS

|   | <u>Page</u> |
|---|-------------|
| ABSTRACT  | i           |
| LIST OF TABLES  | iv          |
| LIST OF FIGURES   | v           |
| SUMMARY   | 1           |
| 1.0 INTRODUCTION  | 4           |
| 2.0 TECHNICAL APPROACH AND METHODS OF ANALYSIS  | 6           |
| 2.1 SITE CONDITIONS   | 6           |
| 2.2 MECHANISMS FOR MODIFYING PERMEABILITY ADJACENT TO A SHAFT   | 9           |
| 2.2.1 Effects of Stress Redistribution  | 10          |
| 2.2.2 Effects of Blasting   | 13          |
| 2.3 METHODOLOGY FOR DEVELOPING THE MODIFIED PERMEABILITY ZONE MODEL   | 16          |
| 3.0 STRESS ANALYSIS FOR A SHAFT IN WELDED TUFF  | 18          |
| 3.1 GENERAL DESCRIPTION OF ROCK MASS RESPONSE TO SHAFT EXCAVATION   | 18          |
| 3.2 ROCK MASS STRENGTH  | 18          |
| 3.3 ROCK MASS DEFORMABILITY   | 22          |
| 3.4 IN SITU STRESS  | 22          |
| 3.5 ELASTIC ANALYSIS  | 23          |
| 3.6 ELASTOPLASTIC ANALYSIS  | 23          |
| 4.0 CONSTITUTIVE RELATIONSHIPS BETWEEN STRESS ON FRACTURES AND ROCK MASS PERMEABILITY                           | 30          |
| 4.1 THEORETICAL BASIS FOR OBTAINING A ROCK MASS STRESS-PERMEABILITY RELATIONSHIP FROM TESTS ON SINGLE FRACTURES | 30          |
| 4.2 LABORATORY STUDIES OF SINGLE FRACTURES IN WELDED AND NONWELDED TUFF   | 32          |
| 4.3 FIELD STUDIES OF SINGLE FRACTURES IN WELDED TUFF  | 35          |
| 4.4 STRESS PERMEABILITY RELATIONSHIPS   | 35          |
| 5.0 EVALUATION OF PERMEABILITY CHANGES RESULTING FROM STRESS RELIEF   | 40          |
| 5.1 SUMMARY OF INPUT PARAMETERS   | 40          |
| 5.2 RESULTS   | 41          |
| 6.0 EVALUATION OF PERMEABILITY CHANGES RESULTING FROM BLASTING  | 44          |
| 6.1 REVIEW OF CASE HISTORIES  | 44          |
| 6.1.1 Colorado School of Mines Test Mine  | 44          |

**TABLE OF CONTENTS**  
(Continued)

|   | <u>Page</u> |
|---|-------------|
| 6.1.2 Stripa Mine, Sweden   | 48          |
| 6.1.3 Nevada Test Site  | 49          |
| 6.1.4 Rolla Experimental Mine   | 52          |
| 6.1.5 Tunnel in Basalt  | 52          |
| 6.1.6 U.S. Bureau of Mines Studies                                    | 52          |
| 6.2 BLAST DAMAGE EXTENT BASED UPON CHARGE DENSITY                     | 55          |
| 6.3 PERMEABILITY CHANGES AND EXTENT OF BLAST DAMAGE IN<br>WELDED TUFF | 56          |
| 7.0 MODEL OF THE MODIFIED PERMEABILITY ZONE                           | 58          |
| APPENDIX A - ROCK MASS STRENGTH                                       | 61          |
| APPENDIX B - ROCK DAMAGE CAUSED BY BLASTING - BIBLIOGRAPHY            | 69          |
| REFERENCES  | 75          |

## LIST OF FIGURES

| <u>Figure</u> | <u>Title</u>  | <u>Page</u> |
|---------------|---|-------------|
| 1             | Elevations of Shafts and Repository in Relation to Stratigraphy   | 7           |
| 2             | Cross-section Through a Shaft in Welded Tuff Showing Fracture Spacing Relative to Shaft Radius                                      | 8           |
| 3             | Stress Analysis for a Circular Opening in a Homogeneous, Elastic Medium   | 11          |
| 4             | Near-hole Blast Cracking (From Dowding, 1985, Figure 15-2 and Dupont, 1977, Figure 26-A)  | 14          |
| 5             | Comparison of Fracture Patterns Resulting From Smooth Blasting and Conventional Blasting  | 15          |
| 6             | Strength Envelopes for Welded Tuff  | 21          |
| 7             | Strength Envelopes for Nonwelded Tuff   | 21          |
| 8             | Development of a Plastic Zone in Welded Tuff for Assumptions of Lower Bound Strength and Upper Bound In Situ Stress                 | 27          |
| 9             | Extent of the Plastic Zone as a Function of Depth For Low Strength Tuff   | 28          |
| 10            | Comparison of Radial Displacements (Elastic and Elastoplastic Solutions) at 310 m Depth   | 29          |
| 11            | Permeability as a Function of Normal Stress From Laboratory Testing by Peters et al. (1984)   | 33          |
| 12            | Comparison of Relative Permeability Relationships From Laboratory Testing by Peters et al. (1984)                                   | 34          |
| 13            | Permeability vs. Effective Normal Stress, G Tunnel Block Test - Path 21 (After Zimmerman et al., 1985)                              | 36          |
| 14            | Permeability vs. Effective Normal Stress, G Tunnel Block Test - Path 23 (After Zimmerman et al., 1985)                              | 37          |
| 15            | Comparison of Field, Laboratory, and Modeling Studies of the Relationship Between Effective Normal Stress and Fracture Permeability | 38          |
| 16            | Upper and Lower Bounds to Sensitivity of Rock Mass Permeability to Effective Normal Stress in Welded Tuff Normalized to 12 MPa      | 39          |
| 17            | Rock Mass Permeability-Stress Relationships Normalized to Stress Levels Used in Modified Permeability Zone Analyses                 | 42          |
| 18            | Estimated Change in Axial Rock Mass Permeability at 100 m and 310 m Depths Resulting From Stress Relief                             | 43          |
| 19            | Macroporosity Test, Stripa, Sweden  | 50          |

## LIST OF FIGURES

(Continued)

| <u>Figure</u> | <u>Title</u>   | <u>Page</u> |
|---------------|--|-------------|
| 20            | Typical Displacement Profiles in Large Excavated Caverns at the Nevada Test Site   | 51          |
| 21            | Depth of Disturbance Measured by Seismic Refraction in a Tunnel in Dolomite for Various Blasting Methods (From Worsey, 1985)     | 53          |
| 22            | Primary Seismic Wave Velocity in Vertical and Horizontal Directions Between Boreholes, Tunnel in Basalt (From King et al., 1984) | 54          |
| 23            | Method for Estimating the Thickness of the Blast-Damaged Zone in Relation to Explosive Charge Density                            | 57          |
| 24            | Modified Permeability Zone Model for Topopah Spring Welded Tuff for Expected Conditions at 310 m Depth                           | 60          |

## LIST OF TABLES

| <u>Table</u> | <u>Title</u>  | <u>Page</u> |
|--------------|---|-------------|
| 1            | Properties of Welded and Nonwelded Tuff Used in Stress Analyses                         | 20          |
| 2            | Results of Elastoplastic Stress Analyses for Welded Tuff                                | 25          |
| 3            | Case Histories of Blast Damage Measured in Tunnels                                      | 45          |
| 4            | Equivalent Permeability of the Modified Permeability Zone                               | 59          |
| A-1          | Properties of Welded and Nonwelded Tuff Used in Stress Analyses                         | 64          |
| A-2          | Comparison of the Calculated and Recommended Empirical Strength Parameter, $m$ , Values | 66          |

## SUMMARY

The development and operation of an underground repository in tuff at Yucca Mountain will require access to the repository horizon through a number of vertical shafts. As part of the Nevada Nuclear Waste Storage Investigations Project (NNWSI), Sandia National Laboratories (SNL) is conducting studies to determine whether shafts can become pathways that compromise radioactive waste isolation by providing a means for water to enter the repository. Conceptually, water- or air-flow through a sealed shaft could occur through three zones as follows: 1) the seal material placed within the original opening, 2) the interface between the seal material and the host rock, and 3) a zone surrounding the original opening in which the permeability might be modified by the excavation process. The purpose of this report is to provide a model of the modified permeability zone that can be used in future analyses of the performance of the repository. The report specifically considers modification of permeability in fractured, welded tuff of the Topopah Spring unit, which will be the major stratigraphic unit encountered in the shafts at Yucca Mountain.

It is postulated in the report that the dominant processes which may lead to modification of permeability are stress redistribution and damage by blasting due to excavation. It should be noted that while care might be taken to limit damage due to blasting by selection of an alternate method of excavation, the effects of stress redistribution will occur regardless of the excavation method used. The redistribution of stresses around an opening in fractured tuff might affect the permeability of the rock mass in two ways; namely, 1) by the fracturing of originally intact rock due to excessive compressive or tensile stresses, and 2) by the opening or closing of preexisting fractures due to changes in the normal stresses acting across the fractures, or to shearing along the fractures. The potential for fracturing of intact rock is evaluated by means of a simple analysis for the case of a circular shaft excavated in a homogeneous, isotropic and linearly elastic medium. This analysis shows that the maximum tensile or compressive stresses at the shaft wall at repository depth should not exceed approximately 10 percent of the reported mean values for tensile and unconfined compressive strength of intact rock. The analysis shows that fracturing of intact rock, due to stress concentrations around a shaft at repository depth, is unlikely, even allowing for variation from the mean reported strength values and potential anisotropy in the stress field. Whereas stress redistribution around a shaft should not lead to fracturing of intact rock (which could in turn lead to increased permeability), the effects of stress changes across fractures may have a significant effect on permeability. This arises because the rock mass is densely fractured and because the permeability of fractures is sensitive to the stress applied across the fractures.

It is currently planned that three of the four shafts at Yucca Mountain will be excavated by blasting. It is expected that blasting will, to some degree, damage the remaining rock adjacent to the excavation wall by creation of new cracks and extending or widening of preexisting cracks. This damage may lead to increases in permeability in the zone in which new fractures are created.

It is postulated that the significant mechanisms for modifying permeability in fractured, welded tuff are 1) opening or closing of fractures in response to stress changes, and 2) creating new fractures or causing the opening of

pre-existing fractures by blasting. The approach for developing the modified permeability zone model includes the following five steps:

1. Calculate stress changes around a shaft by using an appropriate closed-form solution for elastic or elasto-plastic analysis of a circular shaft located in a uniform stress field (Section 3.0).
2. Obtain relationships from published laboratory and field testing results which describe the effects of stress on the permeability of single fractures and fractured rock (Section 4.0).
3. Calculate rock mass permeability as a function of radius away from the shaft, based on the calculated stresses and the stress-permeability relationships obtained from testing (Section 5.0).
4. Estimate permeability changes due to blasting from evaluation of case histories which indicate the depth of damage, and estimate the probable increase in fracture frequency in the damaged zone (Section 6.0).
5. Combine the results derived from performing steps 3 and 4 to obtain the combined effects of stress redistribution and blasting (Section 7.0).

For the sake of simplification, the analyses are based on general assumptions that are described in detail in the text (Section 2.0).

Analyses are conducted for shaft depths of 100 m and 310 m. The 100-m depth is representative of the upper part of the Topopah Spring unit, whereas 310 m is the depth at which the Exploratory Shaft intersects the repository horizon. Analyses are conducted to represent a range of expected rock conditions at each of these depths as follows:

- A lower-bound estimate of the increase in rock mass permeability is obtained by considering an upper bound for the expected rock mass strength properties, a lower bound for the expected in situ stresses, and a lower bound for the sensitivity of permeability to stress as indicated by laboratory and field testing.
- An expected estimate of the probable increase in rock mass permeability is obtained using the expected mean values for strength and in situ stresses and values for the mean sensitivity of permeability to stress.
- An upper bound estimate of the increase in rock mass permeability is obtained by using values for lower-bound strength properties, upper-bound in situ stresses, and the upper-bound sensitivity of permeability due to stress.

In these analyses, the intact rock compressive strength varies from 110 to 230 MPa, with an expected value of 171 MPa. Values for the rock mass quality, as indicated by the Rock Mass Rating, vary from 48 to 84, with an expected value of 65. Values for the in situ stress varies from 0.25 to 1.0 times the weight of overburden with an expected value of 0.6 times the weight of overburden. Depending upon these properties, a wide range of rock mass behavior is predicted. At both depths, the combination of lower-bound rock mass strength and upper-bound in situ stress results in inelastic behavior adjacent to the shaft wall; whereas for the other cases analyzed, the predicted behavior is elastic. This difference in rock mass response is significant with respect to the effects on rock mass permeability. Under elastic conditions (using values for the lower-bound sensitivity of permeability to stress), the maximum increase in rock mass permeability resulting from redistribution of stress at the shaft wall is less than an order of magnitude. Given the potential resolution of in situ permeability measurements and potential variability in the rock mass, such a zone of increased permeability may not be measurable. On the other hand, inelastic deformation (combined with values for the upper-bound sensitivity of permeability to stress) results in predicted changes in rock mass permeability at the shaft wall as high as two orders of magnitude.

Estimates of the effects of blasting on rock mass permeability are based initially on a review of case histories which indicate the extent of blast damage around underground openings. Because these case histories indicate only the width of the damaged zone and not the permeability, it is necessary to base the estimates of increased permeability on assumptions regarding the increased fracture frequency within the damaged zone. Case histories suggest that the width of blast damage may vary from approximately 0.3 m, for cases in which controlled blasting methods such as smooth blasting are used, to approximately 2.0 m, for cases in which conventional blasting methods are used. For purposes of estimating increases in rock mass permeability due to blasting, it is assumed that blasting will be controlled and results in a three-fold increase in fracture frequency within a zone extending 0.5 m from the shaft wall. In a second upper bound blast damage model, it is assumed that the annulus extends 1.0 m from the shaft wall.

The results of the stress redistribution and blast damage analyses are combined to form a series of models for the modified permeability zone representing a range of rock mass properties and in situ stress conditions. These models are most easily compared by considering an equivalent rock mass permeability of the modified permeability zone, which is averaged over an annulus one radius wide around the shaft and normalized to the permeability of the undamaged rock (Table 4). For the expected conditions at 310 m depth (i.e., considering mean values for rock mass strength, in situ stress, and stress permeability sensitivity, and a 0.5-meter wide blast-damaged zone), the equivalent rock mass permeability averaged over an annulus one radius wide is 20 times the permeability of the undamaged rock mass. For the upper bound condition at 310 m depth (considering low values for rock mass strength, a high value for in situ stress, high stress-permeability sensitivity, and a one meter wide blast damaged zone), the equivalent rock mass permeability is 80 times the undisturbed permeability.

## 1.0 INTRODUCTION

The work described in this report was performed for Sandia National Laboratories (SNL) as a part of the NNWSI project. SNL is one of the principal organizations participating in the project, which is managed by the U.S. Department of Energy's Nevada Operations Office (DOE-NVO). The project is a part of the DOE's program to safely dispose of the radioactive waste from nuclear power plants.

The DOE has determined that the safest and most feasible method currently known for the disposal of such wastes is to emplace them in mined geologic repositories. The NNWSI project is conducting detailed studies of an area on and adjacent to the Nevada Test Site (NTS) in southern Nevada to determine its feasibility as a site for the development of a repository.

The technical criteria developed by the Nuclear Regulatory Commission (NRC) for disposal of high-level radioactive wastes in geologic repositories include the general design criterion that "seals for shafts and boreholes shall be designed so that following permanent closure they do not become pathways that compromise the geologic repository's ability to meet the performance objectives . . ." (NRC, 1983, ¶60.134). SNL is currently conducting studies to determine whether shafts and boreholes can become pathways for radionuclide migration or influence radionuclide release by providing a means for water to enter the repository.

Conceptually, water or air flow through a sealed shaft could occur through three zones: 1) the seal materials placed within the original opening; 2) the interface between the seal materials and the host rock; and 3) a zone surrounding the original opening in which the permeability might be modified (i.e., increased or reduced) by the excavation process. The specific purpose of this report is to provide a model of the modified permeability zone which can be used in future analyses of the performance of the repository. These future analyses will demonstrate whether the modified permeability zone is significant with respect to performance and whether it is necessary to control the degree of disturbance around the shaft by appropriate selection of excavation methods. The technical method used for developing the modified permeability zone model is described in Section 2.0 and is based on an approach used previously for a shaft in basalt (Kelsall et al., 1982, 1984).

Elastic and elastoplastic stress analyses are presented in Section 3.0 for a range of expected underground conditions. These conditions include the range of rock mass strength and the state of in situ stress. In Section 4.0, constitutive relationships between stress on fractures and rock mass permeability are presented from theoretical considerations, laboratory investigations on single fractures in welded and nonwelded tuff, and field permeability tests on single fractures in welded tuff. Comparisons are made between field and laboratory measurements and bounds for stress permeability measurements are selected.

In Section 5.0, an evaluation of permeability changes resulting from stress relief is performed by combining the stress analysis in Section 3.0 with the constitutive relationships in Section 4.0. Analyses are conducted for depths in a shaft of 100 m and 310 m. The 100-m depth is selected to be representative of the upper part of the Topopah Spring unit, whereas 310 m is the depth

at which the Exploratory Shaft intersects the repository horizon. Analyses are conducted to represent a range of expected rock conditions at each of these depths as follows:

- A lower-bound estimate of the increase in rock mass permeability is obtained by considering an upper bound for the expected rock mass strength properties, a lower bound for the expected in situ stresses, and a lower bound for the sensitivity of permeability to stress as indicated by laboratory and field testing.
- A "likely" estimate for the increase in rock mass permeability is obtained using the expected mean values for strength and in situ stresses and the mean sensitivity of permeability to stress.
- An upper bound estimate of the increase in rock mass permeability is obtained using lower-bound strength properties, upper-bound in situ stresses, and the upper-bound sensitivity of permeability due to stress.

An evaluation of permeability changes resulting from blasting is presented in Section 6.0 by review of pertinent case histories and a prediction of the extent of blast damage using some measures to control blasting. Section 7.0 combines the results of stress-induced damage and blast-induced damage in a single modified permeability zone model over a range of different depths and conditions.

## 2.0 TECHNICAL APPROACH AND METHODS OF ANALYSES

This chapter presents the technical approach and methods of analysis for the evaluation of the modified permeability zone. Fundamental assumptions made in the analysis are presented. Consideration is given, first, toward defining the objectives of the study in terms of the expected site conditions. A discussion of potential mechanisms for modifying rock mass permeability is then presented. The final section describes the specific methodology used for developing the modified permeability zone model.

### 2.1 SITE CONDITIONS

The repository is to be developed in the Topopah Spring welded tuff unit (TSw2) at an approximate depth of 310 m. The proposed repository lies in the unsaturated zone 200 m to 400 m above the ground-water table (Fernandez et al., 1987). The repository would be accessed by a series of ramps and shafts on the northeast boundary with mains driven to the southwest.

The major shafts accessing the repository include the Exploratory Shaft (4.4 m excavated diameter) and adjacent Escape Shaft (2.4 m excavated diameter), the Men and Materials Shaft (6.9 m excavated diameter) and the Emplacement Exhaust Shaft (6.9 m excavated diameter). These shafts, as illustrated in Figure 1 will penetrate through the Tiva Canyon welded tuff, Yucca Mountain and Pah Canyon nonwelded tuff, and Topopah Spring welded tuff units. In addition, the Exploratory Shaft will penetrate to the top of the Calico Hills (CHn1) unit.

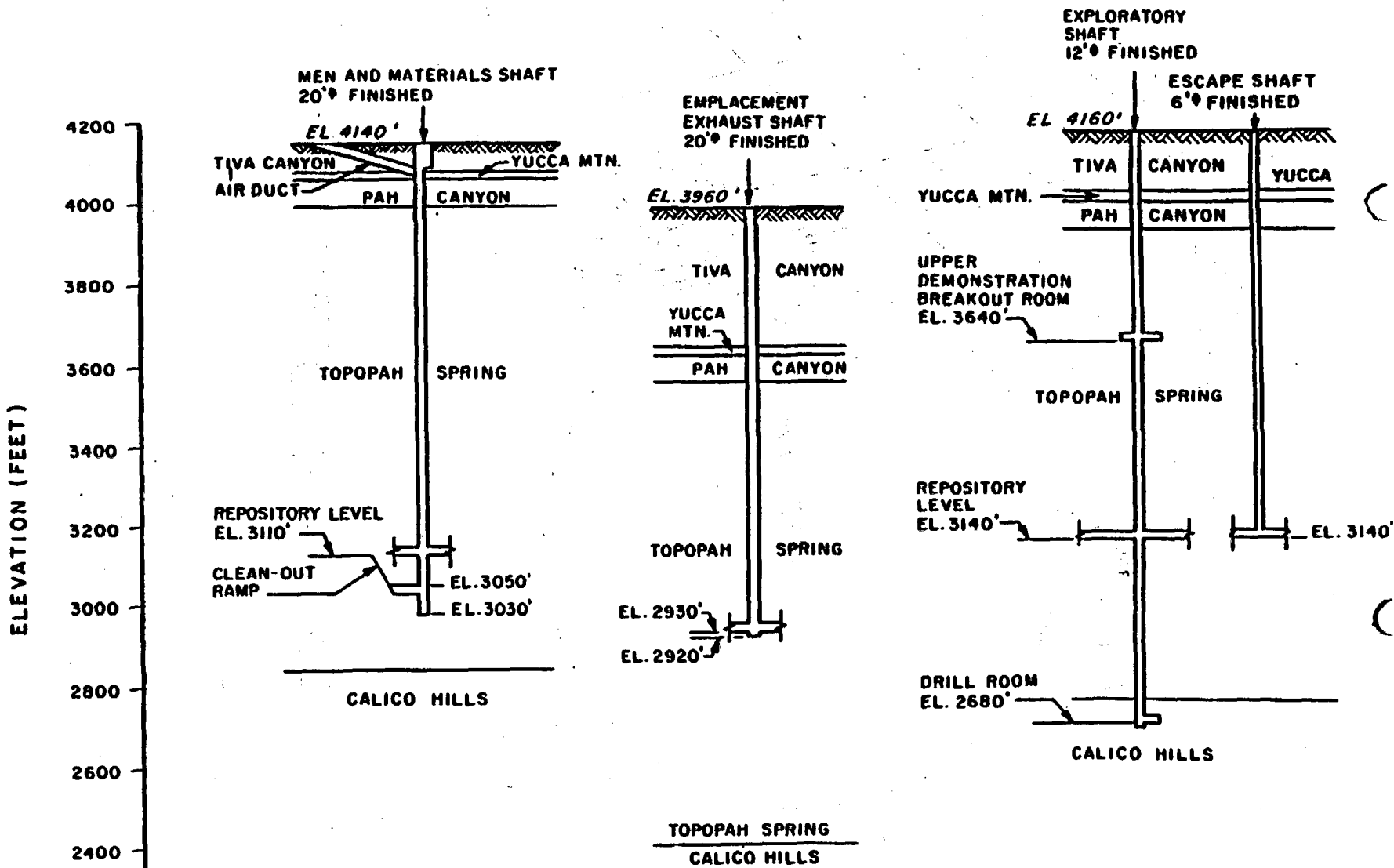
Figure 1 shows that the shafts are excavated mainly through the Topopah Spring and Tiva Canyon welded tuff units. It is thus appropriate to develop a modified permeability zone model for welded tuff. The response of the Yucca Mountain and Pah Canyon nonwelded units is less significant because their thickness is small relative to that of the welded units. The response of the Calico Hills nonwelded unit is not considered here, but may be considered in future design analyses, if necessary. It is noted that only the Exploratory Shaft will penetrate partially into the unit.

Both the Topopah Spring and Tiva Canyon welded tuffs are characterized as "densely fractured" (Sinnock et al., 1984, p. 8). Scott et al. (1983, p. 318) estimate a fracture density of 20 to 40 per unit  $m^3$ , and Langkopf and Gnirk (1986, p. 66) estimate a fracture frequency of 2 to 16 per meter corresponding to a spacing of 6 to 50 cm. Fracture orientations are evaluated by Langkopf and Gnirk (1986, p. 40-47) based on the mapping of surface exposures of Tiva Canyon, and the mapping of the welded portion of the Grouse Canyon Member in the G-tunnel complex at Rainier Mesa.

Figure 2 shows the range of fracture spacing obtained from Langkopf and Gnirk (1986) for welded tuff, drawn to scale in relation to the planned diameter of the Exploratory Shaft. The figure is intended to show that the fracture spacing is small relative to the shaft diameter. Considering a representative volume of rock adjacent to the shaft, it is to be expected that the geomechanical response to excavation will be influenced by rock mass properties (which

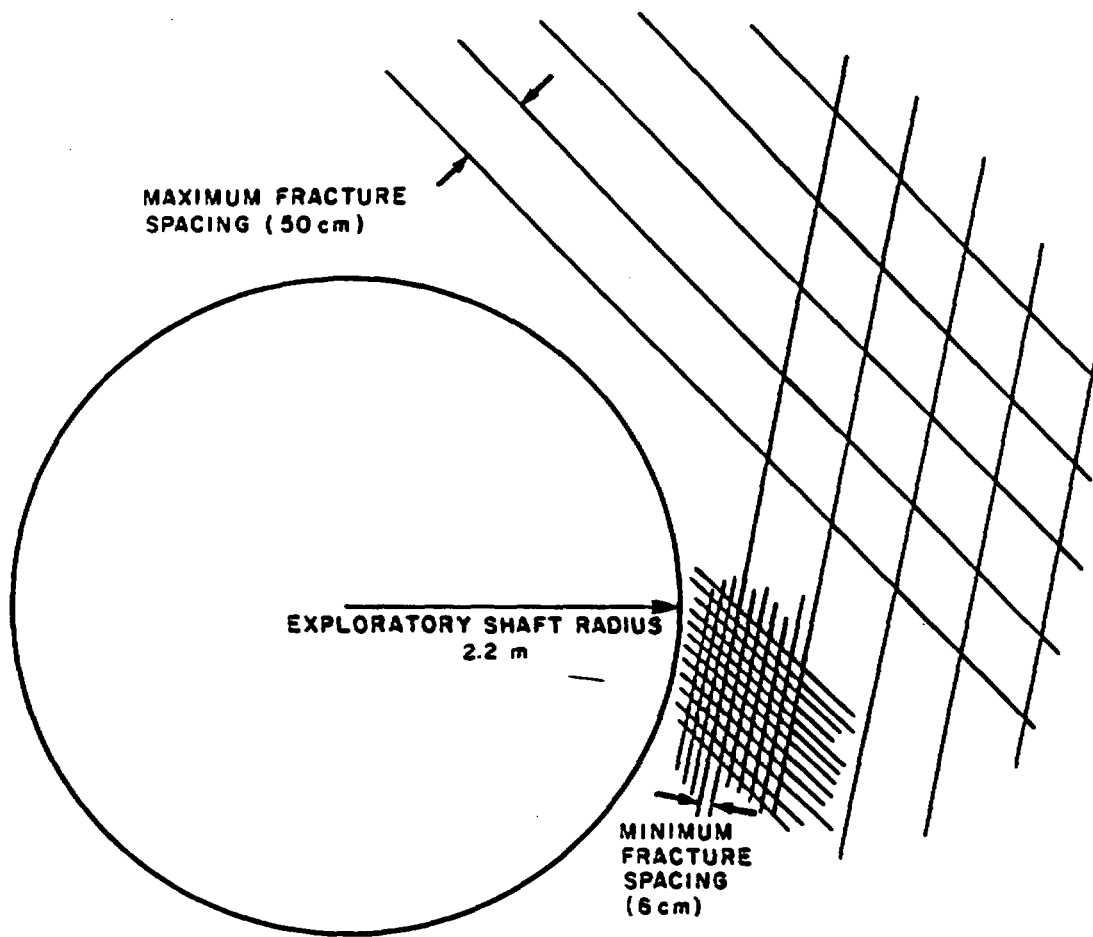
---

\* Thermal/mechanical stratigraphy nomenclature from Ortiz et al. (1985, Figure B-1).



REFERENCES: SNL DRWG. NO. R07001  
GEOLOGY ESTIMATED FROM BENTLEY (1984) AND  
SCOTT AND BONK (1984)

FIGURE 1. ELEVATIONS OF SHAFTS AND REPOSITORY IN RELATION TO STRATIGRAPHY



**NOTE: FRACTURE ORIENTATIONS SCHEMATIC**



**FIGURE 2. CROSS-SECTION THROUGH A SHAFT IN WELDED TUFF SHOWING FRACTURE SPACING RELATIVE TO SHAFT RADIUS**

take into account the effect of fractures) rather than by the properties of the intact rock. Similarly, the permeability of the rock mass will be influenced by fractures, as well as, by the rock matrix. (This discussion applies specifically to welded tuff and may be less applicable to nonwelded units in which the typical fracture spacing is 80 cm to 200 cm [Langkopf and Gnirk, 1986, p. 66].) The fracture orientations shown in Figure 2 are schematic; actual fracture patterns in welded tuff are expected to range from two sets plus random to three sets plus random (Langkopf and Gnirk, 1986, p. 48).

The potential for water flow through fractured welded tuff is governed by properties of the rock mass (i.e., intrinsic permeability) and by the degree of saturation. As described by Sinnock et al. (1984, p. 16), two types of hydraulic conductivity, matrix and fracture, are pertinent to understanding water flow through the unsaturated zone. If the ground-water flux exceeds the product of the matrix conductivity multiplied by the gradient, saturation occurs and water flows through the fractures at a rate governed by the rock mass hydraulic conductivity. For Tiva Canyon and Topopah Spring welded tuff, the rock mass hydraulic conductivity is expected to vary from  $10^{-2}$  to  $10^{-5}$  cm/s (Scott et al., 1983, p. 299). If the ground-water flux is less than the matrix conductivity times the gradient, the rock mass is not saturated, and flow will be relatively slow through the high effective porosity of the matrix at a rate limited by the hydraulic conductivity of the matrix. From Sinnock et al. (1984, p. 11), the saturated matrix hydraulic conductivity for Tiva Canyon and Topopah Spring welded tuff is 2.5 to  $3.5 \times 10^{-9}$  cm/s.

Because of the combined effects of low average rainfall and permeability and capillary barriers between stratigraphic units, the flux through most of the Topopah Spring welded tuff is probably restricted to a value equal to or less than the matrix conductivity; i.e., about 1 mm/year (Montazer and Wilson, 1984, p. 51). For these expected conditions, it would be appropriate to consider only how excavation could result in modification of the matrix conductivity. It is possible, however, that the shafts could act as preferential pathways for water flow. For example, extreme rainfall could lead to local flooding in surface washes and flood waters could be directed into the shafts (Fernandez et al., 1987). Under these conditions, local saturation could occur around a shaft, resulting in fracture flow. For these conditions, it is appropriate to consider how rock mass conductivity might be modified by excavation.

In the remainder of this report, reference is made to rock mass permeability. This term implies a property of the rock mass (i.e., intrinsic permeability) which is independent of the fluid permeant. The modified permeability zone model which is developed can be applied to water flow (in saturated conditions) or air flow (in unsaturated conditions) through fractures.

## 2.2 MECHANISMS FOR MODIFYING PERMEABILITY ADJACENT TO A SHAFT

In general terms, three processes may contribute to the formation of a modified permeability zone around an underground opening as follows:

- Stress redistribution,
- Damage (i.e., fracturing or loosening) by the excavation process, especially if blasting is used, and
- Weathering or ground-water/rock interaction.

Emphasis is placed in this report on the evaluation of the effects of mechanical disturbance around a shaft, i.e., the effects of stress redistribution and blasting due to excavation on the permeability of the rock mass surrounding the shaft. It is the authors' judgment that weathering and chemical effects of ground-water/rock interaction are relatively insignificant mechanisms for modifying permeability. Generally, it is believed that dissolution does not occur in the Topopah Spring tuff at low temperatures (USDOE, 1986, p. 6-254). This report gives no further attention to changes in permeability due to chemical processes.

As discussed in the following sections, the relative importance of stress redistribution and blast damage will depend on factors such as intact rock strength, spacing and properties of fractures in the rock mass, rock strength, in situ stress state, depth, shape of the opening and excavation method. It is noted that stress redistribution will occur around all shafts, although the manifestation will vary depending upon the same factors listed above. Hence, some degree of modification of permeability may occur around all shafts, and not only around those that are excavated by blasting.

### 2.2.1 Effects Of Stress Redistribution

It is postulated that the redistribution of stresses around an opening in tuff might affect the permeability of the rock mass in one of two ways, as follows:

- By the fracturing of originally intact rock due to excessive compressive or tensile stresses.
- By opening or closing of pre-existing fractures due to changes in the normal stresses acting across the fractures, or shear stresses along the fractures.

The potential for fracturing of intact rock is evaluated by means of a simple analysis for the case of a circular shaft excavated in a homogeneous, isotropic, and linearly elastic medium (Figure 3). At any point, the tangential stress is given by the Kirsch solution (Jaeger and Cook, 1976, p. 251) as:

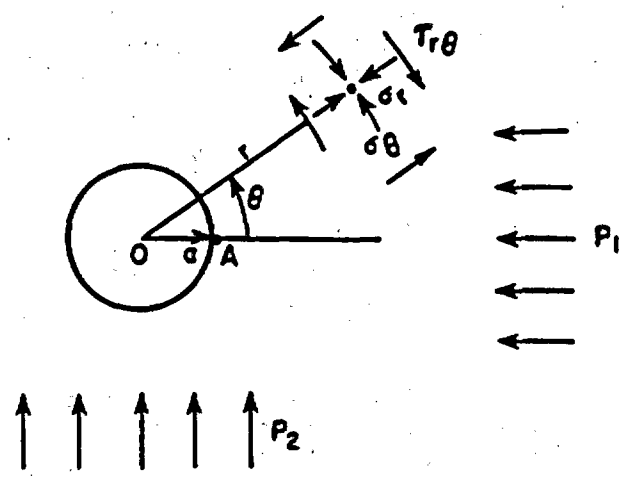
$$\sigma_{\theta} = \frac{P_1 + P_2}{2} \left(1 + \frac{a^2}{r^2}\right) - \frac{P_1 - P_2}{2} \left(1 + \frac{3a^4}{r^4}\right) \cos 2\theta \quad (2-1)$$

where

- $\sigma_{\theta}$  = tangential stress,
- $P_1, P_2$  = maximum and minimum far-field (undisturbed) in situ stresses,
- $a$  = radius of the shaft, and
- $r, \theta$  = polar coordinates (Figure 3).

For the case where  $r = a$  (i.e., considering points on the shaft wall where the maximum tangential stress will occur in an elastic medium), Equation (2-1) reduces to

$$\sigma_{\theta} = (P_1 + P_2) - 2 \cos 2\theta (P_1 - P_2). \quad (2-2)$$



*After Goodman (1980)*

**FIGURE 3. STRESS ANALYSIS FOR A CIRCULAR OPENING IN A HOMOGENEOUS, ELASTIC MEDIUM**

Bauer et al. (1985) evaluated the in situ stresses at Yucca Mountain by the finite element method, and compared the results to hydrofracturing measurements made in boreholes. The finite element method was used for evaluating gravitational effects, and indicated that the ratio of horizontal to vertical stress ( $K_0$ ) might range from 0.2 to 0.4, due to variation in topographic relief at Yucca Mountain and variations in elastic properties between welded and nonwelded units. The  $K_0$  values from hydrofracturing measurements, as reported by Bauer et al. (1985), ranged from 0.4 to 0.8, indicating that tectonic or residual stress may contribute to horizontal stress. It was suggested that a working range of  $0.3 < K_0 < 0.8$  is consistent with regional tectonics, field measurements and finite element calculations.

For a bounding calculation using Equation 2-2, the minimum horizontal stress ( $P_2$ ) is set equal to 0.25 times the vertical stress and the maximum horizontal stress ( $P_1$ ) is set equal to the vertical stress, which is calculated on the basis of the weight of overburden as

$$\sigma_v = \rho gh \quad (2-3)$$

where

$\sigma_v$  = vertical stress,  
 $\rho$  = mass density (= 2250 kg/m<sup>3</sup>, Nimick et al., 1984, p. 4)  
 $g$  = acceleration constant, and  
 $h$  = depth.

For a depth of 310 m (the depth at which the repository intersects the Exploratory Shaft), the calculated vertical stress is 6.84 MPa (about 990 psi). Substituting  $P_1 = 6.84$  MPa and  $P_2 = 0.25 \times 6.84 = 1.7$  MPa in Equation 2-2, the tangential stress around the opening is calculated as a function of the angle  $\theta$ :

| $\theta$ (deg) | tangential stress (MPa) |
|----------------|-------------------------|
| 0              | -1.72 (tension)         |
| 20             | +0.68                   |
| 40             | +6.77                   |
| 60             | +13.69                  |
| 80             | +18.20                  |
| 90             | +18.82                  |

These stresses may be compared with the strength values for Topopah Spring (TSw2) tuff given by Nimick et al. (1984, p. 2). The maximum tensile stress, as calculated, is 1.72 MPa, whereas the mean intact rock tensile strength is 16.9 MPa. The maximum compressive stress, as calculated, is 18.9 MPa, whereas the mean intact rock compressive strength is 171 MPa. These comparisons indicate that fracturing of intact rock due to stress concentrations around a shaft at 310 m depth is unlikely, even allowing for variations from the mean reported strength values.

Whereas stress redistribution around a shaft should not lead to fracturing of intact rock (which could in turn lead to increased permeability), the effects of stress changes across fractures may have a significant effect on permeability. This arises because the rock mass is densely fractured and because the permeability of fractures is sensitive to the stress applied across the fractures (Section 4.0). Conceptually, permeability should be increased where

normal stresses are reduced across fractures or shear stresses are increased, while permeability should be reduced where normal stresses are increased.

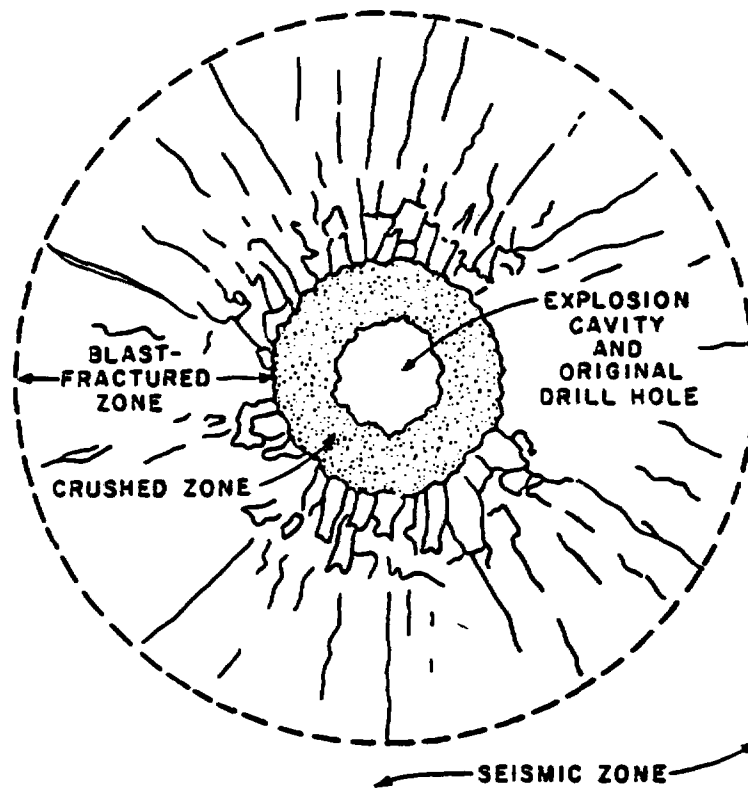
### 2.2.2 Effects of Blasting

It is currently planned that three of the four shafts at Yucca Mountain will be excavated by blasting. It is conceivable to expect that blasting may damage the remaining rock adjacent to the excavation wall by creating new cracks and extending or widening of pre-existing cracks. It is known from underground construction practice (e.g., Hoek and Brown, 1980, Chapter 10) that the visible degree of damage can be limited (if necessary) by the use of "controlled" methods such as smooth blasting.

Several investigators have described the mechanics of blasting in rock (Langefors and Kihlstrom, 1978, Chapter 1; Hoek and Brown, 1980, Chapter 10; Brady and Brown, 1985, Chapter 17). It is generally recognized that three zones form near the explosion hole (Figure 4). The first zone is comprised of a crushed annulus which is formed by intergranular cracking, the collapse of voids, differential compression of the rock matrix, and other modes of microscopic deformation. Outside this zone is the blast fractured zone where a pattern of radial cracks form. Fracturing in this zone may be due to the quasi-static gas pressure that sets up tensile tangential stresses outside the crushed annulus over a period of short duration, or by crack propagation where gas pressure actually enters the radial fractures and extends them over a period of time much longer in duration. Outside this zone is an extended seismic zone where the blast wave travels at sonic velocity characteristic of the rock and the peak particle velocity attenuates rapidly with distance. Tensile or shear failure of the rock may occur where compressive waves are reflected in part off of free surfaces (open fractures or void space) near existing fractures, and in part are refracted to the surrounding rock.

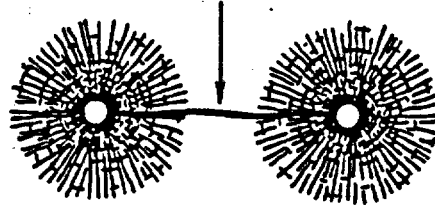
In actual rock masses, the extent and pattern of fracturing will be influenced by rock properties such as strength, anisotropy, pre-existing cracks in the rock mass and in situ stress. Cracking is also influenced by the blasting method and by the charge weight of explosives. Perimeter blasting is the process by which controlled methods are used in order to limit the number and extent of new cracks in the completed excavation. Two techniques are available for controlled perimeter blasting; these include pre-splitting and smooth blasting. Smooth blasting, which is common in tunnel and shaft excavations, involves drilling a number of closely spaced parallel boreholes along the final excavation surface, placing low-density charges in these holes, and detonating all of the perimeter charges simultaneously (by the use of milli-second delays) after the remainder of the production blastholes (i.e., those holes inside the perimeter holes) in the face have been detonated. The effect is to cause preferential crack growth along the line between the boreholes, producing a relatively smooth excavation contour. Because relatively low charge weights can be used in the perimeter holes, the damage to the rock beyond the perimeter can be limited.

Figure 5 is an idealization of the different results obtained with conventional and smooth blasting methods. As noted above, the actual results of blasting may be influenced by rock properties and blasting methods, and by how well the blasting is executed. For example, smooth blasting requires more accurate drilling of the perimeter holes. The extent of blast damage around shafts and tunnels, as indicated by case histories, is further reviewed in Section 6.0.

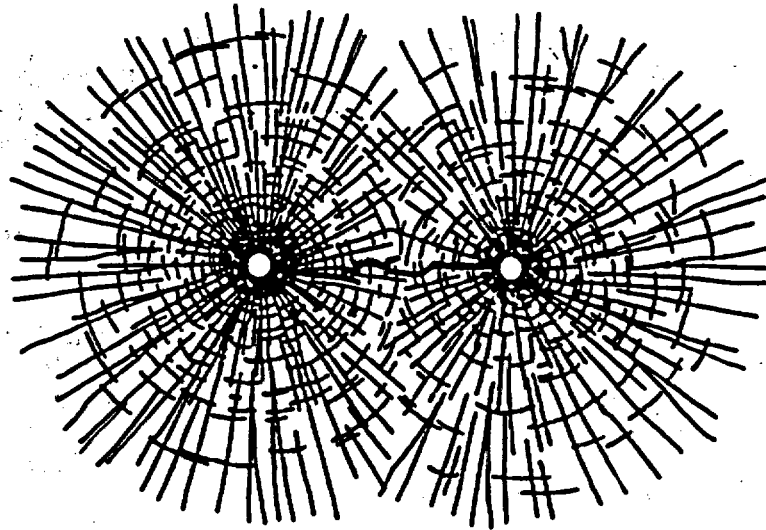


**FIGURE 4. NEAR-HOLE BLAST CRACKING (FROM DOWDING, 1985, FIGURE 15-2, AND DUPONT, 1977, FIGURE 26-A)**

MAJOR CRACK, PRODUCING SMOOTH CONTOUR



SMOOTH BLASTING  
DAMAGE ZONE 5-10 TIMES  
BOREHOLE DIAMETER



CONVENTIONAL BLASTING  
DAMAGE ZONE 15-20 TIMES  
BOREHOLE DIAMETER

*After Hocking and St. John, 1979*

**FIGURE 5. COMPARISON OF FRACTURE PATTERNS RESULTING FROM SMOOTH BLASTING AND CONVENTIONAL BLASTING**

### 2.3 METHODOLOGY FOR DEVELOPING THE MODIFIED PERMEABILITY ZONE MODEL

It is postulated that the significant mechanisms for modifying permeability in fractured, welded tuff are 1) the opening or closing of fractures in response to stress changes, and 2) creating new fractures or the opening of old fractures by blasting. The approach for developing the modified permeability zone model includes the following five steps which are described in detail in subsequent sections:

1. Calculate stress changes around a shaft by using an appropriate closed-form solution for elastic or elastoplastic analysis of a circular shaft located in a uniform stress field (Section 3.0).
2. Obtain relationships from published laboratory and field testing results which describe the effects of stress on the permeability of single fractures and fractured rock (Section 4.0).
3. Calculate rock mass permeability as a function of radius away from the shaft based on the calculated stresses and the stress-permeability relationships obtained from testing (Section 5.0).
4. Estimate permeability changes due to blasting from evaluation of case histories which indicate the depth of damage and estimate the probable increase in fracture frequency in the damaged zone (Section 6.0).
5. Combine the results derived from performing steps 3 and 4 to obtain the combined effects of stress redistribution and blasting (Section 7.0).

In order to perform the analysis, it is necessary to consider a simplified representation of the fracture system and the stress regime in the rock mass, as described below. The discussion and subsequent analysis refer mostly to Topopah Spring tuff; but they are also representative of Tiva Canyon tuff, which has similar hydrologic and mechanical properties (Scott et al., 1983, p. 300; Sinnock et al., 1984, p. 12).

It has been noted (Section 2.1) that the Topopah Spring welded tuff is densely fractured and that several fracture sets (i.e., with different orientations) are present. Prior to excavation, each fracture is subjected to normal and shear stress, depending on its orientation relative to the direction of the principal in situ stresses. After excavation, these stresses will change in the zone adjacent to the excavation; depending on such factors as the shape and proximity of the opening, in situ stress state, rock mass strength, and the orientation of a fracture, the stresses across an individual fracture could be reduced or increased (see Section 3.1). In the interest of simplification, three assumptions form the basis for modified permeability zone analysis, as follows:

1. Prior to excavation, the in situ stress state is isotropic and the normal stress acting across each fracture is equal to the average far-field value.

2. Stresses existing around the opening after excavation are calculated by using closed-form solutions as normal principal stresses acting in the radial and tangential (or hoop) directions; shear stresses are ignored.
3. The stress acting across each fracture after excavation is the calculated radial stress at the appropriate location relative to the shaft wall. (Note that the radial stress is always less than the tangential stress in an isotropic stress field.)

These assumptions are conservative for the isotropic state of stress (i.e., they tend to over-predict increases in permeability) in that stress increases across some fractures are ignored and each fracture is, in effect, assumed to be perpendicular to the direction of maximum stress relief. Conversely, the simplified analysis does not account for the effects of shearing along fractures. On balance, it is the authors' judgment that the model is a reasonable representation of permeability changes in fractured welded tuff.

It should be noted that the actual spacings, orientations and continuity of fractures in the rock mass need not be considered, because the model predicts the change in rock mass permeability relative to the undisturbed case. As a result of the assumptions described above, the modified permeability zone will extend equally in all directions around a circular shaft (assuming an isotropic stress field). If one or two fracture sets are, in fact, dominant in the rock mass, the extent of the zone in which permeability is increased will be greater where fractures are oriented, approximately, tangential to the shaft wall (Kelsall, 1982, p. 41-42).

### 3.0 STRESS ANALYSIS FOR A SHAFT IN WELDED TUFF

The first stage in developing the modified permeability zone model involves calculating the stress distribution around a shaft excavated in welded tuff. The calculated stresses will be used in Section 5.0 to estimate changes in rock mass permeability.

#### 3.1 GENERAL DESCRIPTION OF ROCK MASS RESPONSE TO SHAFT EXCAVATION

When a shaft is excavated, there is a redistribution of the original in situ stresses around the opening. The nature of this redistribution depends upon the original in situ stresses (as affected by depth), on the shape of the opening, and on rock strength and deformability properties. Relatively strong and stiff rocks, when confined at shallow depths, in general behave essentially elastically whereby deformations are theoretically reversible and produce no failure. At greater depths, the same rock might respond with proportionately greater deformation due to slippage along fractures. In this case also, there is no significant failure of intact rock material, but deformations in the plastic zone adjacent to the opening may be nonreversible. The extent of the plastic zone depends upon the rock mass strength and the in situ state of stress. At progressively greater depths, the in situ stress is generally larger and the plastic zone extends further from the shaft if rock mass strength is uniform with depth. However, in a layered stratigraphy, as discussed subsequently in this report, the type and extent of disturbance might vary from one layer to another, with greater disturbance observed in weaker materials.

The distinction between the elastic and plastic zones around an underground opening is important with respect to stress distributions and the resultant effects on fracture permeability. In the case of elastic deformations adjacent to an opening, the radial stress is reduced to zero at the shaft or tunnel wall, whereas the tangential stress is increased relative to the undisturbed or far-field value. In this case, it is expected that the permeability of fractures tangential to the opening (perpendicular to the radial stress) should be increased, whereas the permeability of radial fractures should be reduced. In the case of plastic deformations adjacent to an opening, both the radial and tangential stresses are reduced close to the wall in the plastic zone so that the permeability of both tangential and radial fractures should be increased.

#### 3.2 ROCK MASS STRENGTH

Rigorous analysis of stress changes and deformation in a jointed rock mass requires consideration of the strength of the rock mass, as affected by discontinuities as well as by intact rock. Rock mass strength has not been measured directly in welded tuff and comparative methods are required for obtaining estimates. According to Bieniawski (1984, p. 81) two methods seem to be particularly promising, those proposed by Hoek and Brown (1980) and Protodyakonov (1964). Both of these approaches are used in Appendix A to obtain rock mass strength parameters for welded tuff (with emphasis placed on the method proposed by Hoek and Brown). The remainder of this section presents a summary of the Hoek and Brown method and its results.

Hoek and Brown's (1980, p. 175) criterion for the strength of discontinuous rock masses is expressed as

$$\frac{\sigma_1}{\sigma_u} = \frac{\sigma_3}{\sigma_u} + \sqrt{m \frac{\sigma_3}{\sigma_u} + s}, \quad (3-1)$$

where

$\sigma_u$  = unconfined compressive strength of intact rock,  
 $m, s$  = rock mass strength constants dependent upon rock quality, and  
 $\sigma_1, \sigma_3$  = major and minor principal stresses at failure.

Hoek and Brown (1980, pp. 133-182) provide a detailed discussion of the factors that influence rock mass strength, and provide methods for estimating the  $m$  and  $s$  constants from laboratory testing and field investigations. The laboratory testing includes performing triaxial compression tests on samples of intact rock over the range of confining pressures expected in the field. The field investigations include rock mass classification, either by the Geomechanics Classification System (RMR System, Bieniawski, 1984, p. 112) or the Q System (Barton et al., 1974; p. 189).

Rock mass failure envelopes are presented in Figures 6 and 7 for the Topopah Spring nonlithophysal welded unit (TSw2) and the Calico Hills unit (CHn1). These envelopes are derived from Equation 3-1 and data presented in Table 1. The rock mass strength constants are derived from the RMR as described in detail in Appendix A and as summarized in this table. The three envelopes in Figure 6 for the Topopah Spring tuff include the following cases:

Case 1: An upper bound estimate corresponding to the upper bound RMR (84) and the mean unconfined compressive strength plus one standard deviation.

Case 2: An expected estimate corresponding to the mean RMR (65) and the mean unconfined compressive strength.

Case 3: A lower bound estimate corresponding to the lower bound RMR (48) and the mean unconfined compressive strength minus one standard deviation (110 MPa).

The two envelopes in Figure 7 for the Calico Hills tuff include the following cases:

Case 4: An upper bound estimate corresponding to the upper bound RMR (71) and the mean unconfined compressive strength plus one standard deviation (36 MPa).

Case 5: A lower bound estimate corresponding to the lower bound RMR (49) and the mean unconfined compressive strength minus one standard deviation (18 MPa).

The range of failure strength or maximum principal stress at failure under confining stress is from the lower bound envelope to the upper bound envelope as shown in the figures. The magnitude of the range of failure strength increases with increased confining pressure for welded and nonwelded tuff. For comparison, failure envelopes based upon data from Nimick et al. (1984, p. 4) are shown for welded tuff (TSw1 and TSw2) and nonwelded tuff (PTn) in Figures 6 and 7 respectively.

**TABLE 1**  
**PROPERTIES OF WELDED AND NONWELDED TUFF USED IN STRESS ANALYSES**

| UNIT                     | ESTIMATE | ROCK MASS (a)<br>CLASSIFICATION | RMR(a) | UNCONFINED<br>COMPRESSIVE<br>STRENGTH (MPa)(b) | $m$ (c) | $s$ (c)               |
|--------------------------|----------|---------------------------------|--------|--|---------|-----------------------|
| Topopah Spring<br>(TSw2) | High     | I, Very Good                    | 84     | 230  | 6.0     | 0.079                 |
|                          | Expected | II, Good                        | 65     | 171  | 1.4     | $3.9 \times 10^{-3}$  |
|                          | Low      | III, Fair                       | 48     | 110  | 0.084   | $2.60 \times 10^{-4}$ |
| Calico Hills<br>(Chn1)   | High     | II, Good                        | 71     | 36   | 0.78    | 0.01                  |
|                          | Low      | III, Fair                       | 49     | 18   | 0.046   | $3.0 \times 10^{-4}$  |

(a) Classification and rock mass rating are presented by Langkopf and Gnirk (1986, p. 90).

(b) Mean values for compressive strength from Nimick et al. (1984, p. 2). The ranges of unconfined compressive strength ( $\pm 1S.D.$ ) for intact rock are obtained from Table 2-7 of the SCP (Sandia National Laboratories, 1985).

(c) See Section 3.2 and Appendix A for definition and method of computing  $m$  and  $s$  constants.

MAJOR PRINCIPAL STRESS  
AT FAILURE ( $\sigma_1$  MPa)

RANGE OF UNCONFINED  
ROCK MASS STRENGTH  
BY PROTOYAKONOV METHOD  
WELDED

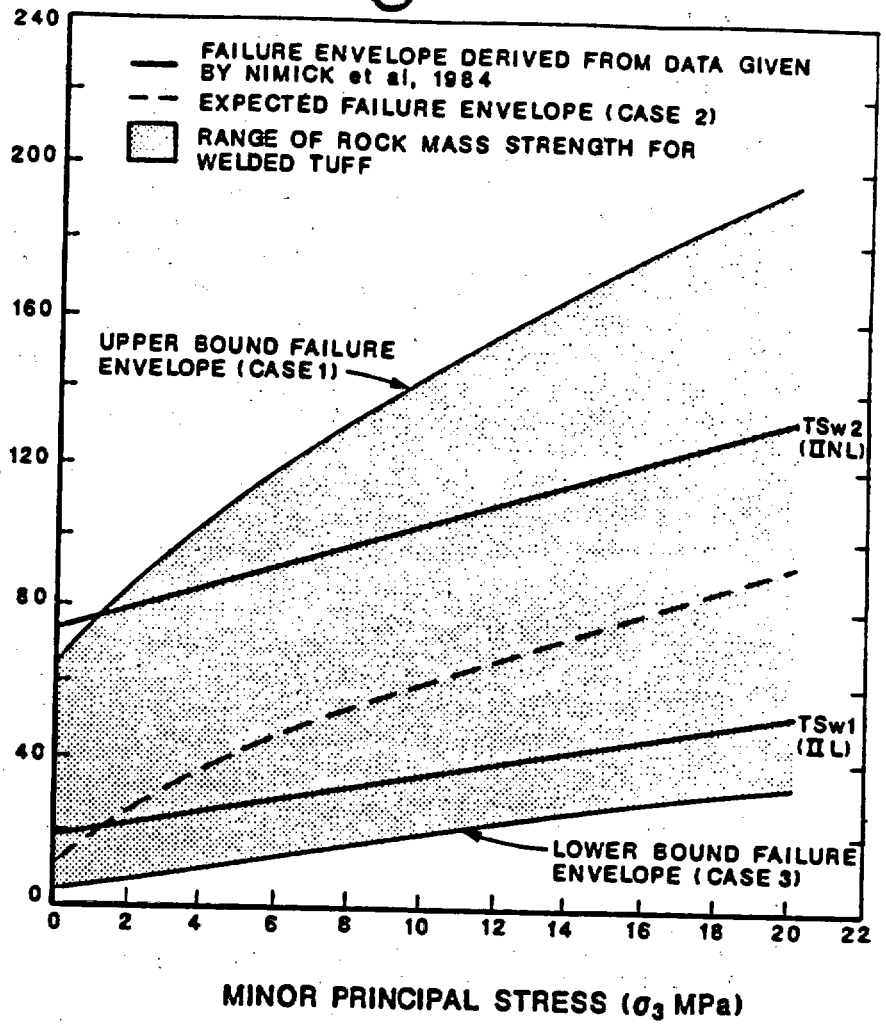


FIGURE 6. ROCK MASS FAILURE ENVELOPES FOR WELDED TUFF

MAJOR PRINCIPAL STRESS  
AT FAILURE ( $\sigma_1$  MPa)

RANGE OF UNCONFINED  
ROCK MASS STRENGTH  
BY PROTOYAKONOV METHOD  
NON-WELDED

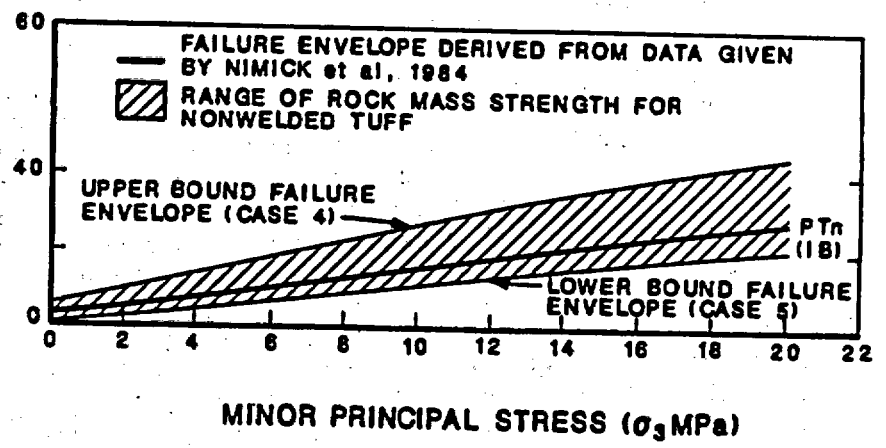


FIGURE 7. ROCK MASS FAILURE ENVELOPES FOR NONWELDED TUFF

The data in Table 1 and the failure envelopes in Figure 6 refer to peak rock mass strength, which is the maximum stress at failure that the rock can sustain under given conditions. After its peak strength has been exceeded, a rock mass may still be able to sustain load; after significant strain, this load capacity may reduce to a minimum, known as the residual strength (Brady and Brown, 1985, p. 87). Determination of the extent of the plastic or inelastic zone and the stress distributions within the inelastic zone requires estimates of residual strength, as well as peak rock strength properties. Barton et al. (1985, pp. 127-128) have performed modeling studies of the stress-displacement relationships for welded tuff. These studies indicate that there is little difference between peak and residual shearing stress at confining stresses less than 10 MPa. In contrast, the estimated rock mass strength relationships in Figure 6 shows a wide variation in peak strength due to rock mass quality. For purposes of analysis, it is assumed that residual rock mass strength is equal to peak rock mass strength, and that evaluation of the upper and lower estimates of peak rock mass strength shown in Figure 6 provides a reasonable bound to differences in peak and residual strength.

### 3.3 ROCK MASS DEFORMABILITY

The rock mass deformability, or modulus, is used for calculating displacements at the shaft wall. These displacements are not used for determining changes in permeability, but are useful for comparing plastic and elastic behavior. When the shaft is excavated, the measured displacements can be compared against the calculated values to provide an indication of whether inelastic deformations are occurring. Nimick et al. (1984, p. 4) report that the rock mass modulus of deformation for welded tuff (TSw2) is estimated to be 15.1 GPa.

### 3.4 IN SITU STRESS

Under perfect confinement, where no horizontal displacement occurs, the ratio of horizontal to vertical stress is given by (Jaeger and Cook, 1976, p. 369)

$$K_0 = \frac{\nu}{1 - \nu} \quad (3-2)$$

where

$K_0$  = ratio of horizontal to vertical stress, and  
 $\nu$  = Poisson's ratio.

Considering a rock mass Poisson's ratio of 0.2 (Nimick et al., 1984, p. 4), the value of  $K_0$  is 0.25.

As reported in Section 2.2.1 there is evidence from field and analytical studies that the  $K_0$  ratio at Yucca Mountain may be higher than 0.25. To cover a range of conditions which may occur at depth, the analyses in this report consider both an upper and lower bound estimate for the far-field horizontal stress. For an upper bound estimate, the far-field horizontal stress is set equal to the vertical stress. For a lower bound estimate, the far-field horizontal stress is set equal to 0.25 times the vertical stress. In both cases, the horizontal stresses are assumed to be equal in all directions, and the vertical stress is calculated on the basis of the weight of overburden, by using Equation 2-3. The weight of the overlying strata is calculated using the weight density of the Topopah Spring, i.e., 2250 kg/m<sup>3</sup> (Nimick et al., 1984, p. 4). Because the nonwelded tuff and alluvium above the Topopah Spring unit exhibit a lower density, the effect of using the above relation is to slightly overestimate vertical stress at depth.

### 3.5 ELASTIC ANALYSIS

Analysis of stresses and displacements within the elastic zone is based upon the Kirsch solution (Jaeger and Cook, 1976, p. 251). For an elastic material that is unsupported, the solution is

$$\sigma_r = p (1 - a^2/r^2), \text{ and} \quad (3-3)$$

$$\sigma_\theta = p (1 + a^2/r^2) \quad (3-4)$$

where

$r$  = radius at point of stress calculation,  
 $a$  = radius of shaft,  
 $\sigma_r$  = radial stress,  
 $\sigma_\theta$  = tangential stress, and  
 $p$  = far-field hydrostatic stress.

In this analysis, the far-field hydrostatic stress is the isotropic horizontal stress, calculated as described in Section 3.4. The solution predicts that the radial stress at the shaft is equal to zero. The tangential stress at the shaft is twice the far-field hydrostatic stress. These equations are used for elastic analysis of stress distribution around a shaft. If the tangential boundary stress ( $\sigma_\theta$ ) exceeds the unconfined compressive strength of the rock mass ( $\sigma_u$ ), failure is predicted and elastoplastic analysis is applicable.

### 3.6 ELASTOPLASTIC ANALYSIS

Hoek and Brown (1980, p. 250) present an elastoplastic solution based upon the failure criterion in Equation 3-1 for the ultimate and residual strength of the rock mass. Hoek and Brown express the elastic stresses as

$$\sigma_r = p - (p - \sigma_{re}) (r_e/r)^2, \text{ and} \quad (3-5)$$

$$\sigma_\theta = p + (p - \sigma_{re}) (r_e/r)^2, \quad (3-6)$$

where

$r_e$  = radius to the elastoplastic boundary,  
 $\sigma_{re}$  = constant, and  
 $p$  = far-field stress.

The radius  $r_e$  represents the extent of plastic deformation and is calculated as follows:

$$r_e = a \exp \left[ N - 2/m_r / \sigma_u (m_r \sigma_u p_1 + s_r \sigma_u^2)^{\frac{1}{2}} \right], \quad (3-7)$$

where

$N = [2/(m_r \sigma_u)] \{ (m_r \sigma_u p + s_r \sigma_u^2 - m_r \sigma_u^2 M)^{\frac{1}{2}} \}$ ,  
 $m_r, s_r$  = residual strength parameters (note that in this analysis, the residual strength properties ( $m_r, s_r$ ) are equal to the peak strength properties ( $m, s$ ), as discussed in Section 3.2),  
 $\sigma_u$  = unconfined compressive strength,  
 $p_1$  = internal support stress, and  
 $M = \frac{1}{2} \left[ (m/4)^2 + mp/\sigma_u + s \right]^{\frac{1}{2}} - (m/8)$ .

The constant  $\sigma_{re}$  is given by

$$\sigma_{re} = p - M\sigma_u. \quad (3-8)$$

The radial and tangential stresses in the plastic zone, where the rock mass exhibits residual (in the present case, peak) strength, are given by

$$\sigma_r = (m_r \sigma_u / 4) [\ln(r/a)]^2 + [\ln(r/a) (m_r \sigma_u p_i + s_r \sigma_u^2)^{\frac{1}{2}}] + p_i, \text{ and} \quad (3-9)$$

$$\sigma_\theta = \sigma_r + (m_r \sigma_u \sigma_r + s_r \sigma_u^2)^{\frac{1}{2}}. \quad (3-10)$$

The displacement analysis that follows assumes that the stress distribution and radius  $r_e$  to the elastoplastic boundary are determined according to the relations presented above. Let  $e_{av}$  be the average plastic volumetric strain associated with the passage from the original state to the failed state. By comparing volumes (per unit length of shaft) of the plastic zone before and after failure, the following expression is obtained

$$\pi (r_e^2 - r^2) = \pi [(r_e + u_e)^2 - (r + u)^2] (1 - e_{av}) \quad (3-11)$$

where

- $r_e$  = radius to elastoplastic boundary,
- $u_e$  = displacement at elastoplastic boundary,
- $r$  = radius,
- $u$  = displacement at radius  $r$ ,
- $e_{av}$  = average volumetric plastic strain, (see Hoek, and Brown, 1980, pp. 251-252).

The value of  $u_e$  is determined by the following formula:

$$u_e = \frac{(1 + \nu)}{E} (p - \sigma_{re}) M\sigma_u r_e,$$

$E$  = rock mass deformation modulus,

$\nu$  = rock mass Poisson's ratio, and all other parameters are as previously defined.

Equation 3-11 is a quadratic equation in which  $u$  can be solved. The elastic displacement ( $u_e$ ) is readily determined at the elastoplastic boundary by substituting elastic stresses into the equation presented above. The displacement in the plastic zone becomes

$$u = \frac{[-2a + \sqrt{(2a)^2 - 4Ta}]}{2}, \quad (3-12)$$

where

$$T = a \left( \frac{-e_{av}}{1 - e_{av}} \right) + \frac{r_e^2}{a} \left( \frac{e_{av}}{1 - e_{av}} \right) - 2 \left( \frac{r_e}{a} \right) u_e - \frac{u_e^2}{a}. \quad (3-13)$$

The relationship in Equation 3-8 has been used for predicting the development of an inelastic or plastic zone in welded and nonwelded tuff near a shaft. Table 2 summarizes the input parameters used in the analyses for welded tuff and indicates whether the rock mass response was entirely elastic or partly plastic. In these analyses the range of intact rock compressive strength is plus and minus one standard deviation of the mean value of 171 MPa for TSW2

**TABLE 2**  
**RESULTS OF ELASTOPLASTIC STRESS ANALYSES FOR WELDED TUFF**

| ANALYSIS | DEPTH (m) | $\sigma_h/\sigma_v$ | $\sigma_u$ (MPa) | RMR | RESPONSE        |
|----------|-----------|---------------------|------------------|-----|-----------------|
| 1        | 100       | 0.25                | 230              | 84  | Elastic         |
| 2(a)     | 100       | 0.6                 | 171              | 65  | Elastic         |
| 3        | 100       | 1.0                 | 110              | 48  | Plastic/Elastic |
| 4        | 310       | 0.25                | 230              | 84  | Elastic         |
| 5(a)     | 310       | 0.6                 | 171              | 65  | Elastic         |
| 6        | 310       | 1.0                 | 110              | 48  | Plastic/Elastic |

$\sigma_h$  = Horizontal in situ stress

$\sigma_v$  = Vertical in situ stress (assumed equal to the weight of overburden.)

$\sigma_u$  = Unconfined compressive strength of intact rock

RMR = Rock mass rating

(a) These analyses correspond with expected strength properties and level of insitu stress.

tuff, as reported by Nimick et al. (1984, p. 2). The standard deviation is obtained from Table 2-7 of the draft Site Characterization Report (Sandia, 1985). The range of RMR is that quoted by Langkopf and Gnirk (1986, p. 90) for Topopah Spring tuff.

It can be seen that the analyses predict a completely elastic response for both expected properties (analyses 2 and 5) and upper bound properties (analyses 1 and 4). With the combination of lower bound properties and higher in situ stress, however, plastic behavior is observed at the 100 m depth, as well as at 310 m. The stress distributions obtained from these analyses (analyses 3 and 6) are illustrated in Figure 8. For a depth of 310 m in an unsupported shaft, the plastic zone might extend out three to four radii when a high horizontal to vertical stress ratio (1.0) is considered. Figure 9 shows the extent of the plastic zone as a function of depth through the several welded and nonwelded tuff units.

The induced displacements under high horizontal stress ( $\sigma_H = \sigma_V$ ) at the repository level in the Topopah Spring unit (TSw2) are shown in Figure 10. The elastic solution corresponds to the high estimate of rock mass strength properties, whereas the elastoplastic solution corresponds to the low estimate of rock mass strength properties. The figure indicates that the peak displacement for the plastic case is, approximately, one order of magnitude higher than the peak displacement in the elastic case. The form of these curves is similar to that observed in large cavities at the Nevada Test Site, as presented by Cording et al. (1971).

The results indicate that a wide variation in rock mass behavior might be observed depending on depth, in situ stress and rock properties. Because rock strength may vary with depth (due to variations in porosity and fracture spacing) the rock mass behavior may vary even within a lithologic unit. For the welded units, the expected response is elastic in nonlithophysal zones, but plastic response may occur in lithophysal zones or in intensely fractured zones where strength is lower. Plastic behavior is expected for the nonwelded Calico Hills tuff near the base of the shaft because of the low strength (which is similar to the lower bound for welded tuff as shown in Figure 6). For the nonwelded Paintbrush unit overlying the Topopah Spring the behavior may be elastic or plastic depending on rock mass strength and in situ stresses. Formation of a plastic zone may be limited, however, if the shaft liner is placed as quickly as possible after excavation. The effects of rock support in limiting inelastic deformation have not been considered in the analyses in this report.

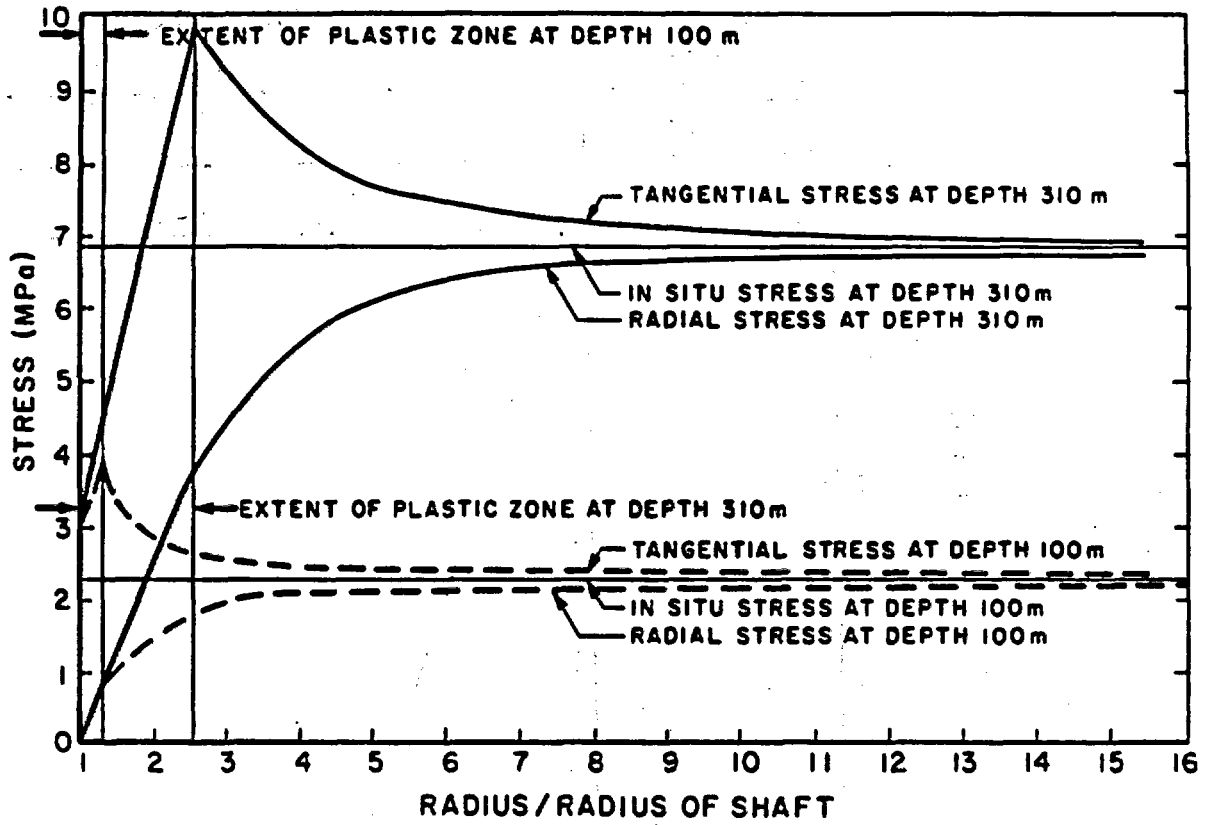
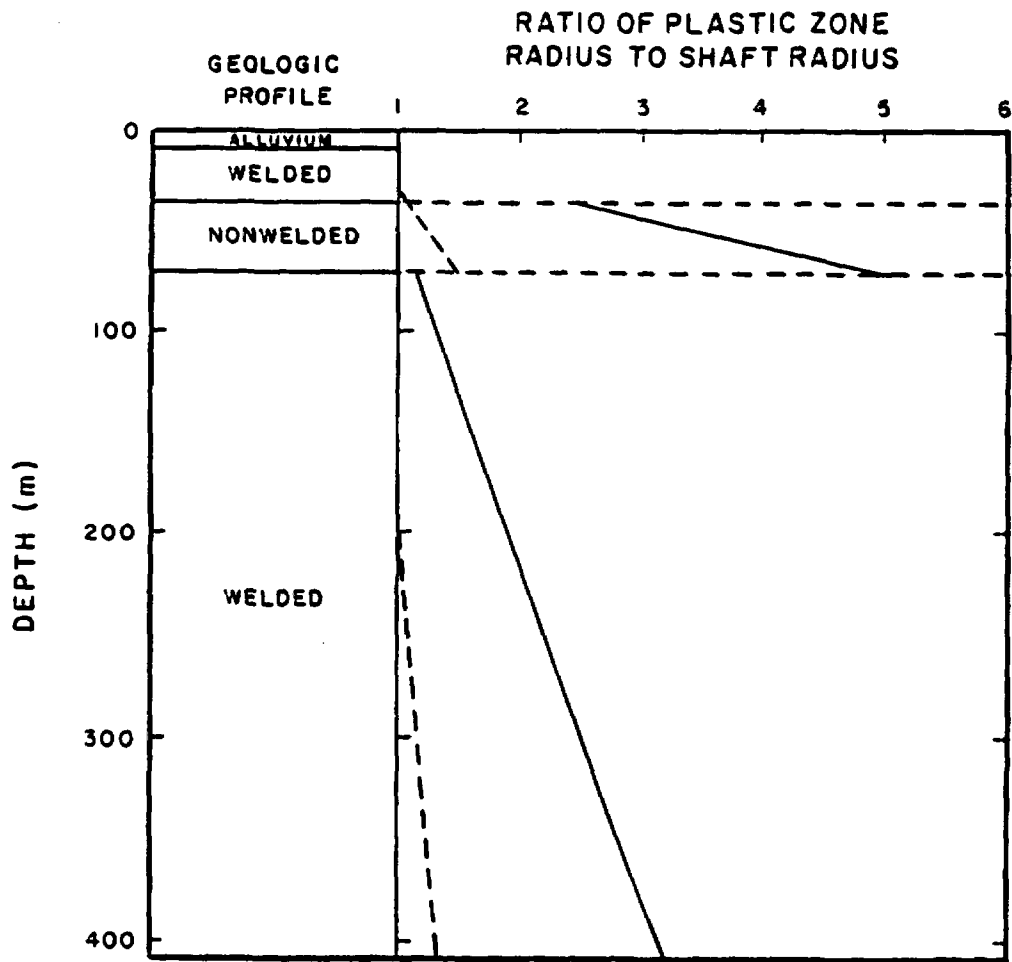


FIGURE 8. DEVELOPMENT OF A PLASTIC ZONE IN WELDED TUFF FOR ASSUMPTIONS OF LOWER BOUND STRENGTH AND UPPER BOUND IN SITU STRESS



**LEGEND**

- LOW HORIZONTAL STRESS
- HIGH HORIZONTAL STRESS

NOTE: GEOLOGIC PROFILE IS BASED UPON INTERPRETATION OF EXPLORATORY HOLE G-4. (BENTLEY, 1984)

**FIGURE 9. EXTENT OF THE PLASTIC ZONE AS A FUNCTION OF DEPTH FOR LOW STRENGTH TUFF**

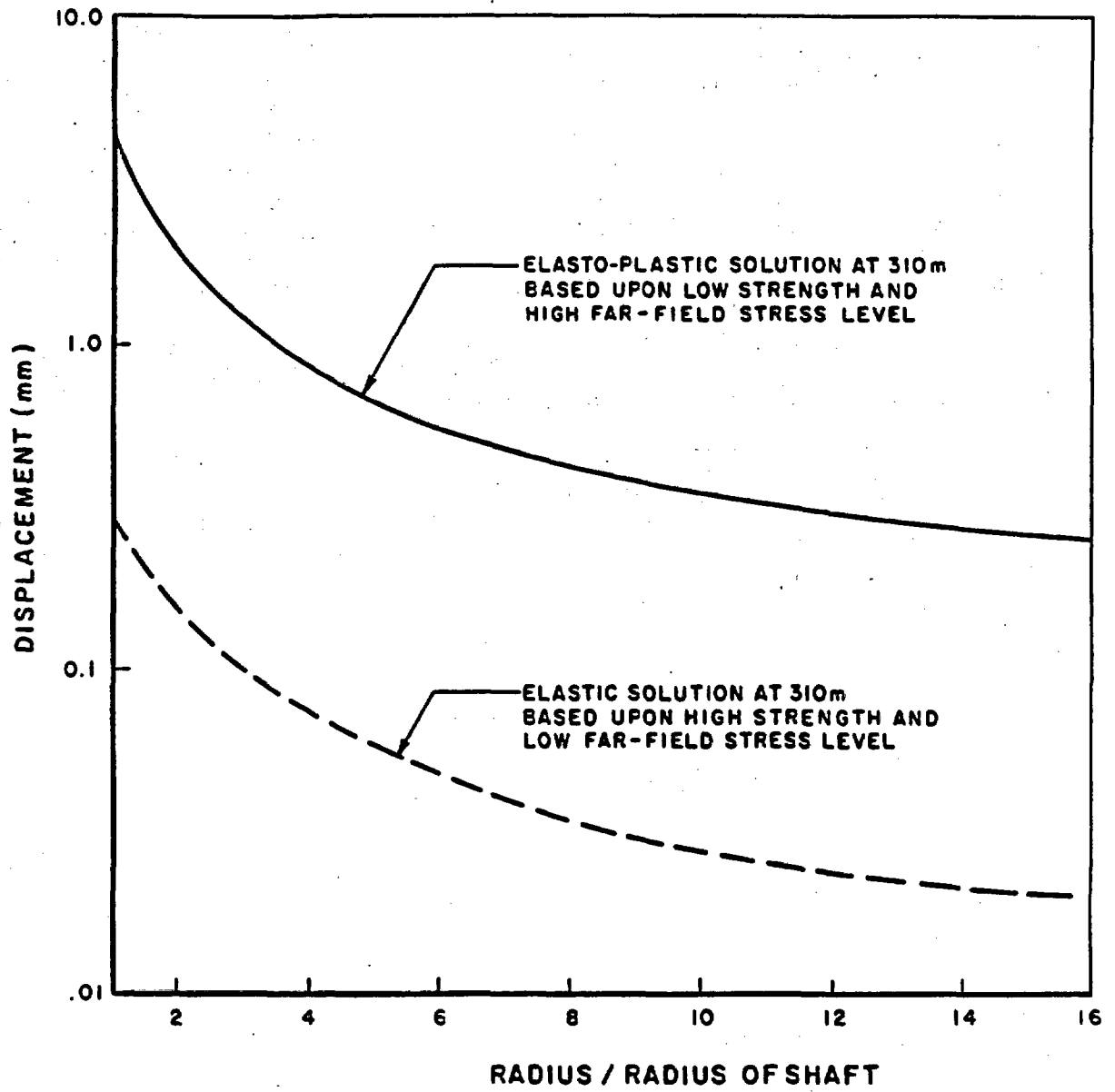


FIGURE 10. COMPARISON OF RADIAL DISPLACEMENTS (ELASTIC AND ELASTOPLASTIC SOLUTIONS) AT 310 m DEPTH

#### 4.0 CONSTITUTIVE RELATIONSHIPS BETWEEN STRESS ON FRACTURES AND ROCK MASS PERMEABILITY

The technical approach used for predicting changes in rock mass permeability around an underground opening requires knowledge of the relationship between permeability and stress. Ideally, this relationship would be obtained from large-scale field tests in which rock mass permeability would be measured as a function of changing stress levels. Because no such field tests have been performed and such tests might be impractical, it is necessary to use measurements made in the laboratory or field on single fractures and extrapolate for determining the effects of stress on rock mass permeability. Section 4.1, below, presents a discussion of the theoretical basis for this extrapolation. Data obtained from laboratory and field tests on single fractures are then reviewed in Sections 4.2 and 4.3 respectively. Finally in this chapter, stress-permeability relationships for single fractures obtained from testing are compared and used for obtaining upper and lower bounds on the expected stress-permeability relationship for the rock mass.

##### 4.1 THEORETICAL BASIS FOR OBTAINING A ROCK MASS STRESS-PERMEABILITY RELATIONSHIP FROM TESTS ON SINGLE FRACTURES

The hydraulic conductivity of a single fracture may be related to the equivalent smooth-wall fracture aperture by the following relationship (Witherspoon et al., 1980, p. 1,016):

$$K = \frac{gb^2}{12\nu}, \quad (4-1)$$

where

K = fracture hydraulic conductivity,  
g = gravitational acceleration.  
b = smooth-wall aperture, and  
ν = kinematic viscosity.

From Freeze and Cherry (1979, p. 27), the intrinsic permeability is related to the hydraulic conductivity by the relation

$$K = \frac{k\rho g}{\mu}, \quad (4-2)$$

where

k = intrinsic permeability,  
ρ = density, and  
μ = dynamic viscosity.

Equation (4-1) can now be rewritten in terms of the intrinsic permeability,  $k_f$ , of a single fracture

$$k_f = \frac{b^2}{12}. \quad (4-3)$$

From Freeze and Cherry (1979, p. 74), the intrinsic rock mass permeability,  $k_m$ , in the direction of a parallel array of fractures is given by:

$$k_m = \frac{Nb^3}{12}, \quad (4-4)$$

where

$N$  = fracture frequency (i.e., fractures per unit distance perpendicular to the orientation).

It can be seen from Equations (4-3) and (4-4) that the permeability of both a single fracture and a rock mass can be related to the fracture aperture. If the fracture aperture is measured from a test on a single fracture, the rock mass permeability in the direction of a parallel array of fractures with similar apertures can be calculated, providing that the fracture frequency is known. Similarly, if the aperture is measured over a range of stress, the change in rock mass permeability over the same range of stress can be calculated by substituting in Equation (4-4)

$$\frac{k_{m1}}{k_{m2}} = \frac{b_1^3}{b_2^3} = \left(\frac{b_1}{b_2}\right)^3, \quad (4-5)$$

where

$k_{m1}$  = rock mass permeability with effective stress  $\sigma_1$  acting across the fractures,  
 $k_{m2}$  = rock mass permeability with effective stress  $\sigma_2$  acting across the fractures,  
 $b_1$  = smooth-wall aperture at effective stress  $\sigma_1$ , and  
 $b_2$  = smooth-wall aperture at effective stress  $\sigma_2$ .

It will be noted that the change in rock mass permeability is independent of the fracture frequency, given the assumption that the frequency does not change in response to stress changes.

The basis for calculating fracture aperture from flow tests on single fractures and termed the "cubic law" (Witherspoon et al., 1980, p. 1,016) is the equation

$$\frac{Q}{\Delta h} = Cb^3, \quad (4-6)$$

where

$Q$  = flow rate,  
 $\Delta h$  = head difference,  
 $b$  = equivalent smooth-wall fracture aperture, and  
 $C$  = constant related to the geometry of the flow regime, and the properties of the fluid.

The validity of the cubic law to natural, nonplanar fractures is the subject of much continuing research. This research has included laboratory testing, field testing of jointed blocks, and phenomenological modeling. Recent reviews of the subject are given by Witherspoon et al. (1980) and Witherspoon (1981). Generally, this work has suggested that the cubic law is valid providing that it is based on a real aperture, which takes into account the roughness and tortuosity of the fracture. The permeability-stress relation is then determined by a number of factors which influence the fracture stiffness, including fracture roughness, fracture wall compressive strength, and the initial aperture. It follows that the relationship will differ according to the rock type, roughness and weathering of the fracture surface, and any fillings that are present. The relationship may also depend on the stress

history of the fracture, and on whether displacements are purely normal or whether shearing occurs. There may be a scale effect, also, related to the fracture roughness.

It is not the purpose of this study to present a detailed evaluation of the validity of the cubic law. For purposes of the analyses presented below, it is proposed that Equation (4-6) can be used for obtaining estimates of fracture apertures from laboratory or field tests on single fractures. Equation (4-4) can then be used to obtain values for intrinsic rock mass permeability, and Equation (4-5) can be used to obtain the ratio of permeabilities at different stress levels.

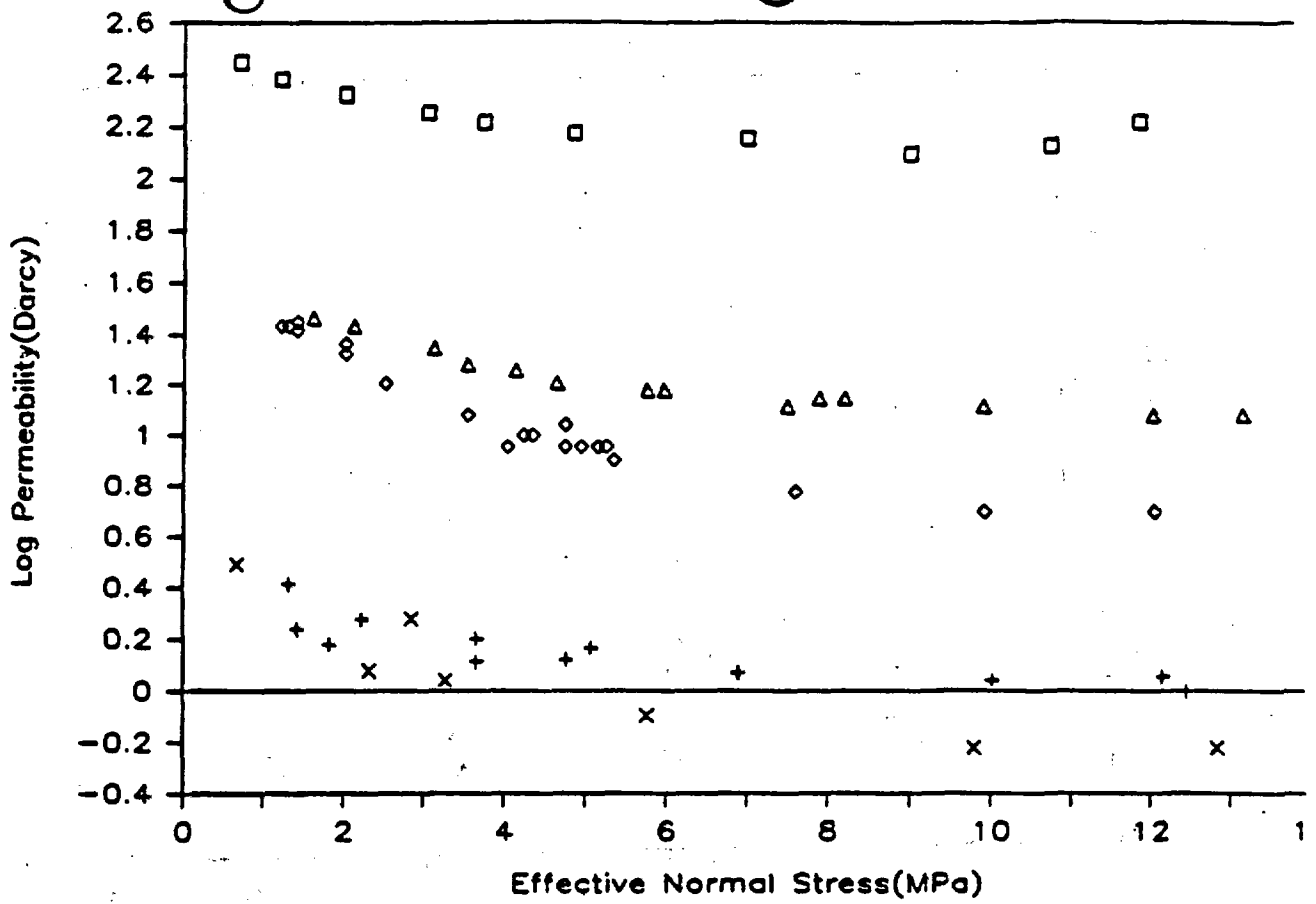
#### 4.2 LABORATORY STUDIES OF SINGLE FRACTURES IN WELDED AND NONWELDED TUFF

Laboratory investigations about the influence of effective confining stress on fracture permeability have been made by Peters et al. (1984, pp. 50-55). Five core samples, each with a single fracture with various aperture and roughness characteristics, were recovered and prepared for testing in a constant flow rate permeameter. Each sample was jacketed and placed in a pressure vessel, which allowed independent application of pore pressure and the external confining pressure. A description of the experimental apparatus, sample preparation, and data reduction methods is provided by Peters et al.

The experimental method included raising the confining pressure and pore pressure to 3.5 and 3.0 MPa respectively. The pore pressure was then held constant and the confining pressure was varied in the range of 3.5 to 15.0 MPa. To simplify analyses of data from Peters et al., only the unloading cycle from the peak confining pressure will be considered on the basis that this is the process (i.e., unloading) that occurs in the field adjacent to an excavation. It is assumed that the effects of loading a sample prior to unloading will return the sample to undisturbed levels of consolidation.

The fracture permeability versus confining pressure data for the five samples are plotted in Figure 11. Fracture permeabilities are inversely proportional to effective normal stress. In each case, the fracture permeabilities approach an asymptotic value, but this value differs widely for the several samples. In other words, the several samples are characterized by different equivalent, smooth-wall apertures at maximum closure. Peters et al. (1984, Tables A.8 - A.11) calculated that the equivalent smooth-wall aperture at maximum closure changed from about 3  $\mu\text{m}$  to about 38  $\mu\text{m}$ .

The fracture permeability versus confining stress relationships also indicate different changes in relative permeability, i.e., the ratio of permeability at zero normal stress to the permeability at high effective normal stress. This is more clearly illustrated in Figure 12, where fracture permeabilities are normalized to their asymptotic values at high effective confining stress. The differences in the relative permeability curves may be partly attributable to fracture roughness. For example, Sample G4-1F is described as a "rough fracture with poorly matched surfaces." Fracture closure under high stress is incomplete, and the relative fracture permeability curves shows little dependence on stress. In contrast, Sample G4-3F is described as a "very planar fracture with well-matched surfaces." Relative permeability is more dependent on stress, suggesting more complete aperture closure under stress. These results are consistent with conclusions drawn by Barton et al. (1985, p. 139), that smooth joints close more completely under applied normal stress than rough joints.

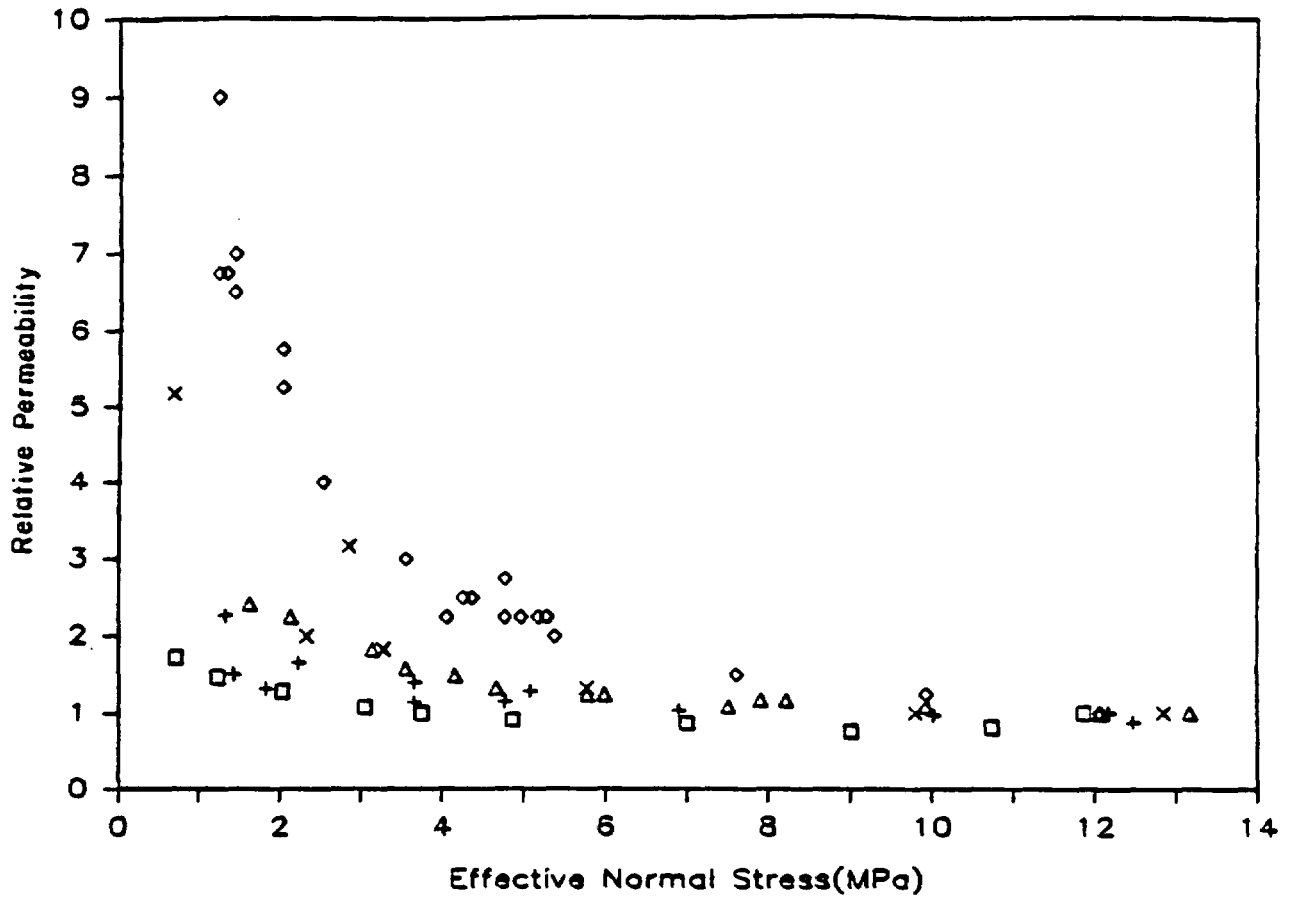


**LEGEND**

SAMPLES TAKEN FROM THE G4 SERIES:

- 1F HIGHLY WELDED, ROUGH
- † 2F HIGHLY WELDED, SMOOTH
- ◇ 3F WELDED, PLANAR
- △ 4F NONWELDED
- x 5F NONWELDED, PLANAR

FIGURE 11. PERMEABILITY AS A FUNCTION OF NORMAL STRESS FROM LABORATORY TESTING BY PETERS et al. (1984)



**LEGEND**

SAMPLES TAKEN FROM THE G4 SERIES:

- 1F HIGHLY WELDED, ROUGH
- + 2F HIGHLY WELDED, SMOOTH
- ◇ 3F WELDED, PLANAR
- △ 4F NONWELDED
- x 5F NONWELDED, PLANAR

**FIGURE 12. COMPARISON OF RELATIVE PERMEABILITY RELATIONSHIPS FROM LABORATORY TESTING BY PETERS et al. (1984)**

### 4.3 FIELD STUDIES OF SINGLE FRACTURES IN WELDED TUFF

Field permeability tests were conducted in the G-Tunnel Heated Block Test (Zimmerman et al., 1985, pp. 755-756). The tests were performed by injecting water under pressure into a packed-off section of a central borehole, which intersects a near-vertical fracture, and monitoring the flow rate in two observation boreholes. The cubic law was then used for calculating the equivalent smooth-wall fracture aperture (Hardin et al., 1982, p. 148). During the test, the fracture was subjected to a complex load-path history that included relief of the in situ stress by slot creation, and subsequent loading and unloading by cycling the flatjack pressure. A summary of the results for two flow paths is presented in Figures 13 and 14 respectively. The two flow paths are identified as paths 21 and 23, and represent the flow of water from a central injection hole 2 to the observation hole 1 or hole 3, respectively. The effective stress is calculated as the difference between the applied total stress from the flatjacks and the water pressure between the packers. Both relationships indicate that fracture permeability is inversely related to normal stress. It is also interesting to note that fracture permeability shows little or no stress-dependence when the effective normal stress exceeds the pre-existing stress of about 3 MPa. The results indicate hysteresis, with path 21 showing a higher stress dependence than path 23. For this reason, path 21 is considered in comparisons between field and laboratory results in the following section.

### 4.4 STRESS-PERMEABILITY RELATIONSHIPS

The combined results from laboratory and field tests provide a basis for bounding the relative fracture permeability versus normal stress relationship. The combined results are shown in Figure 14. These data include

- Two laboratory tests (Samples G4-3F and G4-1F) that showed the least and most change in fracture permeability across the stress change which was used in the tests.
- Field test data from the G-Tunnel Block Test. Note that the data plotted involves the initial unloading due to slot creation, and unloading on a subsequent load cycle.

The comparison shows that the field test data fall within the bounds defined by the available laboratory test data. The results also show that permeability is relatively insensitive to stress changes above a stress level of 3 to 4 MPa. The bounds obtained from Figure 15 can be used to calculate corresponding bounds for rock mass permeability as a function of stress by using the theory described in Section 4.1. The calculated relationships (Figure 16) show rock mass permeability normalized to permeability at a stress level of 12 MPa which was the maximum stress level used in laboratory tests in Peters et al. (1984) (Section 4.2).

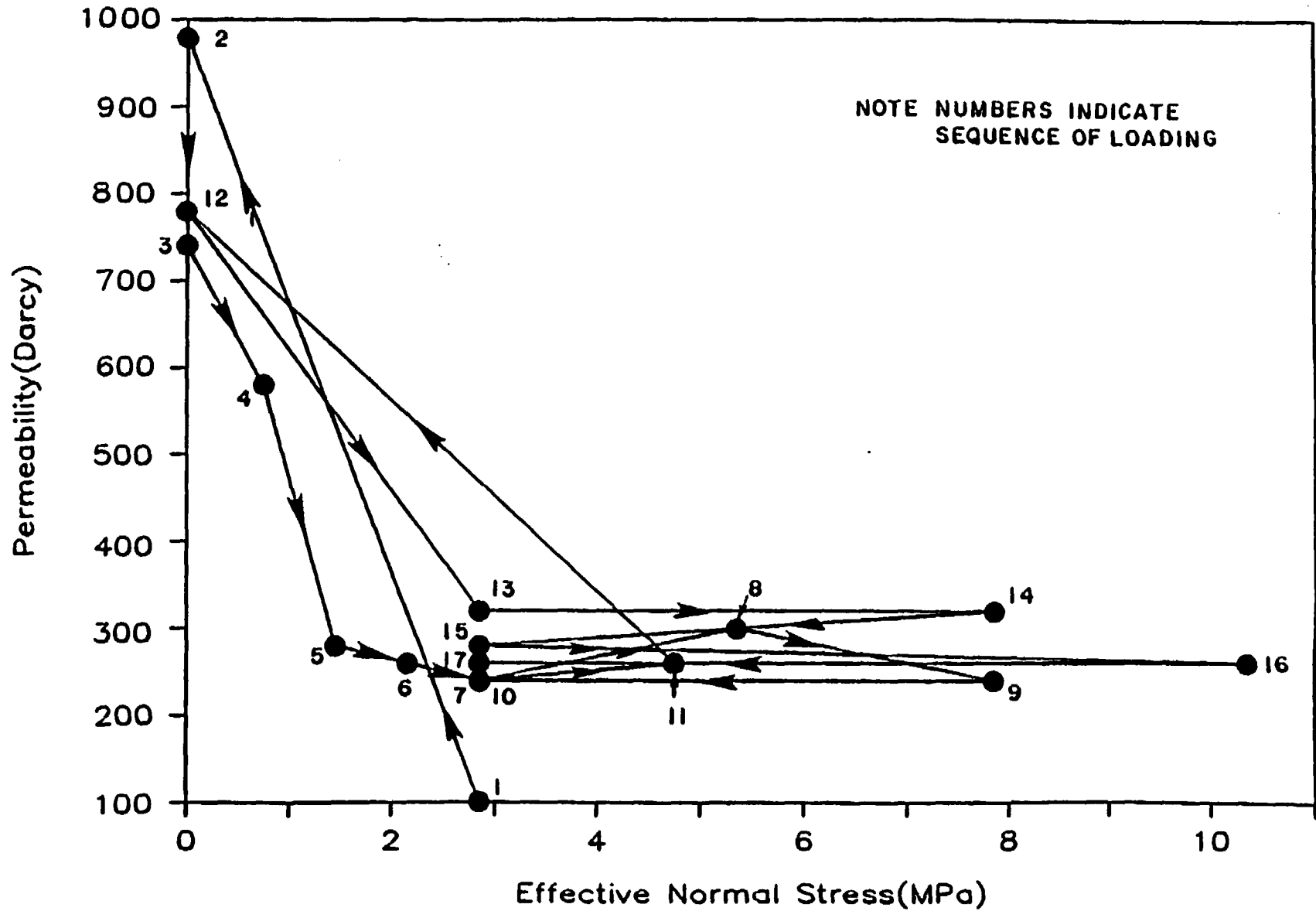


FIGURE 13. PERMEABILITY VS. EFFECTIVE NORMAL STRESS, G TUNNEL BLOCK TEST - PATH 21 (AFTER ZIMMERMAN et al., 1985)

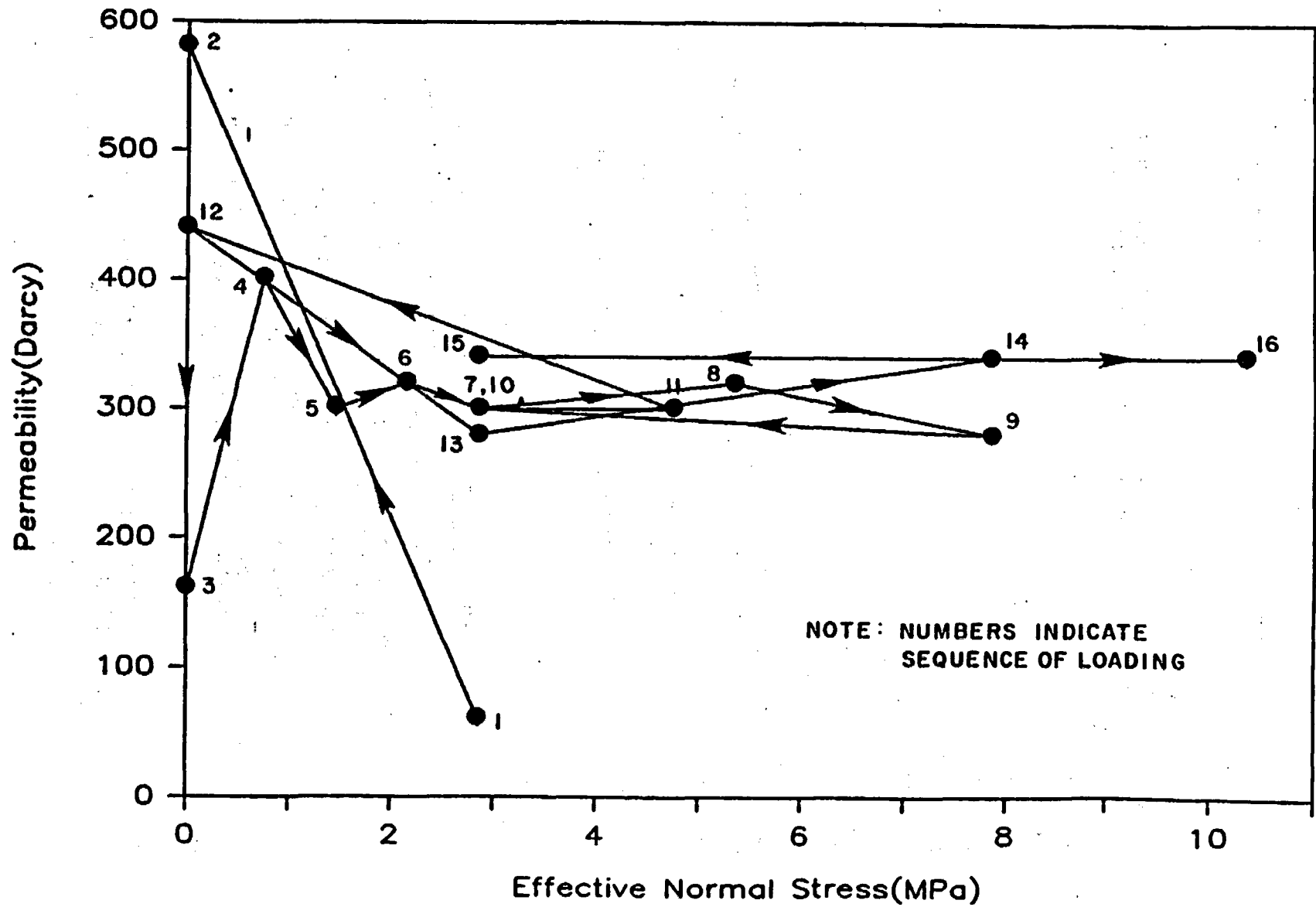
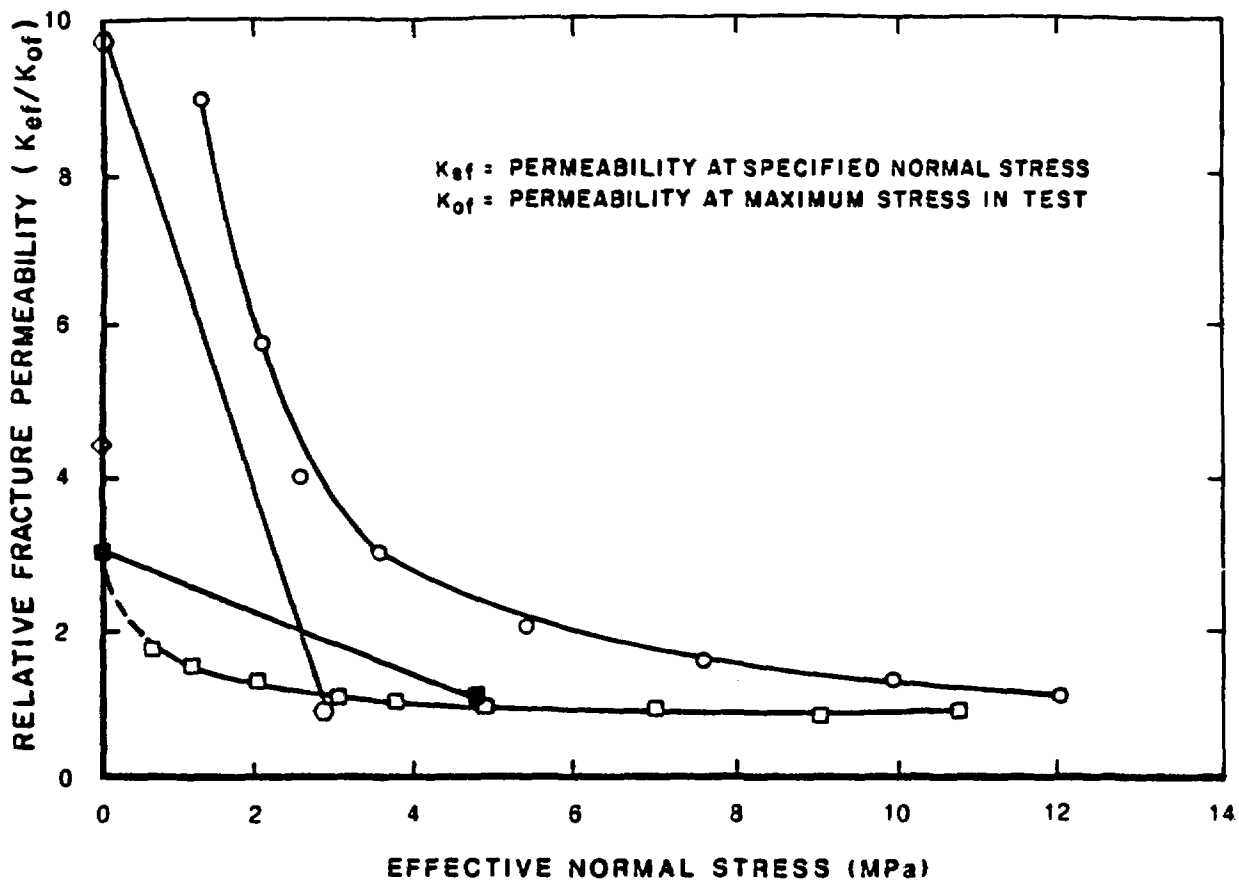


FIGURE 14. PERMEABILITY VS. EFFECTIVE NORMAL STRESS (TUNNEL BLOCK TEST)



LEGEND

LABORATORY TESTING (AFTER PETERS ET AL., 1984)

- ROUGH FRACTURE WITH POORLY MATED SURFACES (SAMPLE G4-1F, WELDED)
- PLANAR FRACTURE WITH WELL MATCHED SURFACES (SAMPLE G4-3F, WELDED)

FIELD TESTING (AFTER ZIMMERMAN ET AL., 1985)

- FRACTURE IN G TUNNEL BLOCK TEST FOR PATH 21 UNLOADED BY SLOT CREATION
- FRACTURE IN G TUNNEL BLOCK TEST FOR PATH 21 AFTER SUBSEQUENT LOADING CYCLE

**FIGURE 15. COMPARISON OF FIELD, LABORATORY, AND MODELING STUDIES OF THE RELATIONSHIP BETWEEN EFFECTIVE NORMAL STRESS AND FRACTURE PERMEABILITY.**

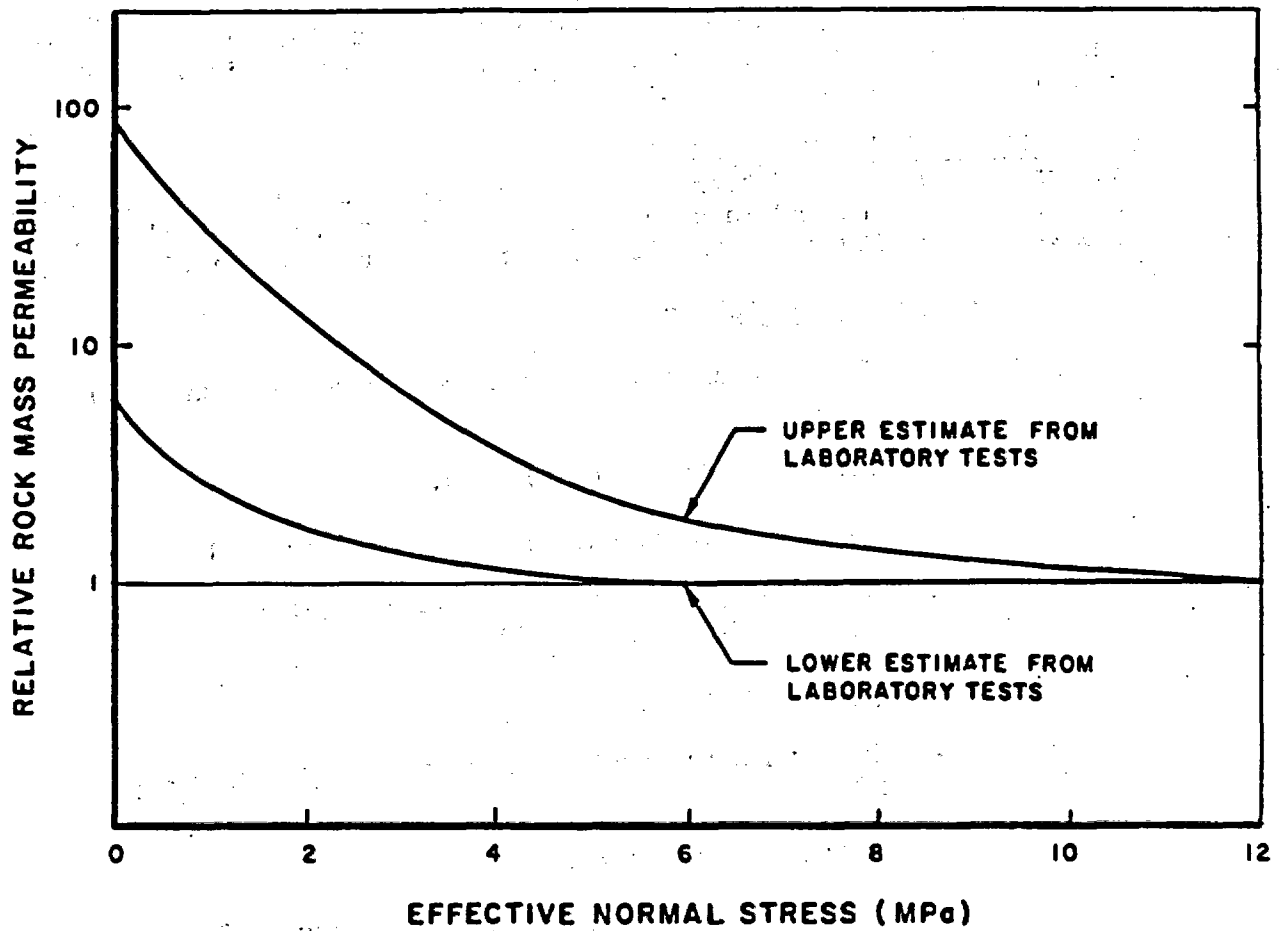


**FIGURE 16. UPPER AND LOWER BOUNDS TO SENSITIVITY OF ROCK MASS PERMEABILITY TO EFFECTIVE NORMAL STRESS IN WELDED TUFF NORMALIZED TO 12 MPa**

## 5.0 EVALUATION OF PERMEABILITY CHANGES RESULTING FROM STRESS RELIEF

The rock mass stress-permeability relationships developed in Section 4.0 may be used with the stress distributions calculated in Section 3.0 to predict changes in the rock mass permeability near a shaft. In the analyses presented in this section, the expected change in relative rock mass permeability is calculated for Topopah Spring welded tuff (TSw2) at depths of 100 m and 310 m. This expected change corresponds to the expected values for rock mass strength, in situ stress, and stress-permeability sensitivity. An upper bound change in permeability is also calculated for a combination of lowest rock mass strength, highest in situ stress, and greatest sensitivity of permeability to stress change.

### 5.1 SUMMARY OF INPUT PARAMETERS

The parameters and conditions used in the calculations are given below. Rock strength parameters and in situ stress conditions are obtained from Table 2. Stress-permeability relationships are obtained from Figure 15.

- Upper Bound Change
  - Intact rock unconfined compressive strength = 110 MPa.
  - Rock Mass Rating (RMR) = 48.
  - Ratio of horizontal to vertical stress = 1.0.
  - Upper bound rock mass stress-permeability relationship (Figure 16).
- Expected Change
  - Intact rock unconfined compressive strength = 171 MPa.
  - Rock Mass Rating = 65.
  - Ratio of horizontal to vertical stress = 0.6.
  - Approximately the mean of the rock mass stress-permeability relationship from Figure 16 (see below).

Permeability has not been calculated for the conditions of upper bound strength and lower bound in situ stress (analyses 1 and 4 in Table 2). Essentially, the results would be the same as those for the expected conditions because the rock response is elastic for both expected and upper bound properties.

The initial stress condition is defined by two equal principal stresses acting in a plane, normal to the shaft axis. In a sense, this isotropic model is a hydrostatic stress condition, although the stress in the direction of the penetration axis is ignored. Also, the effects of pore pressures and temperature changes are currently ignored. In the four analyses conducted, the

undisturbed isotropic stress varies from about 1.3 MPa (i.e., 0.25 times the vertical stress at 100 m depth) to about 7 MPa (i.e., equal to the vertical stress at 310 m depth). In order to obtain stress-permeability relationships for each analysis, it is necessary to normalize permeability to the appropriate undisturbed stress level (so that the relative undisturbed permeability value in each case equals one). Figure 17 shows the relationships actually used in each of the four analyses, obtained from the general stress-permeability relationship previously presented in Figure 16. For the upper bound analyses, the relationships are obtained by straight-line extrapolation between the undisturbed stress value and the maximum predicted relative permeability value determined at zero stress. The value for relative permeability at zero stress for the expected condition is obtained from the G-Tunnel field test (Path 21, Figure 15).

## 5.2 RESULTS

For the expected conditions, the rock mass response to excavation is elastic at depths of 100 m and 310 m (Table 2). The tangential stress is increased (by a factor of two at the excavation surface) and the radial stress is reduced to zero at the surface. Permeability should be increased along tangential fractures orientated perpendicularly to the radial stress and conversely reduced along radial fractures orientated perpendicularly to the tangential stress. For the case of upper bound change with reduced rock mass strength and higher in situ stresses, the rock mass response to excavation is inelastic, and both the radial and tangential stresses are reduced, resulting in an increase in permeability along all fractures.

The predicted upper bound and expected changes in rock mass permeability at the two depths are presented in Figure 18. To provide a conservative estimate and to simplify the analysis, the effects of increased stress across radial fractures in the elastic zone are ignored. This is a reasonable simplification, given the nonlinear stress-permeability relation for fractures (Section 2.3). From Figure 14, it can be seen that an increase in stress levels above 4 to 6 MPa has a relatively minor effect on permeability compared with the effect that would result from reducing stress. Thus, changes in axial rock mass permeability would be dominantly influenced by radial stress relief.

The results indicate a difference in the effects of stress relief depending largely on rock mass strength and in situ stress conditions. Under expected conditions (with the expected change in relative permeability from Figure 17), the maximum increase in rock mass permeability (occurring at the shaft wall) is about one order of magnitude. Given the potential resolution of in situ permeability measurements and potential variability in the rock mass, such a zone of increased permeability may not be measurable. On the other hand, the elastoplastic solution (with the upper bound change in permeability from Figure 17) indicates changes as high as two orders of magnitude at the excavation surface. In this case, the zone in which permeability is increased by at least one order of magnitude extends out about one radii from the shaft wall.

For the case of predicted inelastic behavior, it is noted that the degree of stress relief might be reduced in practice by the application of support (e.g., rock bolts, shotcrete or concrete liner) at the time of excavation. Rock support would probably have little effect on deformations in the elastic zone.

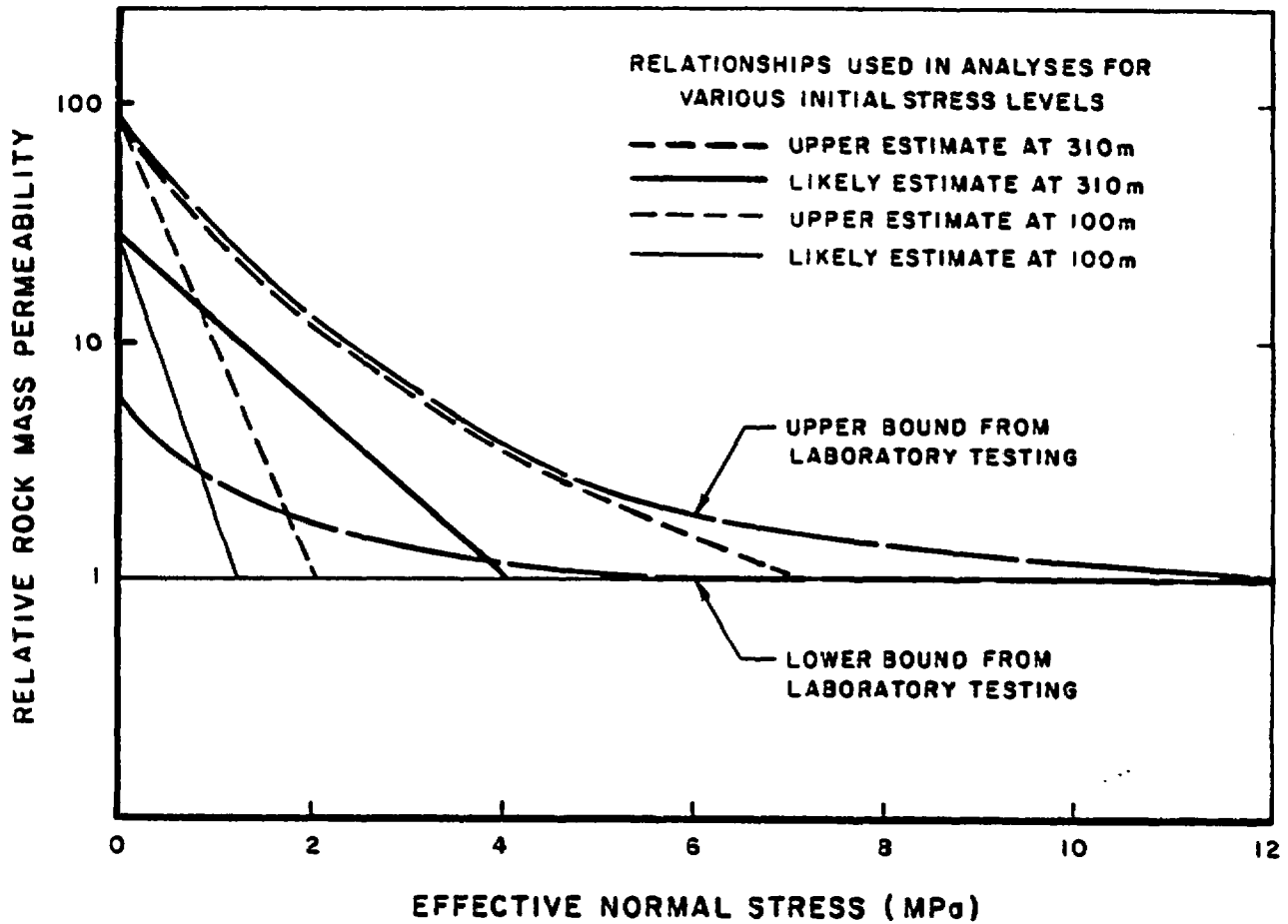


FIGURE 17. ROCK MASS PERMEABILITY-STRESS RELATIONSHIPS NORMALIZED TO STRESS LEVELS USED IN MODIFIED PERMEABILITY ZONE ANALYSES

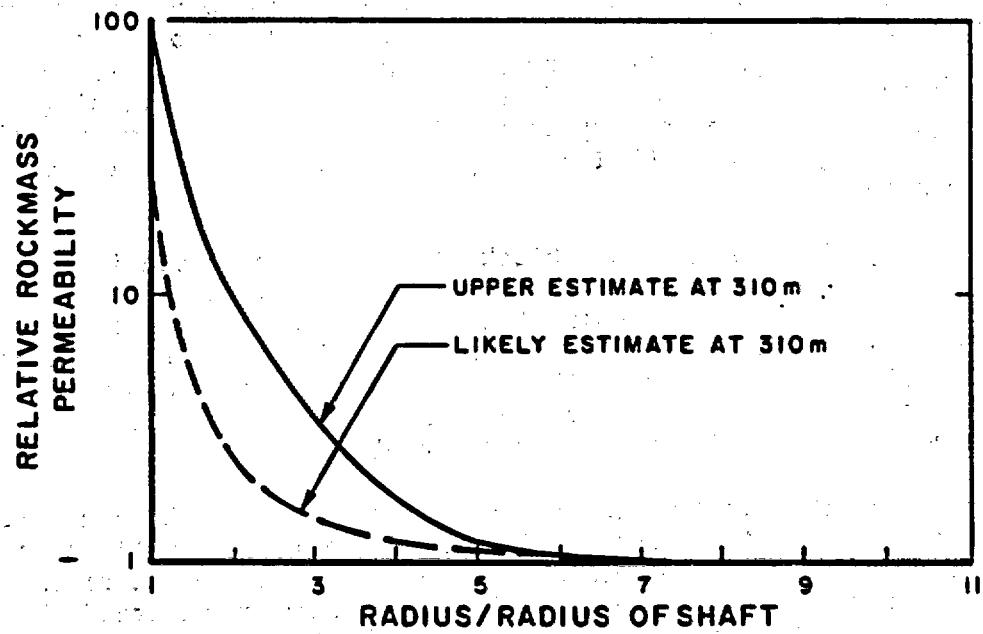
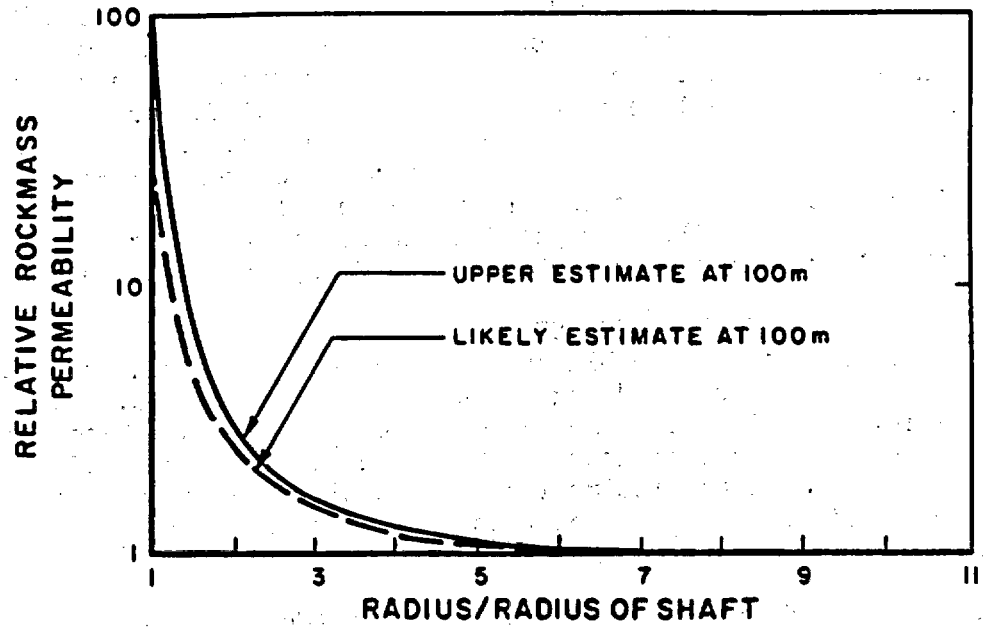


FIGURE 18. ESTIMATED CHANGE IN AXIAL ROCK MASS PERMEABILITY AT 100 m AND 310 m DEPTHS RESULTING FROM STRESS RELIEF

## 6.0 EVALUATION OF PERMEABILITY CHANGES RESULTING FROM BLASTING

Excavation of a shaft by blasting might result in increased permeability in a damaged zone adjacent to the shaft wall. This chapter reviews evidence from field case histories regarding the extent of blast damage and its effects on rock mass permeability. Unfortunately, we have found few case histories in which the permeability of the blast-damaged zone was measured directly. As shown in Section 6.1, case histories are useful for providing evidence of the extent of blast damage, as indicated by increased fracturing. The extent of blast damage can also be estimated by means of general relationships between explosives charge weight and the particle velocity required to produce fracturing (Section 6.2). The possible increases in permeability and the extent of the blast damage zone for welded tuff are presented in Section 6.3.

### 6.1 REVIEW OF CASE HISTORIES

Appendix B contains a bibliography of about 60 references that relate directly or indirectly to blast damage around shafts or tunnels. Table 3 summarizes 14 case histories in which the extent of damage or disturbance around an opening was measured. As indicated in the table, in a majority of these cases no attempt was made to distinguish between blast damage and disturbance due to stress relief. The most relevant case histories are reviewed in the following sections.

#### 6.1.1 Colorado School of Mines Test Mine (Montazer and Hustrulid, 1983; El Rabaa et al., 1982; Montazer et al., 1982; Hustrulid et al., 1980; Sperry et al., 1984)

The Colorado School of Mines (CSM) has established a mining technology research facility at the Edgar Mine located at Idaho Springs, Colorado. A mining technology research program sponsored by the Office of Nuclear Waste Isolation (ONWI) was directed specifically toward evaluating the structural damage caused by various types of blasting and toward measuring permeability in the damaged zone. ONWI also sponsored a heated block test conducted at the same site.

The damaged zone and heated block tests were conducted in an experimental room excavated specifically for the tests. The room is 5 m wide, 3 m high and 30 m long, and was excavated using ten different blasting patterns. Variations of a Swedish smooth-wall technique were used for seven rounds and variations of the Livingstone blasting method, developed in the U.S., were used for the other three. The rock cover above the experimental room is about 100 m, and the room is located above the water table.

The principal rock type in the experimental room is banded, biotite gneiss, which is intruded and recrystallized by granitic migmatites and pegmatites. Fracture patterns have been mapped in detail in the experimental room and in adjacent drifts and raises. At least ten structural trends have been recognized, but there are three main fracture sets, each dipping steeply or vertical. In the heated block, fracture spacing varies from 60 to 100 cm for the three major sets.

The damaged zone evaluation was made by using boreholes drilled from the tunnel. Three 30-m long holes were drilled parallel to the tunnel axis and a pattern of 6.5- and 7.0-m long radial holes was drilled at each of six different blast round locations. The techniques used for damaged zone assessment include:

**TABLE 3**  
**CASE HISTORIES OF BLAST DAMAGE MEASURED IN TUNNELS**

| SITE   | ROCK TYPE       | BLASTING METHOD | TUNNEL DIMENSIONS | DEPTH OF DAMAGE | MEASUREMENT METHOD   | COMMENTS   | REFERENCES                   |
|--|-----------------|-----------------|-------------------|-----------------|--|--|------------------------------|
| Colorado School of Mines (Edgar Mine) Colorado | Biotite gneiss  | Smoothwall      | 5m x 3m           | 0.5m            | Borehole logging, cross-hole permeability (packer tests), borehole deformation | Depth of blast damage not well documented but in agreement with theoretical calculations   | Montazer and Hustrulid, 1983 |
| Stripa Mine Sweden                             | Granite         | Smoothwall      | 4m x 4m           | 0.3m            | Boreholes  | Fracture lengths ranged from 0.1-1.0m, with an average length of 0.3m; permeability of blast damaged zone not measured           | Anderson and Halen, 1978     |
| Rainier Mesa Nevada Test Site                  | Zeolitized tuff | Conventional    | 3m                | <1.7m (?)       | Air permeability   | Blast damage not well distinguished from stress effects  | Miller et al., 1974          |
| Rolla Experimental Mine                        | Dolomite        | Various         | 2.5 x 2.2m        | 0.3-2.5m        | Seismic refraction   | Depth of damage varies according to method of blasting used; blast damage not distinguished from stress relief                   | Worsey, 1985                 |
| Test Drift                                     | Basalt          | Conventional    | 5m                | -2m             | Cross-hole seismic   | Blast damage seen most clearly in vertical travel direction in drift wall, effects of stress relief seen in horizontal direction | King et al., 1984            |

**TABLE 3**  
**CASE HISTORIES OF BLAST DAMAGE MEASURED IN TUNNELS (Continued)**

| SITE                     | ROCK TYPE             | BLASTING METHOD      | TUNNEL DIMENSIONS | DEPTH OF DAMAGE | MEASUREMENT METHOD                                  | COMMENTS   | REFERENCES              |
|--------------------------|-----------------------|----------------------|-------------------|-----------------|---|--|-------------------------|
| Ontario, Canada          | Limestone             | Presplit             | -8m               | -1m             | TV camera in boreholes in crown                     | Separate zones of moderate cracking and hairline cracks; depth of damage varies with charge weight   | Lukajic, 1982           |
| Saimogo, Japan           | Sandstone/shale       | Conventional         | 5.1m              | up to 1.3m      | Seismic refraction                                  | Comparison of blasting with excavation by TBM; difficult to separate blast damage from stress relief | Nishida et al., 1982    |
| Crestmore Mine           | Marble                | Conventional         | 30-70ft           | 4-5ft           | Seismic refraction, borehole jack, borehole logging | The borehole jacking method was used to determine the rock mass deformation modulus                  | Heuze and Goodman, 1974 |
| Churchill Falls, Canada  | Gneiss                | Controlled perimeter | 2.1 x 2.4m        | <1m             | Plate load test                                     | Most damage within 0.3m  | Benson et al., 1970     |
| Straight Creek, Colorado | Granite/gneiss/schist | Conventional         | 4m                | "few ft"        | Seismic refraction                                  | Blast damage depth estimated within overall low velocity layer extending 1-5m                        | Scott et al., 1968      |
| Belledonne, France       | Granite               | Conventional         | 5.9m              | -1m             | Seismic refraction                                  | Blasting and stress relief effects not specifically distinguished                                    | Plichon, 1980           |

**TABLE 3**  
**CASE HISTORIES OF BLAST DAMAGE MEASURED IN TUNNELS (Continued)**

| <b>SITE</b>             | <b>ROCK TYPE</b> | <b>BLASTING METHOD</b> | <b>TUNNEL DIMENSIONS</b> | <b>DEPTH OF DAMAGE</b> | <b>MEASUREMENT METHOD</b> | <b>COMMENTS</b>   | <b>REFERENCES</b>               |
|-------------------------|------------------|------------------------|--------------------------|------------------------|---------------------------|---|---------------------------------|
| Mine                    | Shale            | Conventional           | ?                        | 0.5-1m                 | Seismic refraction        | Blasting and stress relief effects not specifically distinguished | Brizzolari 1981                 |
| Rama Tunnel, Yugoslavia | Dolomite         | Conventional           | 5m                       | <1m                    | Cross-hole seismic        | Blasting and stress relief effects not specifically distinguished | Kujundic, et al., 1970          |
| Turlough Hill, Ireland  | Granite          | Conventional           | 2.5m                     | 0.5-2.5m               | Cross-hole seismic        | Blasting and stress relief effects not specifically distinguished | O'Donoghue and O'Flaherty, 1974 |

- Core logging,
- Borescope and/or TV logging,
- Cross-hole ultrasonic measurements,
- Single-packer, air-injection permeability measurements,
- Guarded-packer, water-injection permeability measurements, and
- Borehole deformation measurements using the CSM Cell and the Goodman Jack.

Other tests in the mine included roof-to-floor and wall-to-wall convergence measurements using convergence meters and tape extensometers, and in situ stress measurements using the CSIRO and USBM gages, as well as the heated block test noted above. The results from the CSM studies permit the following conclusions to be drawn:

- The blast-damaged zone is estimated at about 0.5 m wide (Montazer et al., 1982, Figure 6).
- Tangential stresses close to the excavation are approximately 6 MPa; the total width of the zone of stress increase is about 9 m, i.e., 1.8 times the tunnel width.
- Radial permeability (as measured in boreholes parallel to the tunnel axis) is reduced by 1 to 2 orders of magnitude within about 2 m from the tunnel face.
- Axial permeabilities (as measured in the radial boreholes) close to the tunnel walls are typically several orders of magnitude greater than the radial permeabilities; these results may be affected by communication between the packed-off zone and the tunnel face and by leakage around the packers which were difficult to seal close to the tunnel face.

Generally, the results from the permeability tests tend to confirm the predictions for an elastic stress distribution given in Section 5.0 that axial permeabilities should increase and radial permeabilities decrease close to an excavation.

6.1.2. Stripa Mine, Sweden (Wilson et al., 1983; Kelsall et al., 1982, 1984; Witherspoon et al., 1981; Anderson and Halen, 1978; Nelson and Wilson, 1980)

Evidence regarding changes in permeability around a tunnel in granitic rock was obtained from the macroporosity test conducted at Stripa, Sweden. This test was designed to measure the permeability of a large volume of low-permeability fractured rock by monitoring water inflow into a 33-m long section of a tunnel. Water inflow was monitored as the net moisture pick-up of the ventilation system inside a sealed portion of the tunnel. Hydraulic

gradients around the tunnel were determined by monitoring groundwater pressures in piezometers which were installed in a total of 90 isolated intervals in 15 radial boreholes drilled from the tunnel. The tunnel was excavated by using smooth-blasting techniques at a depth of about 340 m. The major rock type in the tunnel is a medium-grained granite, which is intruded by pegmatite and aplite dikes. Two major joint sets strike obliquely to the tunnel axis. Fracture frequency measured in holes drilled from the tunnel was, on the average, 4.5 joints/m in inclined holes and 2.9 joints/m in vertical holes.

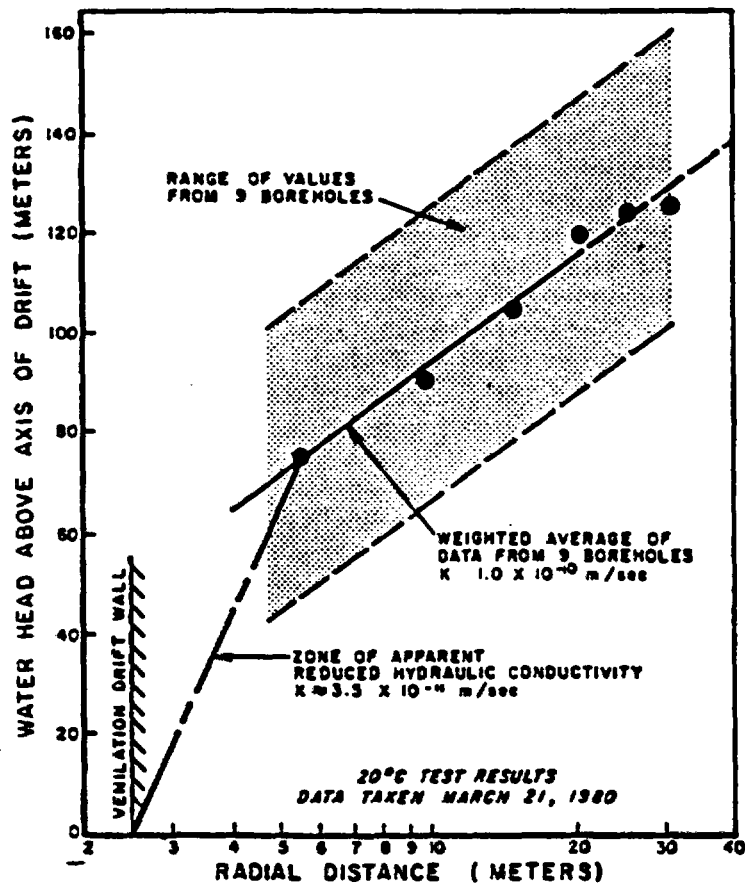
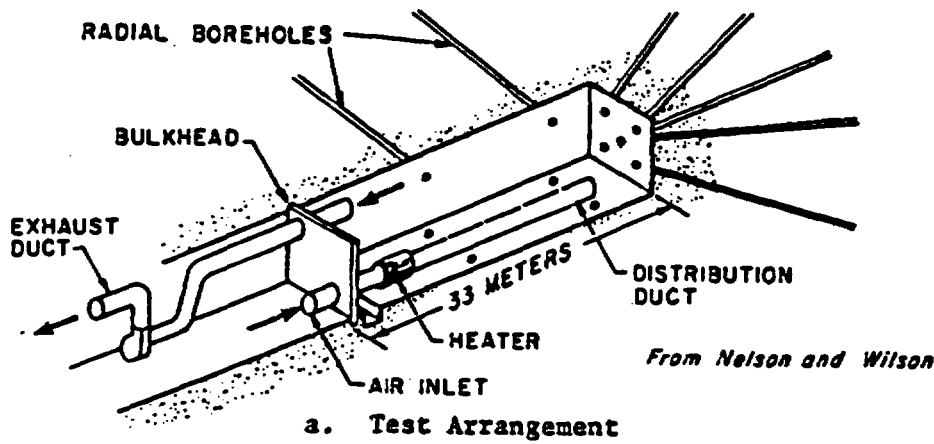
Nelson and Wilson (1980) calculated an average value for rock mass hydraulic conductivity from the observed gradient (the slope of the head-distance plot) and the water inflow monitored in the tunnel. If the weighted average line shown in Figure 19 is projected to the drift wall, it indicates a higher water head than can exist in practice. This indicates that there is a zone, approximately 2.5 m thick, adjacent to the walls of the drift, in which the hydraulic conductivity is reduced by a factor of approximately three relative to the far-field value. Kelsall et al. (1982) presented an analysis to show that this reduction of permeability is consistent with that predicted to occur in response to an increase in the tangential stress around the opening (using the same approach as is used in this report).

The macropermeability test gave no evidence of increases of permeability due to blasting, other than by showing that the blast-damaged zone could not extend more than about 2 m from the wall. Other damaged zone assessments at Stripa were made by direct inspection of fractures produced by blasting and by borehole logging. A detailed inspection of the smooth-blasted tunnel walls showed that about 10 percent of the outer ring holes had wavy fractures along their length. The fractures were caused by blasting; their length ranged from 0.1 to 1.0 m. The extent of these fractures perpendicular to the tunnel walls was investigated by drilling a number of short core holes each intended to follow a particular fracture. The average extent of fractures was found to be about 0.3 m.

#### 6.1.3. Nevada Test Site (Miller et al., 1974; Cording et al., 1971)

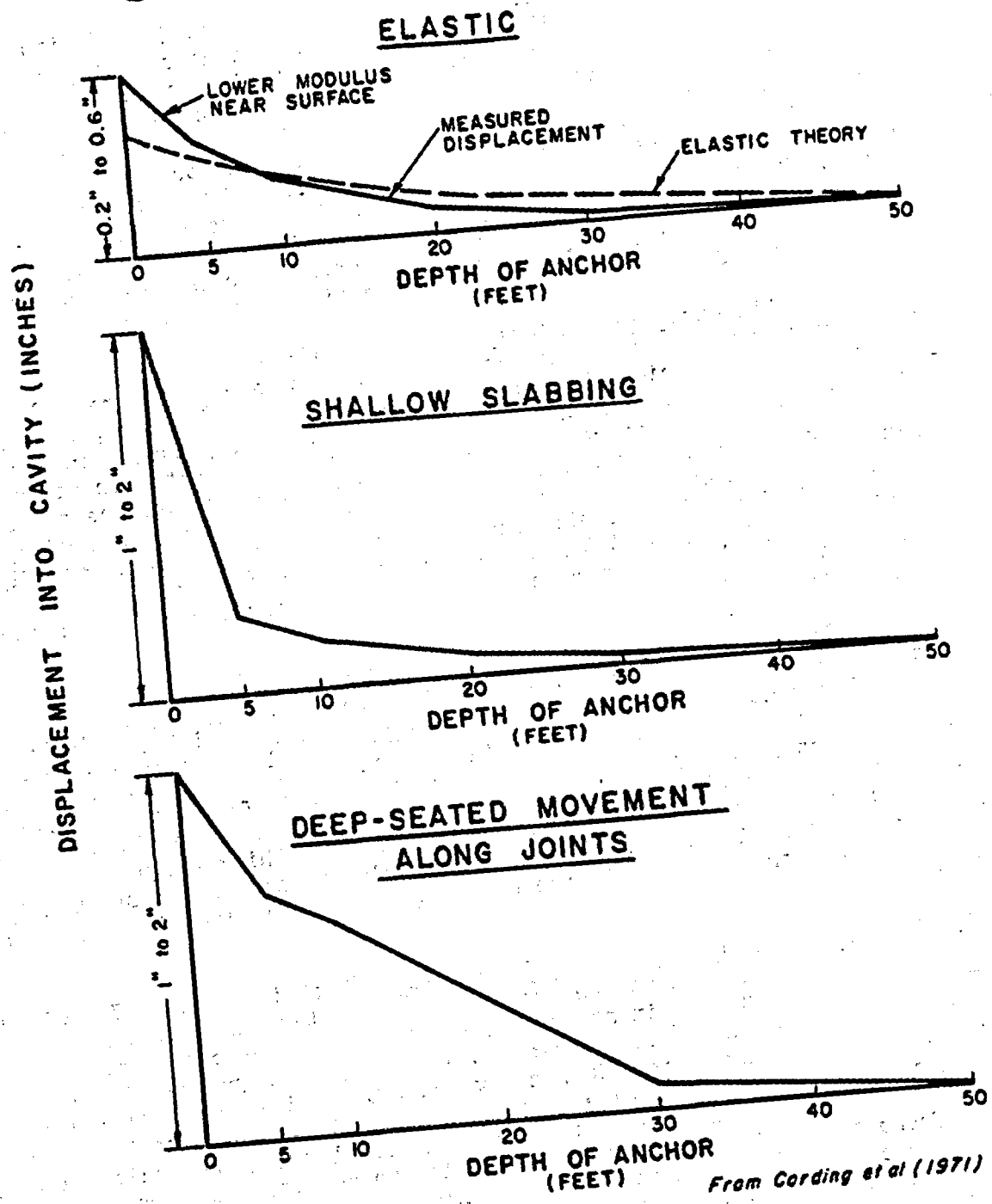
An air-injection method was used by the U.S. Geological Survey to study the intensity of fracturing around a 3-m (10-foot) diameter tunnel in volcanic rocks at the Nevada Test Site (Tunnel u12g.10 at Rainier Mesa), excavated by conventional blasting methods. Injection tests were run at 0.3-m intervals in 17 boreholes drilled from the tunnel. Characteristically, the flow rates obtained were either very low (indicating no fractures present) or relatively high (indicating fractures present in the test interval), with 90 percent of the high flow rates recorded within 1.7 m of the tunnel face (Miller et al., 1974, Figure 7) and 62 percent recorded within about 1 m. Observations in the tunnel revealed many induced fractures attributed to blasting or stresses exceeding the rock strength. These induced fractures were probably responsible for the marked increase in permeability within 1.7 m of the tunnel face. The opening of pre-existing fractures in response to stress relief might be expected to produce a more gradational increase in permeability.

A second case history from the Nevada Test Site does not provide direct evidence of blast damage, but does illustrate a range of rock mass response for different rock properties similar to that predicted in Section 3.0. Figure 20 shows typical displacement-depth profiles obtained from two large cavities excavated in tuff (Cording et al., 1971). The tuff is described as



b. Distance-drawdown Plot at end of 20°C Temperature Experiment

FIGURE 19. MACROPERMEABILITY TEST, STRIPA, SWEDEN



From Gording et al (1971)

FIGURE 20. TYPICAL DISPLACEMENT PROFILES IN LARGE EXCAVATED CAVERNS AT THE NEVADA TEST SITE

low strength and high quality, suggesting a nonwelded tuff with widely spaced joints. Three types of displacement are clearly distinguishable by the extensometer data. Comparisons made by Cording et al. between measured displacements and those predicted from elastic theory indicate a low-modulus loosened zone about 1 to 2 m thick. Other measurements indicated a shallow slabbing zone extending several meters from the excavation, or deep seated movements extending nearly 10 meters from the excavation. These measurements confirm that a thick loosened zone can develop under elastoplastic conditions. As discussed previously in Section 3.6, and as illustrated in Figure 9, the radial displacements at the excavation surface for the elastoplastic case can be an order of magnitude higher than the displacements for the elastic case.

#### 6.1.4. Rolla Experimental Mine (Worsey, 1985)

This study was designed specifically to investigate the degree of damage associated with various blasting methods. An 8 ft x 7 ft experimental heading was driven 7 rounds (~15 m) using fracture control, presplitting, smooth-walling and bulk blasting methods. The drift is excavated in dolomite but the degree of fracturing is not reported. The depth of damage was measured by seismic refraction. The minimum depth of rib damage was achieved by fracture control, followed by presplitting, smooth-wall and bulk blasting (Figure 21). The depth ranged from <0.3 m to >2.5 m for 38 mm ANFO loaded holes. It is noted that no attempt was made by Worsey to distinguish blast effects from stress relief effects.

#### 6.1.5. Tunnel in Basalt (King et al., 1984)

Cross-hole seismic velocities were measured in vertical, horizontal, and diagonal directions between boreholes drilled in the wall of the tunnel. The reference does not describe the site, but it is believed to be the Near Surface Test Facility at Hanford (Basalt Waste Isolation Project) excavated by conventional blasting. A low-velocity zone, attributed to blast damage, appears in vertical travel paths and is about 2 m thick (Figure 22). The horizontal travel paths show a wider low-velocity zone which presumably corresponds to stress relief in the radial (horizontal) direction across vertical joints.

#### 6.1.6. U.S. Bureau of Mines (USBM) Studies (Siskind et al., 1973; Olson et al., 1973; Siskind and Fumanti, 1974; Hocking and St. John, 1979)

The USBM conducted experiments to measure the extent of blast damage around single-shot holes in shale (Siskind et al., 1973) and granite (Olson et al., 1973). Although these experiments may not relate directly to tunnel or shaft excavation, they do illustrate general trends. In the granite tests, the radius of the damaged zone, estimated from core logging and sonic velocities, was found to increase with increased explosive charge, from about 0.25 m for a 0.25 kg charge to 0.77 m for a 2.0 kg charge. Examination of thin sections revealed microfractures extending beyond the damaged zone limit indicated by core logging and velocities. In the shale tests, the extent of the damaged zone was found to be related to the charge and to the type of explosive. Approximate radii of the damaged zone for explosive loadings of about 1 kg/m ranged from 1 to 1.3 m for high-energy dynamite to 0.3 to 0.5 m for low-energy ANFO.

Subsequently, the USBM examined the fracturing produced in the vicinity of large-diameter production blastholes in granite (Siskind and Fumanti, 1974). Damage was assessed by testing cores recovered from the vicinity of the blast-hole. Properties that were measured included porosity, permeability, tensile

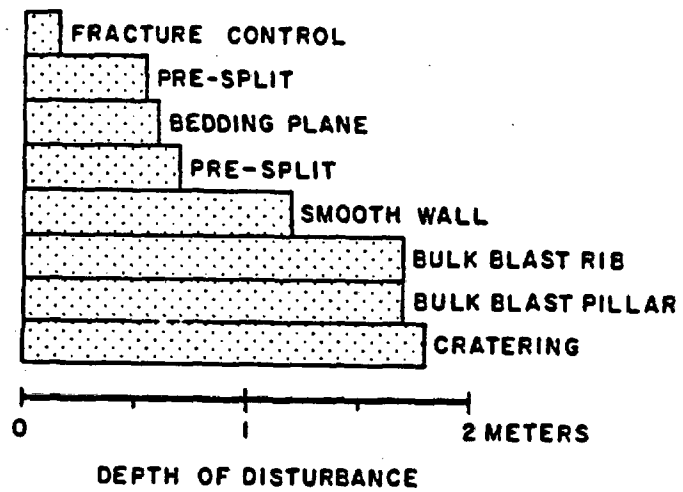


**FIGURE 21. DEPTH OF DISTURBANCE MEASURED BY SEISMIC REFRACTION IN A TUNNEL IN DOLOMITE FOR VARIOUS BLASTING METHODS (FROM WORSEY, 1985)**

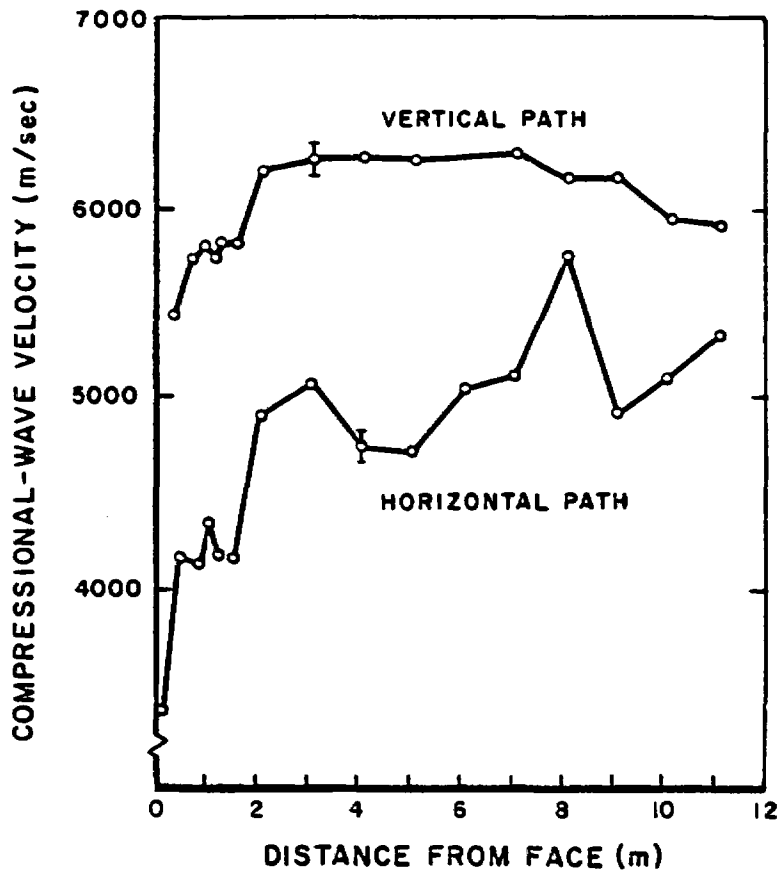


FIGURE 22. PRIMARY SEISMIC WAVE VELOCITY IN VERTICAL AND HORIZONTAL DIRECTIONS BETWEEN BOREHOLES, TUNNEL IN BASALT (FROM KING et al., 1984)

and compressive strength, Young's modulus, and acoustic pulse velocity. The results for a 165-mm diameter hole charged with ANFO indicated that the rock was highly fractured to a radius of 0.65 m (8 blasthole radii), and partly fractured to a radius of 1.14 m (14 blasthole radii). No damage was detected beyond 1.14-m radius.

Hocking and St. John (1979) summarized the USBM work and derived a general conclusion that the diameter of blast-damage zones for a high-energy explosive in hard rock such as granite should range from 15 to 20 charge diameters. For a low-energy explosive, used as a decoupled explosive in smooth blasting, the damaged zone should be only 5 to 10 charge diameters. Figure 5 (Section 2.2.2) shows a comparison between smooth blasting and conventional blasting based on these values. For 35-mm diameter perimeter holes, as used at Stripa (Section 6.1.2), the predicted damage zone would extend about 175 to 350 mm. This is in excellent agreement with the observed 0.3-m thick damaged zone.

## 6.2 BLAST DAMAGE EXTENT BASED UPON CHARGE DENSITY

A general relationship between blast damage and charge density for tunnel blasting conditions has been developed from Swedish experience in granitic rocks by Holmberg and Persson (1980, p. A-37). Figure 23 shows a series of correlations between peak particle velocity and radial distance from the charge for varying charge densities normalized for explosives with the weight strength of ANFO. The potential extent of the damaged zone is indicated by the range of peak particle velocity associated with incipient rock fracture. In the excavation of the shafts, it is assumed that some necessary blasting controls will be used to limit overbreak. These might include the use of perimeter holes that are smaller in diameter than the main holes, or perhaps the perimeter holes contain smaller diameter charges that are decoupled from the surrounding rock. If the charge density of the perimeter holes is assumed to range from 0.45 to 0.5 kg/m of ANFO and the critical particle velocity at incipient rock fracture is 1,000 mm/sec, the expected extent of the blast damaged zone in Figure 23 would be 0.5 m. If a lower peak particle velocity is selected (700 mm/sec), the extent of the blast damaged zone would be greater than 0.5 m.

The range of particle velocities at incipient rock fracture (700-1,000 mm/sec) in the above analysis is based upon experimental data for granitic rock types. Such rock types exhibit higher strength and stiffness than welded tuff. Welded tuff can sustain comparable or higher tensile strain following blast detonation. The above calculations are applicable to estimating the extent of the blast damaged zone in welded tuff for the assumed range of charge density in the perimeter holes.

---

\* A comparison can be made of the tensile strain at failure between granite and welded tuff. The tensile strain at failure for welded tuff is  $5 \times 10^{-4}$  as approximated by the tensile strength (16.9 MPa) divided by the Young's Modulus (31.1 GPa). Note that intact rock properties for welded tuff are taken from Nimick et al., 1984, p. 2. If Stripa Granite is considered (Swan, 1978), the tensile strain at failure is a  $2 \times 10^{-4}$  as approximated by the tensile strength (15 MPa) divided by the Young's Modulus (75.4 GPa).

Figure 23 provides a general guideline for estimating the extent of the blast damaged zone in hard, competent rocks when blasting parameters are known. The trends shown by Figure 23 are supported by several case histories. The data suggest that blast effects are dependent on charge density, and independent of excavation size.

### 6.3 PERMEABILITY CHANGES AND EXTENT OF BLAST DAMAGE IN WELDED TUFF

Rock mass permeability changes associated with blast damage may be estimated from the increase in fracture frequency that is anticipated within the blast damaged zone. Based upon Holmberg and Persson's work on the relationship of peak particle velocity to charge density (Section 6.2) and several case histories (Section 6.1) for controlled blasting, it will be assumed that increases in fracture frequency will be contained within 0.5 m of the wall. It is further assumed for the expected case that any intensely fractured zone which might extend a small distance from the perimeter holes would be removed as overbreak, treated, or subsequently removed if seals were to be emplaced.

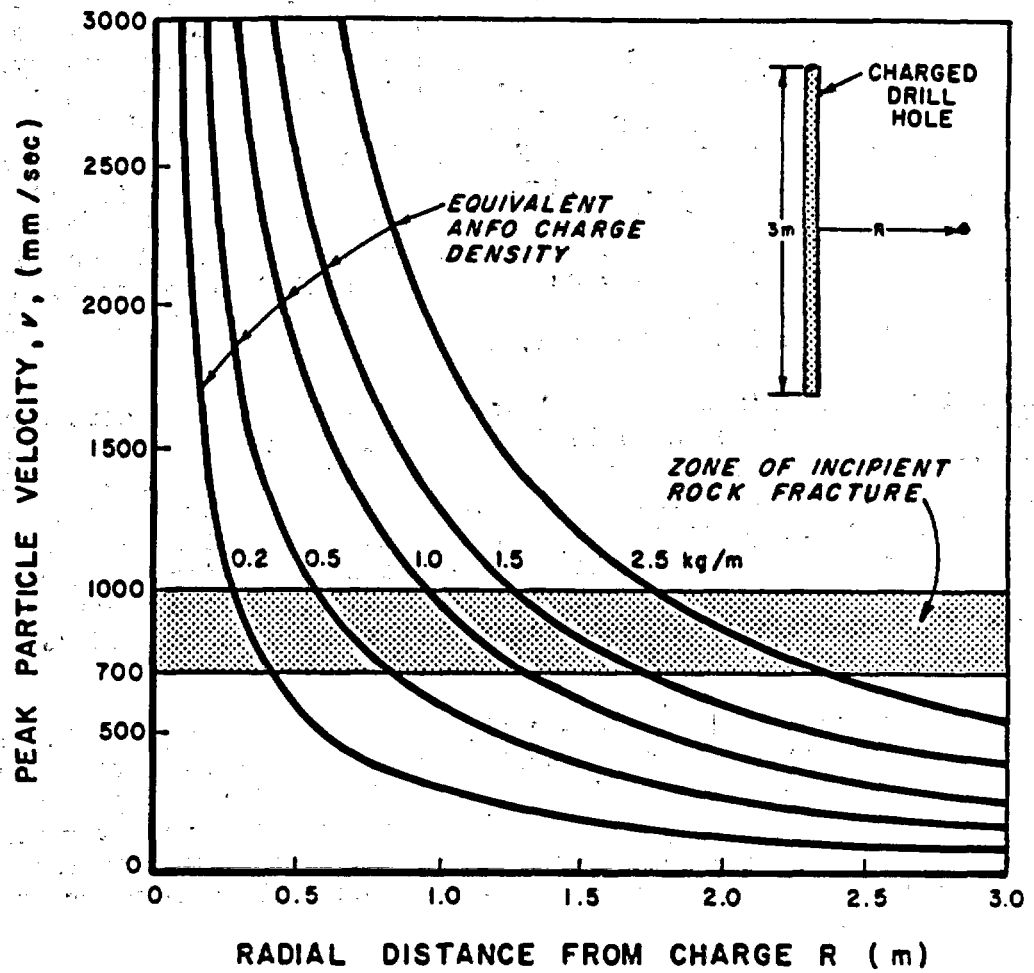
For the upper bound case, it is assumed that the increase in fracture frequency will occur within 1 m of the wall. It is noted that the upper bound extent corresponds approximately to the maximum depth of disturbance measured in dolomite by Worsey (1985) in Figure 21 in which some blasting methods such as fracture control, presplitting, or smooth-wall blasting were utilized.

Blasting is assumed to create new fractures so that the fracture frequency increases by a factor of three in the blast damaged zone. The newly created fractures are assumed to have similar characteristics to the pre-existing fractures. This includes a similar relationship of changes in permeability due to changes in stress. Therefore, the permeability in the blast damaged zone thus increases by a factor of three due to an increase in fracture frequency over the increase that occurs due to stress relief.

Because the changes in fracture frequency associated with blasting have not been well documented, the model for estimating permeability changes associated with blasting must be regarded as preliminary. Also, the assumption that fractures created by blasting have similar characteristics to natural fractures is at present unsubstantiated. It should be noted that the relative changes in permeability resulting from blasting may be greater in unfractured rocks such as nonwelded tuff, if fracturing were to occur by blasting, than in fractured rock in which many fractures already exist. However, because non-welded tuff is more ductile i.e., Young's Modulus equal to 4.8 GPa (Nimick et al., 1984 p. 2) than welded tuff, it might sustain greater strain and be less susceptible to fracturing.

---

\*A similar comparison can be made of the tensile strain at failure between dolomite, and welded tuff. If Lockport dolomite is considered [as reported by Goodman (1980, p. 58, and p. 177)], the tensile strain at failure is  $1.0 \times 10^{-4}$  as approximated by the tensile strength (3.0 MPa) divided by the Young's Modulus (51 GPa). Welded tuff can therefore sustain comparable or somewhat higher strains than dolomite.



From Holmberg and Persson (1980)

FIGURE 23. METHOD FOR ESTIMATING THE THICKNESS OF THE BLAST-DAMAGED ZONE IN RELATION TO EXPLOSIVE CHARGE DENSITY

## 7.0 MODEL OF THE MODIFIED PERMEABILITY ZONE

The results of the modeling and analyses described in previous sections are the basis for developing a model of the modified permeability zone in welded tuff. Figure 24 shows the model developed for the expected conditions at the 310 m depth. In this case the strength properties, rock quality, and in situ stress are as defined for Analysis 5 in Table 2 (i.e.,  $\sigma_c = 171$  MPa, RMR = 65,  $\sigma_H = 0.6 \sigma_v$ ). The stress permeability relation is intermediate between the upper and lower bounds shown in Figure 16 (i.e., the probable estimate shown in Figure 17). The model in Figure 24 also shows the estimated effects of blast damage based on a blast-damaged zone extending 0.5 m from the shaft wall as described in Section 6.3. Permeability is increased by three times over the increase in permeability due to stress relief in an annulus 0.5 m wide around the shaft. It is assumed that any highly fractured zone immediately from the shaft wall will be removed.

The relative contributions of blast damage and stress effects for the exploratory shaft are shown in Table 4, which also summarizes the results of analyses for several conditions and depths of 100 m and 310 m. These include stress redistribution effects without blast damage for elastic and elastoplastic cases, the expected case of elastic deformations with 0.5 m blast and the upper bound case of elastoplastic deformations with a 1 m wide blast damaged zone. The effective rock mass permeability of the modified permeability zone is an equivalent value averaged over an annulus one radius wide around the shaft and normalized to the undamaged rock.

The results reported in Table 4 apply to the exploratory shaft. The effects of stress redistribution scale to the radius of the excavation, while the effects of blast damage, as discussed previously, are independent of shaft radius. The equivalent conductivities for the larger diameter Men and Materials or the Emplacement Exhaust shafts would be smaller than the values given in Table 4 while the converse is true for the smaller diameter Escape Shaft.

TABLE 4  
EQUIVALENT PERMEABILITY OF THE MODIFIED  
PERMEABILITY ZONE (a)

| DEPTH | STRESS REDISTRIBUTION<br>WITHOUT BLAST DAMAGE |               | EXPECTED (b)<br>CASE | UPPER BOUND (c)<br>CASE |
|-------|---|---------------|----------------------|-------------------------|
|       | ELASTIC                                       | ELASTOPLASTIC |                      |                         |
| 100   | 15  | 20            | 20                   | 40                      |
| 310   | 15  | 40            | 20                   | 80                      |

(a) Equivalent permeability is averaged over an annulus 1 radius wide around the 4.4 m (14.5 ft) diameter exploratory shaft.

(b) This is based upon an elastic analysis with expected strength, insitu stress, sensitivity of permeability to stress, and a 0.5 m wide blast damage zone.

(c) This is based upon an elastoplastic analysis with lower bound strength, upper bound insitu stress, greatest sensitivity of permeability to stress, and a 1.0 m wide blast damage zone.

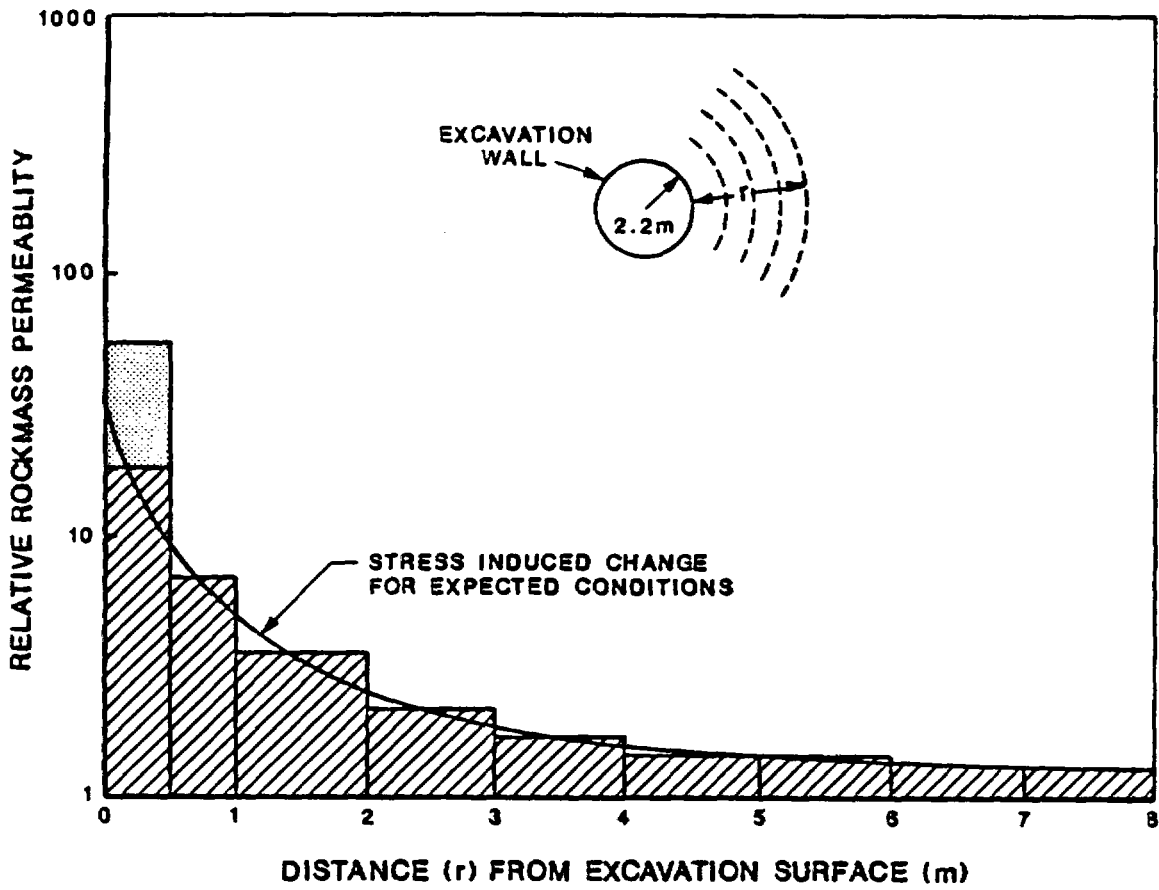


FIGURE 24. MODIFIED PERMEABILITY ZONE MODEL FOR TOPOPAH SPRING WELDED TUFF FOR EXPECTED CONDITIONS AT 310 m DEPTH

APPENDIX A  
ROCK MASS STRENGTH

A-1 HOEK AND BROWN'S EMPIRICAL STRENGTH CRITERION

Hoek and Brown (1980, p. 175) proposed a criterion for the strength of discontinuous rock masses. Laboratory and in situ strength data were compiled and interpreted according to the empirical relation

$$\frac{\sigma_1}{\sigma_u} = \frac{\sigma_3}{\sigma_u} + \sqrt{m \frac{\sigma_3}{\sigma_u} + s}, \quad (A-1)$$

where

$\sigma_u$  = unconfined compressive strength of intact rock,  
 $m, s$  = constants depending on rock quality, and  
 $\sigma_1, \sigma_3$  = major and minor principal stresses at failure;

or alternatively

$$\tau_n = A(\sigma_n - \sigma_{tn})^B, \quad (A-2)$$

where

$\sigma_{tn}$  = tensile strength normalized to uniaxial compressive strength,  
 $A, B$  = constants depending on rock quality, and  
 $\tau_n, \sigma_n$  = shear and normal stress on the failure plane normalized to uniaxial compressive strength.

Hoek and Brown (1980, pp. 133-182) provide a detailed discussion of the factors that influence rock mass strength and propose a method for estimating rock mass strength from laboratory testing and field investigations of rock mass quality. The laboratory testing involves triaxial compression testing of intact rock over the range of confining pressures expected in the field. The test data are then analyzed statistically to obtain the  $m$  constant (Equation A-1) for intact rock (Section A-1.1). The field investigations involve rock mass classification, either by the Geomechanics Classification System (RMR System; Bieniawski, 1984, p. 112) or the Q System (Barton et al., 1974, p. 189). The results obtained are input to empirical relationships to obtain  $m$  and  $s$  constants for the rock mass (Section A-1.3).

The method proposed by Hoek and Brown has been applied to the Topopah Spring nonlithophysal welded unit and the Calico Hills unit (units TSw2 and CHn1) for which laboratory and field data are available. The analysis presented below provides upper and lower bound estimates to the expected rock mass strength for welded and nonwelded tuff.

A-1.1 Analysis of Intact Rock Strength Data

A series of laboratory unconfined and confined compression tests was conducted on welded and nonwelded tuff under a variety of experimental conditions (Price, 1983, p. 6). These conditions included the sample saturation and drainage, as well as temperature and loading rate. The experimental results indicated that degree of saturation and drainage conditions have a significant effect on strength. Elevated temperatures (200°C) were also found to be significant; however the temperatures in the modified permeability zone are not expected to be high (i.e., <90°C), and effects of temperature are not included in the following analysis.

The tests on Topopah Spring (TSw2) and Calico Hills (CHn1) tuffs were conducted under oven-dry, room-dry, and saturated-drained conditions. Several tests on the Calico Hills unit were conducted under saturated-undrained conditions. The test results for welded tuff (Price, 1983, p. 10) reflect a narrow range of cohesion (10.2 to 17.5 MPa) and a broad range of friction angles (25° to 67°). The tests indicate higher friction angles for dry conditions, lower friction angles under saturated-drained conditions, and the lowest values for saturated-undrained conditions. Although these trends are similar to those observed when testing soil or crushed rock, the changes are thought to reflect chemical alteration of the silicates in the tuff (Price, 1983, p. 13).

Price's test data have been analyzed to obtain the  $m$  constant (Equation A-1) for intact rock. For comparison, two methods were used. The first method, described by Hoek and Brown (1980, Appendix 5), used a linear regression analysis to obtain the constant  $m$  for intact rock and the unconfined compressive strength. Equation A-1 is rewritten for intact rock ( $s = 1$ ) as

$$\sigma_1 = \sigma_3 + \sqrt{m_1 \sigma_3 \sigma_u + \sigma_u^2}, \quad (A-3)$$

where

$m_1$  = constant for intact rock, and  
other terms are as defined previously.

This method was applied to the triaxial compression test data given by Price under the assumption that tests conducted under dry conditions would provide data for an upper bound estimate of the constant  $m_1$ , whereas a lower bound estimate would be provided by the test data obtained under saturated, drained conditions. By this method, the upper bound  $m_1$  value for Topopah Spring tuff (TSw2) was 133. This value appears to be very high in comparison to published  $m_1$  values of <29.2 by Hoek and Brown (1980, pp. 141-142), and a quoted range of  $m_1$  values from 5 to 30 by Priest and Brown (1983, p. A-4).

The second method for calculating the  $m_1$  value is based on the ratio of tensile to compressive strength for intact rock ( $s = 1$ ) under unconfined conditions (Hoek and Brown, 1980, p. 177) is

$$-1/R = \sigma_t / \sigma_u = 1/2 [m_1 - \sqrt{m_1^2 + 4}], \quad (A-4)$$

where

$\sigma_t$  = tensile strength ( $\sigma_t < 0$ ),  
 $\sigma_u$  = unconfined compressive strength, and  
 $R$  = absolute value of the ratio of unconfined compressive strength to tensile strength.

The above equation may be solved for  $R$ , and the following relationship obtained:

$$m_1 = R - 1/R. \quad (A-5)$$

For dry conditions, using a tensile strength of 16.9 MPa for Topopah Spring tuff (Nimick et al., 1985, p. 2), the calculated  $m_1$  value is 13.5, which falls

in the range between 5 and 30. The values of  $m_1$  used in the analysis are shown in Table A-1.

#### A-1.2 Assessment of Rock Mass Quality

The rock mass quality for the welded, nonlithophysal Topopah Spring unit (TSw2) and the nonwelded Calico Hills unit (CHn1) was assessed by using the values for Rock Mass Rating (RMR) and Q Systems provided by Langkopf and Gnirk (1986, p. 19-86). The following is a brief summary of the rock mass quality obtained by means of the RMR method:

- Topopah Spring Unit
  - Unconfined Compressive Strength - The unconfined compressive strength ranged from 110 to 230 MPa; this results in the RMR strength rating that ranges from 7 to 15.
  - Rock Quality Designation (RQD) - The average RQD obtained from data for several exploratory boreholes ranged from 35 to 80; this results in an RMR/RQD rating that ranges from 8 to 17.
  - Joint Frequency - The joint frequency values after accounting for bias from sampling near vertical fractures in vertical holes ranged from 2 to 16 fractures per meter; this results in the RMR joint spacing rating that ranges from 10 to 20.
  - Joint Condition - A description of the rock mass condition upon which the lower bound estimate is based, including slightly rough surfaces, separation(s) of less than 1 mm, and hard joint wall rock. The upper bound estimate rating is based on very rough surfaces, noncontinuous, nonseparated, hard joint wall rock.
  - Ground-water Condition - The excavation which is above the ground-water table, is considered dry, and is assigned the highest ground-water RMR of 10.
- Calico Hills Unit
  - Unconfined Compressive Strength - The unconfined compressive strength ranged from 18 to 36 MPa; this results in an RMR strength rating that ranges from 2 to 4.
  - RQD - The average RQD obtained from data for several exploratory boreholes ranged from 85 to 99; this results in an RMR RQD rating that ranges from 17 to 20.
  - Joint Frequency - The joint frequency, after accounting for bias from sampling in vertical

**TABLE A-1**  
**PROPERTIES OF WELDED AND NONWELDED TUFF USED IN STRESS ANALYSES**

| UNIT                     | I<br>ESTIMATE | ROCK MASS (a)<br>CLASSIFICATION | RMR(a) | UNCONFINED<br>COMPRESSIVE<br>STRENGTH (MPa)(b) | $m_i$ | $m^{(c)}$ | $s^{(c)}$             |
|--------------------------|---------------|---------------------------------|--------|--|-------|-----------|-----------------------|
| Topopah Spring<br>(TSw2) | High          | I, Very Good                    | 84     | 230  | 13.5  | 6.0       | 0.079                 |
|                          | Expected      | II, Good                        | 65     | 171  | 13.5  | 1.4       | $3.9 \times 10^{-3}$  |
|                          | Low           | III, Fair                       | 48     | 110  | 2.8   | 0.084     | $2.60 \times 10^{-4}$ |
| Calico Hills<br>(CHn1)   | High          | II, Good                        | 71     | 36   | 4.8   | 0.78      | 0.01                  |
|                          | Low           | III, Fair                       | 49     | 18   | 1.4   | 0.046     | $3.0 \times 10^{-4}$  |

(a) Classification and rock mass rating are presented by Langkopf and Gnirk (1986, p. 90).

(b) Mean values for compressive strength from Nimick et al. (1984, p. 2). The ranges of unconfined compressive strength ( $\pm 1S.D.$ ) for intact rock were obtained from a draft version of the Site Characterization Plan (SCP). The current value for unconfined compressive strength for TSw 2 (see text, page 8) is  $166 \pm 65$  MPa (U.S. DOE, 1987, Table 2-7, p. 2-42).

(c) See text for definition and method of computing  $m$  and  $s$  constants.

boreholes, ranged from 0.5 to 1.2 fractures per meter; this results in an RMR joint spacing rating that ranges from 20 to 25.

- Joint Condition - A description of the condition upon which the estimate is based includes slightly rough surfaces, separation of less than 1 mm, soft-joint wall rock. This condition results in an RMR joint condition rating of 12.
- Ground-water Condition - The excavation is above the ground-water table, is considered dry, and is assigned the highest ground-water RMR of 10.

In the analysis presented by Langkopf and Gnirk, the RMR rating adjustment for joint orientation ranged from 0, for a favorable orientation, to -12 for a very unfavorable orientation. These limits were also adopted herein for a shaft excavated through welded and nonwelded units; a favorable orientation was adopted for an upper-bound estimate and unfavorable orientation was adopted for a lower-bound estimate.

The RMR rating for the Topopah Spring welded unit ranged from 48 to 84 with a corresponding rock mass assessment of very good to fair rock conditions. The RMR rating for the Calico Hills nonwelded unit ranged from 49 to 71 with a corresponding description of from good to fair rock conditions. The Topopah Spring unit exhibits a greater degree of variability reflecting, principally, variations in the RQD and joint spacing indices.

#### A-1.3 Scaling of Peak Rock Mass Strength

Priest and Brown (1983, p. A-4) present empirical relations which scale the  $m$  and  $s$  constants as functions of the RMR as follows

$$m = m_1 \exp [(RMR - 95)/13.4], \text{ and} \quad (A-6)$$

$$s = \exp [(RMR - 100)/6.3],$$

where all terms are as defined previously.

These relations are used for estimating the range of rock mass strength in confined compression for welded and nonwelded tuff. The empirical strength constants are summarized in Table A-2, and failure envelopes are illustrated in Figure 6. For welded tuff, values are given for the expected properties [corresponding to strength properties given by Nimick et al. (1984)] and for upper and lower bounds. The upper bound corresponds to the unconfined compressive strength plus one standard deviation and to the upper bound RMR. The lower bound corresponds to the strength minus one standard deviation and to the lower bound RMR. The discussion in Section A-1.5 highlights the assumptions and limitations of using the empirical strength criterion.

#### A-1.4 Scaling of Residual Rock Mass Strength

Determination of the extent of the plastic or inelastic zone and the stress distributions within the inelastic zone requires estimates of residual strength, as well as ultimate or peak rock strength properties. Barton et al. (1985, pp. 127-128) have performed modeling studies of the stress-displacement

**TABLE A-2**  
**COMPARISON OF THE CALCULATED AND RECOMMENDED EMPIRICAL**  
**STRENGTH PARAMETER,  $m$  VALUES**

| Rock type      | Rock quality           | RMR | Calculated $m^{(a)}$ | Recommended $m^{(b)}$ |
|----------------|------------------------|-----|----------------------|-----------------------|
| Welded Tuff    | Intact<br>(Dry)        |     | 13.5                 | 17.0                  |
|                | (Saturated)            |     | 2.8                  |                       |
|                | Very Good<br>Rock Mass | 85  | 6.0                  | 8.5                   |
|                | Fair<br>Rock Mass      | 44  | 0.084                | 0.34                  |
| Nonwelded Tuff | Intact<br>(Dry)        |     | 4.8                  | 17.0                  |
|                | (Saturated)            |     | 1.4                  |                       |
|                | Good<br>Rock Mass      | 65  | 0.78                 | 1.7                   |
|                | Fair<br>Rock Mass      | 44  | 0.046                | 0.34                  |

(a) These values are used in analyses in this report - from Table A-1.

(b) These values are recommended for fine-grained igneous rocks by Hoek and Brown (1980, p. 176).

relationships for welded tuff. These studies indicate that there is little difference between peak and residual shearing stress at confining stresses less than 10 MPa. In contrast, the estimated rock mass strength relationships in Figure 3-11 show a wide variation in peak or ultimate strength due to rock mass quality. For purposes of analysis, it is assumed that residual rock mass strength is equal to peak rock mass strength, and that evaluation of the upper and lower estimates of peak rock mass strength provides a reasonable bound to differences in peak and residual strength.

#### A-1.5 Assumptions and Limitations

Although the approach adopted by Hoek and Brown provides a promising method for assessing rock mass strength of fractured rock, several assumptions and limitations should be noted. The scaling relationship presented by Priest and Brown (1983) is based upon a comprehensive set of strength data for Paguna andesite. Tests were performed on samples of intact rock, on undisturbed core samples and samples with various degrees of weathering. These samples were classified according to the RMR system, and except for the samples of intact rock, the RMR values ranged from 8 to 46. The range of RMR values (40 to 90) for welded and nonwelded tuff reflects unweathered joints encountered at depth and is somewhat higher than the range for Paguna andesite except for the samples of intact rock and undisturbed core (RMR = 46). Thus, the scaling relationships developed by Priest and Brown in this analysis may reflect a different range of conditions than those that will be encountered for shafts excavated in tuff.

The empirical strength criterion presented by Hoek and Brown is for the brittle failure of rock. The authors established a limitation that rock specimens should be tested and strength data evaluated under the test condition that the major principal stress,  $\sigma_1$ , should be at least twice as great as the confining stress  $\sigma_3$ . In conducting their own analysis, Hoek and Brown evaluated test conditions in which the major principal stress was at least 3.4 times greater than the confining stress; this value corresponds to the transition from the brittle to ductile behavior. The condition of  $\sigma_1 = 2\sigma_3$  is easily satisfied for the higher-strength Topopah Spring (TSw2) tuff. In the case of the lower-strength nonwelded Calico Hills tuff (CHw1), the condition is again satisfied, but test conditions were closer to the conditions in which ductile behavior would be in evidence.

The empirical strength criterion for fractured rock (Equation A-1) assumes that strength is isotropic or that no single discontinuity orientation affects strength. As stated by Hoek and Brown, this condition is satisfied for random jointing or where the discontinuities are grouped in four or more sets. Langkopf and Gnirk (1986, p. 48) have considered fracture orientation sets as mapped from surface outcrops by Scott et al. (1983) at Yucca Mountain, and as determined from oriented core and mapped surface fractures in drifts in Grouse Canyon welded tuff within the G Tunnel complex. Analysis of these data indicated that the Topopah Spring unit (TSw2) would have either two sets plus random joints or three sets plus random joints. In contrast, the joint spacing in the nonwelded tuff of the Calico Hills (CHn1) is such that the rock is characterized as massive with no or few joints. Thus, the effects of shearing on isolated discontinuities may result in strength anisotropy in nonwelded tuff.

The discussion presented above suggests that the Hoek and Brown empirical strength criterion is applicable to welded tuff, and marginally applicable to nonwelded tuff. This evaluation is also borne out by a comparison of  $m$  and  $s$  constants as recommended by Hoek and Brown for fine-grained, polyminerallic, igneous crystalline rocks and the constants presented in Table A-1. Hoek and Brown (1980, p. 176) recommend that for

- An intact rock, the recommended values are  $m = 17.0$  and  $s = 1.0$ ,
- A very good quality rock (RMR = 85), the recommended values are  $m = 8.5$  and  $s = 0.1$ ,
- A good quality rock (RMR = 65), the recommended values are  $m = 1.7$  and  $S = 0.004$ , and
- A fair quality rock (RMR = 44), the recommended values are  $m = 0.34$  and  $s = 0.0001$ .

Comparisons of calculated and recommended  $m$  values are made in Table A-2. Under dry conditions, the calculated  $m_1$  value for welded tuff is comparable to the recommended value. Under saturated drained conditions the calculated value is less and, as pointed out earlier, may reflect chemical alteration. It is interesting to note that Hoek and Brown (1980, p. 154) indicate a reduction in uniaxial compressive strength with no effect on the  $m$  value when water is present in the pores. In the case of nonwelded tuff, the calculated  $m$  values are less, which reflects ductile behavior in this lower strength material.

#### A-2 PROTODYAKONOV'S EMPIRICAL STRENGTH CRITERION

Protodyakonov proposed a strength-size relationship of the following form:

$$\frac{\sigma_d}{\sigma_m} = \frac{d/b + m}{d/b + 1} \quad (A-7)$$

where

- $\sigma_d$  = strength of a cubical specimen with side length  $d$ ,
- $\sigma_m$  = in situ rock mass strength,
- $b$  = distance between discontinuities in the rock mass, and
- $m$  = constant dependent on intact strength as given below.

#### Intact Strength

>75 MPa  
<75 MPa

#### Loading in Compression

2 <  $m$  < 5  
5 <  $m$  < 10

A range of unconfined compressive strength may be determined for welded tuff (TSw2) and nonwelded tuff (CHn1). This range is shown on Figures 6 and 7 and indicates that the Hoek and Brown criterion predicts lower unconfined strength for welded tuff than predicted by the above relation. There is, however, a general correspondence between the unconfined compressive strengths obtained by the two methods.

APPENDIX B  
ROCK DAMAGE CAUSED BY BLASTING  
BIBLIOGRAPHY

Anderson, B., and P. A. Halen, 1978, Mining Methods Used In the Underground Tunnels and Test Rooms at Stripa, LBL-7081, Lawrence Berkeley Laboratory, Berkeley, California.

\* Ash, R. L., 1973, "The Influence of Geological Discontinuities on Rock Blasting," Ph.D. thesis, Department of Civil and Mineral Engineering, University of Minnesota, St. Paul, Minnesota, 289 pp.

Benson, R. P., D. K. Murphy and D. R. McCreath, 1970, "Modulus Testing of Rock at the Churchill Falls Underground Powerhouse, Labrador," Determination of the In Situ Modulus of Deformation of Rock, American Society for Testing and Materials, ASTM STP 477, pp. 89-116.

Bieniawski, Z. T., 1984, Rock Mechanics Design in Mining and Tunneling, A. A. Balkema, Rotterdam, Netherlands.

Brady, B. H. G., and E. T. Brown, 1985, Rock Mechanics for Underground Mining, George Allen & Unwin Ltd., London, England.

Brizzolari, E., 1981, "Miniseismic Investigations in Tunnels: Methodology and Results," Geoexploration, 18, pp. 259-267.

Cording, E. J., A. J. Hendron and D. U. Deere, 1971, "Rock Engineering for Underground Caverns," Underground Rock Chambers, ASCE, New York, New York, pp. 567-600.

Cottam, A. E., 1983, An Evaluation of the Extent and Properties of the Zone of Disturbed Rock Around A Vertical Shaft Excavated Through Basalt Flows At the Basalt Waste Isolation Project Site, SD-BWI-TI-128, Rockwell Hanford Operations, Richland, Washington.

Daemen, J. J. K., S. L. Cobb, W. B. Green, R. G. Jeffrey, S. P. Mathis and D. L. South, 1981, Nuclear Waste Management Research. Annual Report: Rock Mass Sealing, Nuclear Fuel Cycle Research Program, University of Arizona, Tucson, Arizona, Sponsored by the U.S. Nuclear Regulatory Commission.

Dowding, C. H., 1985, Blast Vibration Monitoring and Control, Prentice-Hall, Inc., Englewood Cliffs, New Jersey, 297 pp.

DuPont, 1977, Blaster's Handbook, E. J. DuPont de Nemours and Co., Wilmington, Delaware.

El Rabaa A. W. M. A., W. A. Hustrulid and W. F. Ubbes, 1982, "Spatial Distribution of Deformation Moduli Around the CSM/ONWI Room, Edgar Mine, Idaho Springs, Colorado", Proceedings of the 23rd U.S. Symposium on Rock Mechanics, Berkeley, California, pp. 790-801.

\* Items not reviewed

**BIBLIOGRAPHY**  
(Continued)

- Fisekci, M. Y., and K. Barron, 1975, "Methane Pressure and Flow Measurements in Coal and Surrounding Strata," Canadian Mining and Met. Bull., Vol. 68, No. 763, pp. 91-98.
- Hagan, T. N., 1984, "Basalt Design Considerations For Underground Mining and Construction Operations," ISRM Symposium, Design and Performance of Underground Excavations, British Geotechnical Society, London, England, pp. 255-262.
- Hagan, T. N., 1983, "The Influence of Rock Properties on the Design and Results of Blasts in Underground Construction," Proceedings of the International Symposium on Engineering Geology and Underground Construction, Lisbon, Spain, Vol. 1, pp. III.57-III.66.
- Hendron, A. J., Jr., 1977, "Engineering of Rock Blasting on Civil Projects," Structural and Geotechnical Mechanics: A Volume Honoring Nathan M. Newmark, W. J. Hall, ed., Prentice Hall Inc., Englewood Cliffs, New Jersey, pp. 242-277.
- Heuze, F. E., and R. E. Goodman, 1974, "The Design of 'Room and Pillar' Structures in Competent Jointed Rock. Example: The Crestmore Mine, California," Proceedings of the Second Congress of the ISRM, Belgrade, Yugoslavia, Vol. 2, pp. 679-687.
- Heuze, F. E., W. C. Patrick, R. V. De la Cruz and C. F. Voss, 1981a, In Situ Geomechanics Climax Granite, Nevada Test Site, UCRL-53076, Lawrence Livermore Laboratory, Livermore, California.
- Heuze, F. E., T. R. Butkovich and J. C. Peterson, 1981b, An Analysis of the "Mine-By" Experiment, Climax Granite, Nevada Test Site, UCRL-53133, Lawrence Livermore Laboratory, Livermore, California.
- Hocking, G., and C. M. St. John, 1979, Annual Report--Fiscal Year 1979, Numerical Modeling of Rock Stresses Within A Basaltic Nuclear Waste Repository, RHO-BWI-C-58, Rockwell Hanford Operations, Richland, Washington.
- Hoek, E., and E. T. Brown, 1980, Underground Excavations in Rock, Institution of Mining and Metallurgy, London, England, 527 pp.
- Holmberg, R., (no date) "Damage Criteria for Blasting and A Review of Two Projects Concerning Cautious Blasting," Swedish Detonic Research Foundation, Stockholm, Sweden.
- Holmberg, R., 1983, Hard Rock Excavation at the CSM/OCRD Test Site Using Swedish Blast Design Techniques, BMI/OCRD-4(3), Office of Crystalline Repository Development, Battelle Memorial Institute, Columbus, Ohio, 103 pp.
- Holmberg, R., and K. Maki, 1981, Case Examples of Blasting Damage and Its Influence on Slope Stability, SveDeFo Report DS 1981:9, Swedish Detonic Research Foundation, Stockholm, Sweden.

BIBLIOGRAPHY  
(Continued)

- Holmberg, R., and P. A. Persson, 1980, "Design of Tunnel Perimeter Blasthole Patterns to Prevent Rock Damage," Tunnelling '79, London, England, pp. 280-292.
- Holmberg, R., K. Mäki, W. Hustrulid and H. Sellden, 1983, "Blast Damage and Stress Measurements in the Lkab-Malmberget Fabian Orebody," Proceedings of the Fifth Congress of the ISRM, Melbourne, Australia, Vol. 2, pp. E231-E238.
- Hustrulid, W., R. Cudnik, R. Trent, R. Holmberg, P. E. Sperry, R. Hutchinson and P. Rosasco, 1980, "Mining Technology Development for Hard Rock Excavation," Storage in Excavated Rock Caverns: Rockstore 80, Stockholm, Sweden, Vol. 2, pp. 919-926.
- Hustrulid, W., R. Holmberg and K. Mäki, 1981, Damage Zone Adjacent to Large Hole Blasts at LKAB's Malmberget Mine as Evaluated Using the CSM Cell, SveDeFo Report DS 1981:3, Swedish Detonic Research Foundation, Stockholm, Sweden, 59 pp.
- Kelsall, P. C., J. B. Case and C. R. Chabannes, 1982, A Preliminary Evaluation of the Rock Mass Disturbance Resulting from Shaft, Tunnel, or Borehole Excavation, ONWI-411, Office of Nuclear Waste Isolation, Columbus, Ohio.
- Kelsall, P. C., J. B. Case and C. R. Chabannes, 1984, "Evaluation of Excavation-induced Changes in Rock Permeability," International Journal of Rock Mechanics and Mining Sciences & Geomechanics Abstracts, Vol. 21, No. 3, pp. 123-135.
- Kendorski, F. S., C. V. Jude and W. M. Duncan, 1973, "Effect of Blasting on Shotcrete Drift Linings," Mining Engineering, Vol. 25, No. 12, pp. 38-41.
- King, M. S., L. R. Myer and J. J. Rezowalli, 1984, "Cross-Hole Acoustic Measurements in Basalt," Proceedings of the 25th U.S. Symposium on Rock Mechanics, Evanston, Illinois, pp. 1053-1063.
- Kujundzic, B., L. Joranovic and Z. Radosavljevic, 1970, "A Pressure Tunnel Lining Using High-Pressure Grouting," (in French) Proceedings of the 2nd Congress of the ISRM, Belgrade, Yugoslavia, 4-66, pp. 867-881.
- Langefors, U., and B. Kihlstrom, 1978, Rock Blasting, John Wiley & Sons, New York, New York, 438 pp.
- Lukajic, B. J., 1982, "Geotechnical Experience with Tunnel Portal Construction," 14th Canadian Rock Mechanics Symposium, Vancouver, British Columbia.
- Mäki, K., and R. Holmberg, 1982, "The Shear Strength of Rock Joints with Reference to Cautious Blasting," International Society of Rock Mechanics Symposium, pp. 85-95.
- \* Matheson, G. D., and C. Swindells, 1981, Seismic Detection and Measurement of Blast Disturbance, LF928, Transport and Road Research Laboratory, England.

**BIBLIOGRAPHY**  
(Continued)

McKenzie, C. K., P. D. Forbes, G. E. LeJuge, I. H. Lewis, P. A. Lilly and J. D. Lilly, 1983, "Limit Blast Design Evaluation," Fifth Congress of the ISRM, Melbourne, Australia, Vol. 2, pp. E215-E222.

McKown, A. F., and D. E. Thompson, 1981, "Experiments with Fracture Control in Tunnel Blasting," Proceedings of the 22nd U.S. Symposium Rock Mechanics, Massachusetts Institute of Technology, Cambridge, Massachusetts, pp. 223-230.

Miller, C. H., D. R. Cunningham and M. J. Cunningham, 1974, "An Air-Injection Technique to Study Intensity of Fractures Around a Tunnel in Volcanic Rock," Association of Engineering Geologists, Bulletin, Vol. XI, No. 3, pp. 203-217.

Miller, C. H., and E. H. Skinner, 1980, "The Nature of Fracturing and Stress Distribution in Quartzite Around the 1128 m (3700 ft) Level of the Crescent Mine, Coeur d'Alene Mining District, Idaho," Engineering Geology, 16, pp. 321-338.

Montazer, P. M., and W. A. Hustrulid, 1981, An Investigation of Fracture Permeability Around an Underground Opening in Metamorphic Rocks, Topical Report No. 5, Colorado School of Mines, Golden, Colorado.

Montazer, P. M., and W. A. Hustrulid, 1983, An Investigation of Fracture Permeability Around an Underground Opening in Metamorphic Rocks, BMI/OCRD-4(5), Battelle Memorial Institute, Columbus, Ohio.

Montazer, P. G., G. Chitombo, R. M. King, and W. F. Ubbes, 1982, "Spatial Distribution of Permeability Around the CSM/ONWI Room, Edgar Mine, Idaho Springs, Colorado," Proceedings of the 23rd U.S. Symposium on Rock Mechanics, Berkeley, California, pp. 47-56.

Murphy, V. J., 1972, "Seismic Velocity Measurements for Moduli Determinations in Tunnels," Proceedings of the First North American Rapid Excavation and Tunneling Conference, Chicago, Illinois, 1:209-216.

Nelson, P., and C. Wilson, 1980, "Thermomechanical and Macropermeability Experiments in the Stripa Granite - Status Report," Proceedings of the Workshop on Thermomechanical-Hydrochemical Modeling for a Hardrock Waste Repository, LBL-11204, Lawrence Berkeley Laboratory, Berkeley, California.

Nishida, T., Y. Matsumura, Y. Miyanaga, and M. Hori, 1982, "Rock Mechanical Viewpoint on Excavation of Pressure Tunnel by Tunnel Boring Machine," ISRM Symposium, A. A. Balkema, Rotterdam, Netherlands, Vol., 1, pp. 815-826.

O'Donoghue, L. B., and R. M. O'Flaherty, 1974, "The Underground Works in Turlough Hill: Part I," Water Power, January, pp. 5-12.

Olson, J. J., R. J. Willard, D. E. Fogelson, and K. E. Hjelmstad, 1973, Rock Damage from Small Charge Blasting in Granite, RI 7751, U.S. Bureau of Mines.

BIBLIOGRAPHY  
(Continued)

- Oriard, L. L., 1981a, "Field Tests with Fracture-Control Blasting Techniques," Proceedings of the Rapid Excavation and Tunneling Conference, Vol. 1, pp. 874-884.
- Oriard, L. L., 1981b, "Blasting and Excavation," The Atlanta Research Chamber, D. Rose, ed., Report No. UMTA-GA-06-0007-81-1, U.S. Department of Transportation, Washington, D.C.
- Plichon, J. N., 1980, "Measurement of the Thickness of the Decompressed Zone in an Excavation Under High Overburden Cover," Analysis of Tunnel Stability by the Convergence-Confinement Method, Underground Space, 4, (6):361-402.
- Scott, J. H., F. T. Lee, R. D. Carroll and C. S. Robinson, 1968, "The Relationship of Geophysical Measurements to Engineering and Construction Parameters in the Straight Creek Tunnel Pilot Bore, Colorado," International Journal of Rock Mechanics, Mining Sciences, and Geomechanics Abstracts, Vol. 5, pp. 1-30.
- Siskind, D. E., and R. R. Fumanti, 1974, Blast-Produced Fractures in Lithonia Granite, RI 7901, U.S. Bureau of Mines, 38 pp.
- Siskind, D. E., R. C. Steckley and J. J. Olson, 1973, Fracturing in the Zone Around a Blasthole, White Pine, Michigan, RI 7753, U.S. Bureau of Mines.
- Solyman, Z. V., 1983, "Blasting and Slope Stability," Proceedings of the Fifth Congress of the ISRM, Melbourne, Australia, Vol. 1, pp. C123-C128.
- Sperry, P. E., W. L. Fournery, D. E. Thompson and A. F. McKown, 1979, "Controlled Blasting Experiments at Porter Square Pilot Tunnel," Proceedings of the Rapid Excavation and Tunneling Conference, Atlanta, Georgia, Vol. 2, pp. 1130-1157.
- Sperry, P. E., G. P. Chitombo and W. A. Hustrulid, 1984, Hard Rock Excavation at the CSM/OCRD Test Site Using Crater Theory and Current United States Controlled Smooth Wall Blasting Practices, BMI/OCRD-4(4), Office of Crystalline Repository Development, Battelle Memorial Institute, Columbus, OH, 45 pp.
- Thompson, D. E., A. F. McKown, W. L. Fournery and P. E. Sperry, 1979, Field Evaluation of Fracture Control in Tunnel Blasting, Report No. UMTA-MA-06-0100-79-14, U.S. Department of Transportation, Washington, D.C.
- Wilson, C. R., P. A. Witherspoon, J. C. S. Long, R. M. Galbraith, A. O. DuBois and M. J. McPherson, 1983, "Large-scale Hydraulic Conductivity Measurements in Fractured Granite," International Journal of Rock Mechanics and Mining Sciences & Geomechanics Abstracts, Vol. 20, No. 6, pp. 269-276.
- Witherspoon, P. A., N. G. W. Cook and J. E. Gale, 1981, "Geologic Storage of Radioactive Waste: Field Studies in Sweden," Science, Vol. 211, February 27, 1981.

BIBLIOGRAPHY  
(Continued)

\*Worsey, P. N., 1984, A Comparison of Blast Damage for Different Perimeter Blasting Techniques Underground, Final report to Weldon Springs Research Foundation, 50 pp.

Worsey, P. N., 1985, "In Situ Measurement of Blast Damage Underground by Seismic Refraction Surveys," Proceedings of the 26th U.S. Symposium on Rock Mechanics, Rapid City, South Dakota, pp. 1133-1140.

Worsey, P. N., I. W. Farmer and G. D. Matheson, 1981, "The Mechanics of Pre-Splitting in Discontinuous Rock," Proceedings of the 22nd U.S. Symposium on Rock Mechanics, Massachusetts Institute of Technology, Cambridge, Massachusetts, p. 205-210.

## REFERENCES

- Andersson, B., and P. A. Halén, 1978, Mining Methods Used In the Underground Tunnels and Test Rooms at Stripa, LBL-7081, Lawrence Berkeley Laboratory, Berkeley, California.
- Barton, N., R. Lien and J. Lunde, 1974, "Engineering Classification of Rock Masses for the Design of Tunnel Supports," Rock Mechanics, 6, pp. 189-236.
- Barton, N., S. Bandis, and K. Bakhtar, 1985, "Strength, Deformation and Conductivity Coupling of Rock Joint," International Journal of Rock Mechanics and Mining Sciences & Geomechanic Abstracts, Vol. 22, No. 3, pp. 121-140.
- Bauer, S. J., J. F. Holland and D. K. Parrish, 1985, "Implications About Insitu Stress at Yucca Mountain," Proceedings of the 26th U.S. Symposium on Rock Mechanics, A. A. Balkema, Boston, Massachusetts, Vol. 2, pp. 1113-1120.
- Benson, R. P., D. K. Murphy and D. R. McCreath, 1970, "Modulus Testing of Rock at the Churchill Falls Underground Powerhouse, Labrador," Determination of the In Situ Modulus of Deformation of Rock, American Society for Testing and Materials, ASTM STP 477, pp. 89-116.
- Bentley, C. B., 1984, Geohydrologic Data for Test Well USW G-4, Yucca Mountain Area, Nye County, Nevada, USGS-OFR-84-063 U.S. Geological Survey, Denver, Colorado, 48 pp.
- Bieniawski, Z. T., 1984, Rock Mechanics Design in Mining and Tunneling, A. A. Balkema, Rotterdam, Netherlands, 272 pp.
- Brady, B. H. G., and E. T. Brown, 1985, Rock Mechanics for Underground Mining, George Allen & Unwin Ltd., London, England.
- Brizzolari, E., 1981, "Miniseismic Investigations in Tunnels: Methodology and Results," Geoexploration, 18, pp. 259-267.
- Cording, E. J., A. J. Hendron, and D. U. Deere, 1971, "Rock Engineering for Underground Caverns," Underground Rock Chambers, ASCE, New York, New York, pp. 567-600.
- Dowding, C. H., 1985, Blast Vibration Monitoring and Control, Prentice Hall, Englewood Cliffs, New Jersey, 297 pp.
- DuPont, 1977, Blaster's Handbook, E.I. DuPont de Nemours and Co., Wilmington, Delaware.
- El Rabaa A.W.M.A., W. A. Hustrulid and W. F. Ubbs, 1982, "Spatial Distribution of Deformation Moduli Around the CSM/ONWI Room, Edgar Mine, Idaho Springs, Colorado," Proceedings of the 23rd Symposium on Rock Mechanics, Society of Mining Engineers, AIME, New York, New York, Vol. 1, pp. 790-801.

Fernandez, J. A., P. C. Kelsall, J. B. Case, and D. Meyer 1987, Technical Basis for Performance Goals, Design Requirements and Materials Recommendations for the NNWSI Repository Sealing Program, SAND84-1895, Sandia National Laboratories, Albuquerque, New Mexico (In Preparation).

Freeze, R. A., and J. A. Cherry, 1979, Groundwater, Prentice-Hall, Inc., Englewood Cliffs, New Jersey, 604 pp.

Goodman, R. E., 1980, Introduction to Rock Mechanics, John Wiley & Sons, New York, New York, 468 pp.

Hardin, E., N. Barton, D. Lingle, M. Board and M. Voegele, 1982, A Heated Flatjack Test Series to Measure the Thermomechanical and Transport Properties of In Situ Rock Masses ("Heated Block Test"), ONWI-260, Office of Nuclear Waste Isolation, Battelle Memorial Institute, Columbus, Ohio.

Heuze, F. E., and R. E. Goodman, 1974, "The Design of 'Room and Pillar' Structures in Competent Jointed Rock. Example: The Crestmore Mine, California," Proceedings of the Second Congress of the ISRM, Belgrade, Yugoslavia, Vol. 2, pp. 679-687.

Hocking, G., and C. M. St. John, 1979, Annual Report - Fiscal Year 1979. Numerical Modeling of Rock Stresses Within a Basaltic Nuclear Waste Repository, RHO-BWI-C-58, Rockwell Hanford Operations, Richland, Washington.

Hoek, E., and E. T. Brown, 1980, Underground Excavations in Rock, Institution of Mining and Metallurgy, London, England, 527 pp.

Holmberg, R., and P. A. Persson, 1980, "Design of Tunnel Perimeter Blasthole Patterns to Prevent Rock Damage," Transactions of the Institution of Mining and Metallurgy, London, England, 89:A37-A40.

Hustrulid, W., R. Cudnik, R. Trent, R. Holmberg, P. E. Sperry, R. Hutchinson and P. Rosaco., 1980, "Mining Technology Development for Hard Rock Excavation," Proceedings of the Second International Symposium (Rockstore '80), Stockholm, Sweden, Vol. 2, pp. 919-926.

Jaeger, J. C., and N. G. W. Cook, 1976, Fundamentals of Rock Mechanics, Halsted Press, London, England, 583 pp.

Kelsall, P. C., J. B. Case, and C. R. Chabannes, 1982, A Preliminary Evaluation of the Rock Mass Disturbance Resulting from Shaft, Tunnel or Borehole Excavation, ONWI-411, Office of Nuclear Waste Isolation, Battelle Memorial Institute, Columbus, Ohio.

King, M. S., L. R. Myer and J. J. Rezwali, 1984, "Cross-Hole Acoustic Measurements in Basalt," Proceedings of the 25th U.S. Symposium on Rock Mechanics, Society of Mining Engineers, AIME, New York, New York, pp. 1053-1062.

Kujundzic, B., L. Joranovic and Z. Radosavljevic, 1970, "A Pressure Tunnel Lining Using High-Pressure Grouting," (in French) Proceedings of the 2nd Congress of the ISRM, Belgrade, Yugoslavia, pp. 867-881.

- Langefors, U., and B. Kihlstrom, 1978, Rock Blasting, John Wiley & Sons, New York, New York, 438 pp.
- Langkopf, B. S., and P. R. Gnirk, 1986, Rock Mass Classification of Candidate Repository Units at Yucca Mountain, Nye County, Nevada, SAND82-2034, Sandia National Laboratories, Albuquerque, New Mexico.
- Lukajic, B. J., 1982, "Geotechnical Experience with Tunnel Portal Construction," 14th Canadian Rock Mechanics Symposium, Canadian Institute of Mining and Metallurgy, Vancouver, British Columbia, 15 pp.
- Miller, C. H., D. R. Cunningham and M. J. Cunningham, 1974, "An Air-Injection Technique to Study Intensity of Fractures Around a Tunnel in Volcanic Rock," Bulletin of the Association of Engineering Geologists, Vol. XI, No. 3, pp. 203-217.
- Montazer P. G., G. Chitombo, R. M. King and W. F. Ubbes, 1982, "Spatial Distribution of Permeability Around the CSM/ONWI Room Edgar Mine, Idaho Springs, Colorado," Proceedings of the 23rd Symposium on Rock Mechanics, Society of Mining Engineers, AIME, New York, New York, Vol. 1, pp. 47-56.
- Montazer, P. M., and W. A. Hustrulid, 1983, An Investigation of Fracture Permeability Around an Underground Opening in Metamorphic Rocks, BMI/OCRD-4(5), Battelle Memorial Institute, Columbus, Ohio.
- Montazer, P., and W. E. Wilson, 1984, Conceptual Hydrologic Model of Flow in the Unsaturated Zone, Yucca Mountain, Nevada, USGS Water-Resources Investigations Report 84-3445, United States Geological Survey, Lakewood, Colorado, 55 pp.
- Nelson, P., and C. Wilson, 1980, Thermomechanical and Macropermeability Experiments in the Stripa Granite, Status Report, ONWI-164, Office of Nuclear Waste Isolation, Columbus, Ohio.
- Nimick, F. B., S. J. Bauer and J. R. Tillerson, 1984, Recommended Matrix and Rock-Mass Bulk, Mechanical and Thermal Properties for Thermomechanical Stratigraphy of Yucca Mountain, Keystone Document No. 6310-85-1 (Memorandum to T. O. Hunter), Sandia National Laboratories, Albuquerque, New Mexico.
- Nishida, T., Y. Matsumura, Y. Miyanaga and M. Hori, 1982, "Rock Mechanical Viewpoint on Excavation of Pressure Tunnel by Tunnel Boring Machine", ISRM Symposium, A.A. Balkema, Rotterdam, Netherlands, Vol. 1, pp. 815-826.
- O'Donoghue, L. B., and R. M. O'Flaherty, 1974, "The Underground Works in Turlough Hill: Part I," Water Power, January, pp. 5-12.
- Olson, J. J., R. J. Willard, D. E. Folgelson and K. E. Hjelmstadt, 1973, Rock Damage from Small Charge Blasting in Granite, Report of Investigations 7751, United States Department of the Interior, U.S. Bureau of Mines, 44 pp.
- Ortiz, T. S., R. L. Williams, F. B. Nimick, B. C. Whitlet and D. L. Smith, 1985, A Three-Dimensional Model of Reference Thermal/Mechanical, and Hydrological Stratigraphy at Yucca Mountain, Southern Nevada, SAND84-1076, Sandia National Laboratories, Albuquerque, New Mexico, 76 pp.

Peters, R. R., E. A. Klavetter, I. J. Hall, S. C. Blair, P. R. Heller and G. W. Gee, 1984, Fracture and Matrix Hydrologic Characteristics of Tuffaceous Materials from Yucca Mountain, Nye County, Nevada, SAND84-1471, Sandia National Laboratories, Albuquerque, New Mexico.

Plichon, J. N., 1980, "Measurement of the Thickness of the Decompressed Zone in an Excavation Under High Overburden Cover," Analysis of Tunnel Stability by the Convergence-Confinement Method, Underground Space, 4, (6):361-402.

Price, R. H., 1983, Analysis of Rock Mechanics Properties of Volcanic Tuff Units from Yucca Mountain, Nevada Test Site, SAND82-1315, Sandia National Laboratories, Albuquerque, New Mexico, 80 pp.

Price, R. H., and S. J. Bauer, 1985, "Analysis of the Elastic and Strength Properties of Yucca Mountain Tuff, Nevada," Proceedings of the 26th U.S. Symposium on Rock Mechanics, A. A. Balkema, Boston, Massachusetts, Vol. 1, pp. 89-94.

Priest, S. D., and E. T. Brown, 1983, "Probabilistic Stability Analysis of Variable Rock Slopes," Trans. Instn. Min. Metal. (Sect. A: Min. Industry), 92, pp. A1-A12.

Protodyakonov, M. M., 1964, "The Size Effect in Investigations of Rock and Coal," Proceedings of the International Conference on Stress in the Earth's Crust, Henry Krumb School of Mining, New York, New York, Unpaginated Addendum.

Scott, J. H., F. T. Lee, R. D. Carroll and C. S. Robinson, 1968, "The Relationship of Geophysical Measurements to Engineering and Construction Parameters in the Straight Creek Tunnel Pilot Bore, Colorado," International Journal of Rock Mechanics, Mining Sciences, and Geomechanics Abstracts, Vol. 5, pp. 1-30.

Scott, R. B., R. W. Spengler, S. Diehl, A. R. Lappin and M. P. Chornack, 1983, "Geologic Character of Tuffs in the Unsaturated Zone at Yucca Mountain, Southern Nevada," Role of the Unsaturated Zone in Radioactive and Hazardous Waste Disposal, J. Mercer, ed., Ann Arbor Sciences, Ann Arbor, Michigan, pp. 289-335.

Scott, R. B., and J. Bonk, 1984, Preliminary Geologic Map of Yucca Mountain, Nye County, Nevada with Geologic Section, Open-File Report 84-494, United States Geological Survey, Denver, Colorado.

Sinnock, S., Y. T. Lin and J. P. Brannon, 1984, Preliminary Bounds on the Expected Postclosure Performance of the Yucca Mountain Repository Site, Southern Nevada, SAND84-1492, Sandia National Laboratories, Albuquerque, New Mexico, 82 pp.

Siskind, D. E., R. C. Steckley and J. J. Olson, 1973, Fracturing in the Zone Around a Blasthole, White Pine, Michigan, Report on Investigation 7753, United States Department of the Interior, U.S. Bureau of Mines, 18 pp.

Siskind, D. E., and R. R. Fumanti, 1974, Blast-Produced Fractures in Lithonia Granite, Report of Investigations 7901, United States Department of the Interior, U.S. Bureau of Mines, 29 pp.

Sperry, P. E., G. P. Chitombo and W. A. Hustrulid, 1984, Hard Rock Excavation at the CSM/OCRD Test Site Using Crater Theory and Current United States Controlled Smooth Wall Blasting Practices, BMI/OCRD-4(4), Office of Crystalline Repository Development, Battelle Memorial Institute, Columbus, Ohio, 45 pp.

Swan, G., 1978, "The Mechanical Properties of Stripe Granite," LBL-7074, Lawrence Berkeley Laboratory, Berkeley, California, 25 pp.

U.S. Department of Energy, 1986, "Environmental Assessment, Yucca Mountain Site, Nevada Research and Development Area, Nevada," DOE/RW-0073, U. S. Department of Energy, Office of Civilian Radioactive Waste Management, Washington, D. C.

U.S. Department of Energy, 1987, "Draft, Site Characterization Plan--Yucca Mountain Site, Nevada Research and Development Area, Nevada," U.S. Department of Energy, Office of Civilian Radioactive Waste Management, Washington, D.C.

Wilson, C. R., P. A. Witherspoon, J. C. S. Long, R. M. Galbraith, A. O. DuBois and M. J. McPherson, 1983, "Large-Scale Hydraulic Conductivity Measurements in Fractured Granite," International Journal of Rock Mechanics and Mining Sciences, Vol. 20, No. 6, pp. 269-276.

Witherspoon, P. A., J. S. Y. Wang and J. E. Gale, 1980, "Validity of the Cubic Law for Fluid Flow in a Deformable Rock Fracture," Water Resources Research, Vol. 6, No. 6, pp. 1016-1024.

Witherspoon, P. A., N. G. W. Cook and J. E. Gale, 1981, "Geologic Storage of Radioactive Waste: Field Studies in Sweden," Science, Vol. 211, pp. 894-900.

Worsey, P. N., 1985, "In Situ Measurement of Blast Damage Underground by Seismic Refraction Surveys," Proceedings of the 26th U.S. Symposium on Rock Mechanics, A. A. Balkema, Boston, Massachusetts, Vol. 2, pp. 1133-1140.

Zimmerman, R. M., and W. C. Vollendorf, 1982, Geotechnical Field Measurements, G-Tunnel, Nevada Test Site, SAND81-1971, Sandia National Laboratories, Albuquerque, New Mexico.

Zimmerman, R. M., M. L. Wilson, M. P. Board, M. E. Hall and R. L. Schuch, 1985, "Thermal-Cycle Testing of the G-Tunnel Heated Block," Proceedings 26th U.S. Symposium on Rock Mechanics, A. A. Balkema, Boston, Massachusetts, Vol. 2, pp. 749-758.

## DISTRIBUTION LIST

B. C. Rusche (RW-1), Director  
Office of Civilian Radioactive Waste  
Management  
U.S. Department of Energy  
Forrestal Building  
Washington, D.C. 20585

Ralph Stein (RW-23)  
Office of Civilian Radioactive Waste  
Management  
U.S. Department of Energy  
Forrestal Building  
Washington, D.C. 20585

J. J. Fiore (RW-22)  
Office of Civilian Radioactive Waste  
Management  
U.S. Department of Energy  
Forrestal Building  
Washington, D.C. 20585

M. W. Frei (RW-23)  
Office of Civilian Radioactive Waste  
Management  
U.S. Department of Energy  
Forrestal Building  
Washington, D.C. 20585

E. S. Burton (RW-25)  
Siting Division  
Office of Geologic Repositories  
U.S. Department of Energy  
Forrestal Building  
Washington, D.C. 20585

C. R. Cooley (RW-24)  
Geosciences & Technology Division  
Office of Geologic Repositories  
U.S. Department of Energy  
Forrestal Building  
Washington, D.C. 20585

V. J. Cassella (RW-22)  
Office of Civilian Radioactive Waste  
Management  
U.S. Department of Energy  
Forrestal Building  
Washington, D.C. 20585

T. P. Longo (RW-25)  
Program Management Division  
Office of Geologic Repositories  
U.S. Department of Energy  
Forrestal Building  
Washington, D.C. 20585

Cy Klingsberg (RW-24)  
Geosciences and Technology Division  
Office of Geologic Repositories  
U.S. Department of Energy  
Forrestal Building  
Washington, D.C. 20585

B. G. Gale (RW-22)  
Office of Civilian Radioactive Waste  
Management  
U.S. Department of Energy  
Forrestal Building  
Washington, D.C. 20585

R. J. Blaney (RW-22)  
Program Management Division  
Office of Geologic Repositories  
U.S. Department of Energy  
Forrestal Building  
Washington, D.C. 20585

R. W. Gale (RW-40)  
Office of Civilian Radioactive Waste  
Management  
U.S. Department of Energy  
Forrestal Building  
Washington, D.C. 20585

J. E. Shaheen (RW-44)  
Outreach Programs  
Office of Policy, Integration and  
Outreach  
U.S. Department of Energy  
Forrestal Building  
Washington, D.C. 20585

J. O. Neff, Manager  
Salt Repository Project Office  
U.S. Department of Energy  
505 King Avenue  
Columbus, OH 43201

Engineering & Licensing Division  
Office of Isotopic Repositories  
U.S. Department of Energy  
Forrestal Building  
Washington, D.C. 20585

O. L. Olson, Manager  
Basalt Waste Isolation Project Office  
Richland Operations Office  
U.S. Department of Energy  
P.O. Box 550  
Richland, WA 99352

D. L. Vieth, Director (4)  
Waste Management Project Office  
U.S. Department of Energy  
P.O. Box 14100  
Las Vegas, NV 89114

D. F. Miller, Director  
Office of Public Affairs  
U.S. Department of Energy  
P.O. Box 14100  
U.S. Department of Energy  
Las Vegas, NV 89114

P. M. Bodin (12)  
Office of Public Affairs  
U.S. Department of Energy  
P.O. Box 14100  
Las Vegas, NV 89114

B. W. Church, Director  
Health Physics Division  
U.S. Department of Energy  
P.O. Box 14100  
Las Vegas, NV 89114

Chief, Repository Projects Branch  
Division of Waste Management  
U.S. Nuclear Regulatory Commission  
Washington, D.C. 20555

Document Control Center  
Division of Waste Management  
U.S. Nuclear Regulatory Commission  
Washington, D. C. 20555

S. A. Mann, Manager  
Crystalline Rock Project Office  
U.S. Department of Energy  
9800 South Cass Avenue  
Argonne, IL 60439

A. Street, Jr.  
Lawrence Livermore National Laboratory  
P.O. Box 808  
Mail Stop L-209  
Livermore, CA 94550

L. D. Ramspott (3)  
Technical Project Officer for NNWS  
Lawrence Livermore National Laboratory  
P.O. Box 808  
Mail Stop L-204  
Livermore, CA 94550

W. J. Purcell (RW-20)  
Associate Director  
Office of Civilian Radioactive Waste  
Management  
U.S. Department of Energy  
Forrestal Building  
Washington, D.C. 20585

D. T. Oakley (4)  
Technical Project Officer for NNWSI  
Los Alamos National Laboratory  
P.O. Box 1663  
Mail Stop F-619  
Los Alamos, NM 87545

W. W. Dudley, Jr. (3)  
Technical Project Officer for NNWSI  
U.S. Geological Survey  
P.O. Box 25046  
418 Federal Center  
Denver, CO 80225

NTS Section Leader  
Repository Project Branch  
Division of Waste Management  
U.S. Nuclear Regulatory Commission  
Washington, D.C. 20555

V. M. Glanzman  
U.S. Geological Survey  
P.O. Box 25046  
913 Federal Center  
Denver, CO 80225

P. T. Prestholt  
NRC Site Representative  
1050 East Flamingo Road  
Suite 319  
Las Vegas, NV 89109

M. E. Spaeth  
Technical Project Officer for NNWSI  
Science Applications International  
Corporation  
Suite 407  
101 Convention Center Drive  
Las Vegas, NV 89109

SAIC-T&MSS Library (2)  
Science Applications International  
Corporation  
Suite 407  
101 Convention Center Drive  
Las Vegas, NV 89109

W. S. Twenhofel, Consultant  
Science Applications International  
Corporation  
820 Estes Street  
Lakewood, CO 89215

A. E. Gurrola  
Vice President and General Manager  
Energy Support Division  
Holmes & Narver, Inc.  
Mail Stop 580  
P.O. Box 14340  
Las Vegas, NV 89114

J. A. Cross, Manager  
Las Vegas Branch  
Fenix & Scisson, Inc.  
Mail Stop 514  
P.O. Box 14308  
Las Vegas, NV 89114

Neal Duncan (RW-44)  
Office of Policy, Integration, and  
Outreach  
U.S. Department of Energy  
Forrestal Building  
Washington, D.C. 20585

J. S. Wright  
Technical Project Officer for NNWSI  
Westinghouse Electric Corporation  
Waste Technology Services Division  
Nevada Operations  
P.O. Box 708  
Mail Stop 703  
Mercury, NV 89023

ONWI Library  
Battelle Columbus Laboratory  
Office of Nuclear Waste Isolation  
505 King Avenue  
Columbus, OH 43201

W. M. Hewitt, Program Manager  
Roy F. Weston, Inc.  
955 L'Enfant Plaza, Southwest, Suite 800  
Washington, D.C. 20024

H. D. Cunningham, General Manager  
Reynolds Electrical & Engineering  
Co., Inc.  
P.O. Box 14400  
Mail Stop 555  
Las Vegas, NV 89114

T. Hay, Executive Assistant  
Office of the Governor  
State of Nevada  
Capitol Complex  
Carson City, NV 89710

R. R. Loux, Jr., Director (3)  
Nevada Agency for Nuclear Projects  
Nuclear Waste Project Office  
State of Nevada  
Capitol Complex  
Carson City, NV 89710

C. H. Johnson, Technical Program Manager  
Nevada Agency for Nuclear Projects  
Nuclear Waste Project Office  
State of Nevada  
Capitol Complex  
Carson City, NV 89710

John Fordham  
Desert Research Institute  
Water Resources Center  
P.O. Box 60220  
Reno, NV 89506

Department of Comprehensive Planning  
Clark County  
225 Bridger Avenue, 7th Floor  
Las Vegas, NV 89155

Lincoln County Commission  
Lincoln County  
P.O. Box 90  
Pioche, NV 89043

Community Planning and Development  
City of North Las Vegas  
P.O. Box 4086  
North Las Vegas, NV 89030

City Manager  
City of Henderson  
Henderson, NV 89015

N. A. Norman, Project Manager  
Bechtel National Inc.  
P.O. Box 3965  
San Francisco, CA 94119

Flo Butler  
Los Alamos Technical Associates  
1650 Trinity Drive  
Los Alamos, NM 87544

Timothy G. Barbour  
Science Applications International  
Corporation  
1626 Cole Boulevard, Suite 270  
Golden CO 80401

E. P. Binnall  
Field Systems Group Leader  
Building 50B/4235  
Lawrence Berkeley Laboratory  
Berkeley, CA 94720

Dr. Martin Mifflin  
Desert Research Institute  
Water Resources Center  
Suite 1  
2505 Chandler Avenue  
Las Vegas, NV 89120

Planning Department  
Nye County  
P.O. Box 153  
Tonopah, NV 89049

Economic Development Department  
City of Las Vegas  
400 East Stewart Avenue  
Las Vegas, NV 89101

Director of Community Planning  
City of Boulder City  
P.O. Box 367  
Boulder City, NV 89005

Commission of the European Communities  
200 Rue de la Loi  
B-1049 Brussels  
BELGIUM

Technical Information Center  
Roy F. Weston, Inc.  
955 L'Enfant Plaza, Southwest, Suite 800  
Washington, D.C. 20024

R. Crig  
Parsons Brinkerhoff Quade &  
Douglas, Inc.  
1625 Van Ness Avenue  
San Francisco, CA 94109-3678

Dr. Madan M. Singh, President  
Engineers International, Inc.  
98 East Naperville Road  
Westmont, IL 60559-1595

Roger Hart  
Itasca Consulting Group, Inc.  
P.O. Box 14806  
Minneapolis, Minnesota 55414

T. H. Isaacs (RW-22)  
Office of Civilian Radioactive Waste  
Management  
U.S. Department of Energy  
Forrestal Building  
Washington, D.C. 20585

D. H. Alexander (RW-23)  
Office of Civilian Radioactive Waste  
Management  
U.S. Department of Energy  
Forrestal Building  
Washington, D.C. 20585

B. J. King, Librarian (2)  
Basalt Waste Isolation Project Library  
Rockwell Hanford Operations  
P.O. Box 800  
Richland, WA 99352

David K. Parrish  
RE/SPEC Inc.  
3815 Eubank, N.E.  
Albuquerque, NM 87191

D. L. Fraser, General Manager  
Reynolds Electrical & Engineering  
Co., Inc.  
Mail Stop 555  
P.O. Box 14400  
Las Vegas, NV 89114-4400

Gerald Parker (RW-25)  
Office of Geologic Repositories  
U.S. Department of Energy  
Forrestal Building  
Washington, D.C. 20585

J. P. Knight (RW-24)  
Office of Civilian Radioactive Waste  
Management  
U.S. Department of Energy  
Forrestal Building  
Washington, D.C. 20585

Allen Jelacic (RW-23)  
Office of Civilian Radioactive Waste  
Management  
U.S. Department of Energy  
Forrestal Building  
Washington, D.C. 20585

J. R. Rollo  
Deputy Assistant Director for  
Engineering Geology  
U.S. Geological Survey  
106 National Center  
12201 Sunrise Valley Drive  
Reston, VA 22092

R. Lindsay Mundell  
U.S. Bureau of Mines  
P.O. Box 25086  
Building 20  
Denver Federal Center  
Denver, CO 80225

Vincent Gong  
Technical Project Officer for NNWSI  
Reynolds Electrical & Engineering  
Co., Inc.  
Mail Stop 615  
P.O. Box 14400  
Las Vegas, NV 89114-4400

Christopher M. St. John  
J. F. T. Agapito Associates, Inc.  
27520 Hawthorne Boulevard, Suite 137  
Rolling Hills Estates, CA 90274

J. P. Pedalino  
Technical Project Officer for NNWSI  
Holmes & Narver, Inc.  
Mail Stop 605  
P.O. Box 14340  
Las Vegas, NV 89114  
Eric Anderson  
Mountain West Research-Southwest, Inc.  
398 South Mill Avenue, Suite 300  
Tempe, AZ 85281

Judy Foremaster (5)  
City of Caliente  
P.O. Box 158  
Caliente, NV 89008

S. D. Murphy  
Technical Project Officer for NNWSI  
Fenix & Scisson, Inc.  
Mail Stop 940  
P.O. Box 15408  
Las Vegas, NV 89114

S. H. Kale (RW-20), Associate Director  
Office of Civilian Radioactive Waste  
Management  
U.S. Department of Energy  
Forrestal Building  
Washington, D.C. 20585

6300 R. W. Lynch  
6310 T. O. Hunter  
6310 60/124233/1.3/Q2  
6311 L. W. Scully  
6311 C. Mora  
6312 R. W. Bingham  
6312 B. S. Langkopf  
6312 R. R. Peters  
6313 T. E. Blejwas  
6313 L. E. Shephard  
6313 R. M. Zimmerman  
6314 J. R. Tillerson (3)  
6314 J. A. Fernandez (20)  
6314 S. J. Bauer  
6314 T. E. Hinkebein  
6314 R. E. Stinebaugh  
6315 S. Sinnock  
6315 M. J. Eatough  
6332 WMT Library (20)  
6430 N. R. Ortiz  
3141 S. A. Landenberger (5)  
3151 W. L. Garner (3)  
8024 P. W. Dean  
3154-3 C. H. Dalin (28)  
for DOE/OSTI  
6311 V. Hinkel (2)